UNIVERSITY OF MODENA AND REGGIO EMILIA

PhD in Food Sciences, Technologies and Biotechnologies

XXXII Cycle

CIRCULAR ECONOMY STRATEGIES FOR THE MANAGEMENT AND VALORISATION OF SOME BY-PRODUCTS OF THE WINE INDUSTRY

PhD Candidate Umberto Cancelli

Supervisor (Tutor): Prof. Andrea Antonelli

Co-Supervisor (Co-Tutor): Dr. Giuseppe Montevecchi

Coordinator of Doctorate Course: Prof. Alessandro Ulrici

Academic year 2019/2020

INDEX

AIM OF THE WORK

7. MATERIALS AND METHODS

7.1 CHEMICALS

7.2 DISTILLATION FRACTIONS

7.2.1 CLASSIFICATION OF THE DISTILLATION FRACTIONS

7.2.2 ANALYSIS OF THE DISTILLATION FRACTIONS

7.2.3 PREPARATION OF THE DISTILLATION FRACTIONS SAMPLES AND GC-MS ANALYSIS

7.2.4 PREPARATION OF THE STANDARD SOLUTIONS

7.2.5 CALCULATION OF THE RESPONSE FACTOR AND DETERMINATION OF THE ANALYTES CONCENTRATION

7.2.6 DETERMINATION OF THE ALCOHOL BY VOLUME OF THE DISTILLATION FRACTIONS

7.3 DETERMINATION OF THE CHEMICAL PROFILE OF THE DISTILLATION FRACTIONS USED FOR ELECTRICITY PRODUCTION IN THE FUEL CELL TECHNOLOGY

7.3.1 DETERMINATION OF RELATIONSHIP OF VOLTAGE, CURRENT INTENSITY AND APPARENT POWER DURING DMFC EXPERIMENTS

7.4 GRAPE STALKS

7.4.1 PRETREATMENT OF THE GRAPE STALKS

7.4.2 ACETYLATION AND SILYLATION OF THE GRAPE STALKS POWDER

7.4.2.1 ACETYLATION

7.4.2.2 SILYLATION

7.4.3 TESTS FOR THE REALISATION OF BIO-COMPOSITES

7.5 ELECTROSTATIC SEPARATION OF GRAPE STALK POWDER

7.5.1 EXTRACTION TESTS ON GRAPE STALKS POWDER

7.5.2 HPLC DETERMINATION OF SUGARS AND FURANIC COMPOUNDS

7.5.3 COLOUR DETERMINATION

7.5.4 TOTAL PHENOLIC CONTENT

7.6 BIOCATALYTIC TREATMENT OF THE GRAPE STALKS POWDER

7.7 STATISTICAL ANALYSIS

8. RESULTS AND DISCUSSION

ABSTRACT

This Ph.D. project focused on the development of solutions for the valorisation of some minor by-products of the wine industry, such as grape stalks and distillation fractions.

Grape stalks are made of lignocellulose biomass formed by three different bio-polymers: cellulose, hemicellulose and lignin and represent a source of sugars, phenolic compounds, and fibre. Since lignocellulosic biomass is a very complex material, a fractionation of these components and the breaking of their interactions are necessary. The different pretreatment methods allow breaking down the lignocellulosic biomass into its fundamental units and increasing the accessibility for the subsequent treatments on these biopolymers. The grape stalks were subjected to drying, milling and electrostatic separation. The latter allowed to obtain nine fractions by triboelectric effect and these were treated by extraction with water and 2% sulphuric acid in order to obtain extracts for the HPLC analysis to search sugars and furans.

The aqueous/acid treatment led to the extraction of sugars and furans from the cleavage of lignocellulosic biomass. In aqueous extracts the concentrations of glucose and fructose are in the range of 9.4-13.5 g/100 g d.w. and 7.46-11.6 g/100 g d.w. respectively. In the acid extracts the concentration of xylose, deriving from the cleavage of hemicellulose, is in the range 8.26-17.53 g/100 g d.w., while those of furfural and HMF are 1996.19-260.24 mg/kg d.w. and 290.58-144.41 mg/kg d.w respectively.

In addition, a possible use of grape stalk powder as filler in bio-plastic formation was explored using polybutylene succinate as polymer. The specimens produced using 10% grape stalk powder such as, acetylated and silylated were characterized for their mechanical properties.

The obtained bio-composites were shown more rigid than the polymer with an increase of the Young's module passing from value of 623 MPa for the poly-butylene succinate to the 713 MPa of bio-composite with acetylated grape stalk powder.

Distillation process produces fractions containing high concentrations of ethanol and methanol. Their application in the fuel cell technology for the production of electricity was investigated. The fractions were first analyzed by gas chromatography coupled with mass spectrometry and after proper dilution used in experiments with direct methanol fuel cell.

The concentrations of ethanol and methanol were suitable for the experiments with direct methanol fuel cells. In particular the fractions of heads and tails from grape pomace showed the highest values of ethanol 74% and methanol 3.8%.

The results obtained are very interesting, even if the used cells used, suitable for the use of methanol gave lower performances when the fractions of distillation were used. This behaviour is due to the presence of ethanol and of the other volatile congeners.

The experiments carried out showed the possibility of enhancing the grape stalks as source of sugars and furanic compounds and as fillers for the production of bio-composite materials. The experimental tests carried out with the distillation fractions in direct methanol fuel cells represented a possible use for the valorisation of these bio-blends in fuel cell technology.

RIASSUNTO

Questo progetto di dottorato si è focalizzato sullo sviluppo di soluzioni per la valorizzazione di alcuni sottoprodotti dell'industria enologica, ancora poco considerati, come raspi d'uva e residui di distillazione. I raspi d'uva sono costituiti da biomassa lignocellulosica formata essemzialmente da tre biopolimeri (cellulosa, emicellulosa e lignina), i quali possono rappresentare una fonte di zuccheri, di composti fenolici e di fibra. Poiché la biomassa lignocellulosica è un materiale molto complesso, un frazionamento dei suoi componenti e la rottura delle loro interazioni sono necessarie. I differenti metodi di pre-trattamento permettono di rompere la biomassa lignocellulosica nelle sue componenti fondamentali e incrementare l'accessibilità per i successivi trattamenti sui biopolimeri.

I raspi d'uva sono stati sottoposti a essiccazione, macinazione e separazione elettrostatica. Quest'ultima ha permesso di ottenere nove frazioni per effetto triboelettrico e queste sono state trattate mediante estrazione con acqua/acido solforico diluito alla fine di ottenere estratti per l'analisi HPLC per la ricerca di zuccheri e furani.

Il trattamento acquoso / acido ha portato all'estrazione di zuccheri e furani dalla scissione della biomassa lignocellulosica. Negli estratti acquosi le concentrazioni di glucosio e fruttosio sono rispettivamente nell'intervallo di 9,4-13,5 g/100 g peso secco e 7,46-11,6 g/100 g peso secco. Negli estratti acidi la concentrazione di xilosio, derivante dalla scissione dell'emicellulosa, è nell'intervallo 8,26-17,53 g/100 g peso secco, mentre quelle di furfurale e HMF sono rispettivamente 1996,19-260,24 mg/kg peso secco e 290,58-144,41 mg/kg peso secco.

Inoltre un possibile uso della polvere di raspi d'uva come *filler* nella produzione di bio-plastica è stato esplorato mediante l'incorporazione nella misura del 10% a polibutilene succinato. I provini formati sono stati caratterizzati mediante test meccanici.

I bio-compositi ottenuti sono stati mostrati più rigidi del polimero con un aumento del modulo di Young passando dal valore di 623 MPa per il polimero poli-butilsuccinato a quello di 713 MPa per il bio-composito ottenuto dalla polvere di raspi acetilata.

Le frazioni di distillazione contengono alte concentrazioni di etanolo e metanolo e la loro applicazione nella tecnologia delle celle a combustibile per la produzione di elettricità è stata investigata. Le frazioni

sono state dapprima analizzate in gascromatografia accoppiata a spettrometria di massa e successivamente usate, previa diluizione, negli esperimenti con cella a combustibile a metanolo diretto. Le concentrazioni di etanolo e metanolo si sono dimostrate adatte per gli esperimenti con celle a combustibile a metanolo diretto. In particolare, la frazioni di testa e coda derivante dalle vinacce ha mostrato i valori più alti di etanolo 74% e metanolo 3,8%.

I risultati ottenuti sono molto interessanti, anche se le celle utilizzate, adatte all'impiego di metanolo hanno dato prestazioni inferiori usando le frazioni della distillazione ricche soprattutto di etanolo e di altre sostanze volatili.

Gli esperimenti condotti hanno mostrato la possibilità di valorizzare i raspi d'uva come fonte di zuccheri e composti furanici e come rinforzanti meccanici per la produzione di materiali bio-compositi. I test sperimentali condotti con le frazioni di distillazione in celle a combustibile a metanolo diretto hanno rappresentato un possibile uso per la valorizzazione di queste bio-miscele nella tecnologia delle celle a combustibile.

INTRODUCTION

1. CIRCULAR VS LINEAR ECONOMY

1.1 ACTIVITIES OF THE FOOD INDUSTRY AND GENERATION OF BY-PRODUCTS

The growing demographic increase of the world population and the continuous development of consumption have led to an expansion of industrial activities for the production of consumer goods and in particular those of the food industry (Maina et al., 2017; Ghisellini et al., 2016). In the various raw material transformation processes of the food industry there is a strong production of by-products also called as food waste. Unlike common waste, by-products can be used as secondary raw materials for the generation of new products or to feed subsequent production cycles. This is extremely important to make industrial activities energetically independent and eco-compatible. A study published by the European Union and dating back to 2010 showed that 90 million tons of food wastes are produced every year by food industry processing activities (Ravindran et al., 2016; Monier et al., 2010). This poses environmental problems relating to the disposal and management of food waste. The approach of converting waste from the food industry or any other waste into high-value added products and turning waste into by-products easily usable in various production cycles is called circular economy and in this case of circular economy applied to food industry. Food supply chain waste is therefore an important resource with great potential to create products with high added value such as bio-plastics, biopolymers, bio-fuels and bio-molecules (fig. 1) obtainable through extraction procedures (Ravindran et al., 2016).

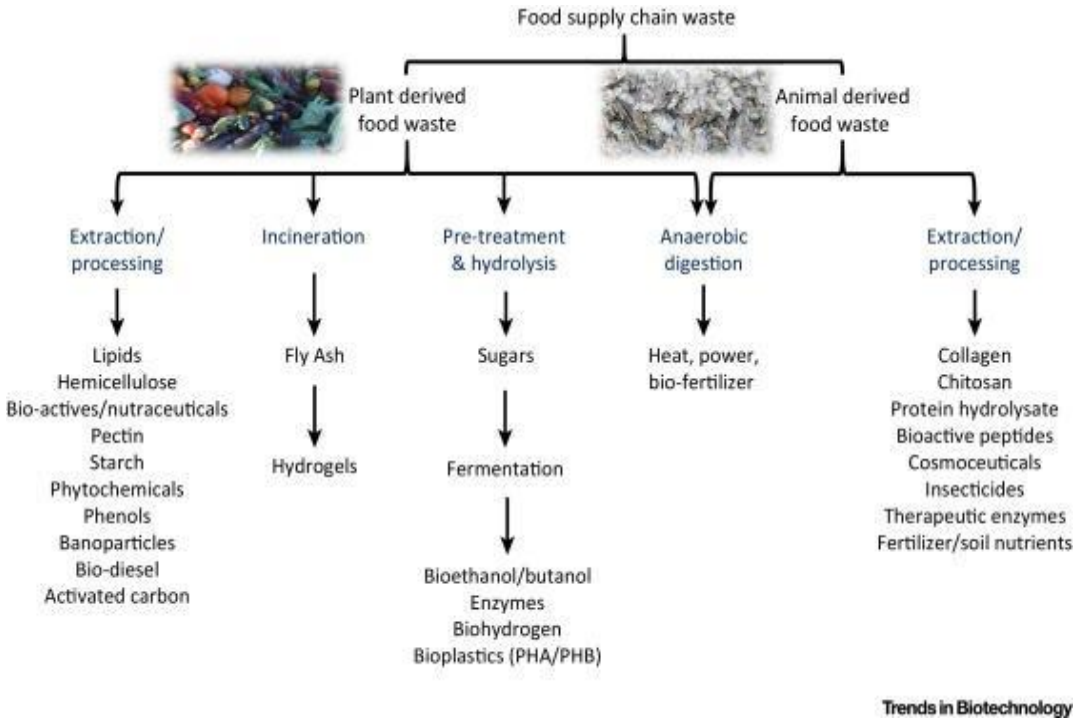

Figure 1: Possible uses of food supply chain waste (Ravindran et al., 2016)

1.2 IMPORTANCE OF RECOVERY AND RECYCLING OF BY-PRODUCTS IN FOOD INDUSTRY

The excessive generation of waste deriving from the activities of linear economy of production, consumption and throwing is one of major socio-economic challenges on a global level to avoid their accumulation and reduce environmental pollution. Food waste can be divided into two categories: **municipal solid waste** (**OMSW**) and **food supply chain waste** (**FSCW**). Municipal solid waste is that produced in cities and sub-urban centres and the overall annual rate of such waste is 1.3 billion tons and it is estimated that could rise to 2.2 billion in 2025 (Maina et al., 2017). The food supply chain waste is generated by the life cycle of the different production processes of the food industry from the production of raw materials to the phases of food processing industry and of the distribution chains (Gustavsson et al., 2011). In fact, various product losses have been documented both in the production phases of the raw material and in the food manufacturing processes. It is estimated that in the European Union the annual amount of food supply chain waste is around 90 million tons every year and that it can increase to 126 million tons in 2020 (Maina et al., 2017). Because of these significant quantities of both municipal solid organic waste and food supply chain waste and their environmental impacts, the European Union has provided various guidelines for sustainable waste management. For these reasons in the food industry it is very important to adopt circular economy approaches, which include

regenerative methods of by-products to convert them into secondary raw materials for the realisation of new products with high added value. The regeneration and reuse of these secondary raw materials for bio-based chemical and polymer production allows obtaining the following advantages (Ellen MacArthur Foundation):

- use and implementation of innovative by-product recycling technologies and investments in research and innovation;
- greater competitiveness in terms of management, production and research for companies, which use regenerative approaches to the circular economy aimed at reaching the titles of zero waste companies;
- creation of new job opportunities and professional figures;
- reduction of raw material of fossil origin and autonomy from the point of view energy and production;
- possibility of processing a large variety of by-products that are part of food supply chain to obtain numerous high added value products;
- best cost savings;
- better resource management and efficiency;
- improvement of environmental performance with the development of eco-friendly production models;
- creation of inclusive development models;
- development of innovative bio-based industries and new market fields for bio-based products.

The importance of waste recycling is therefore now used as a fundamental requirement for assessing environmental impact for all industrial activities, including the food industry, which must reach the objective of zero waste to become eco-compatible and eco-functional. In the environmental impact assessment pyramid (fig. 2) we see how these decreases passing from disposal to re-use, recycling and processing of by-products to reach the zero waste stage. The objective is therefore to develop more and more environmentally techniques to obtain products free of waste.

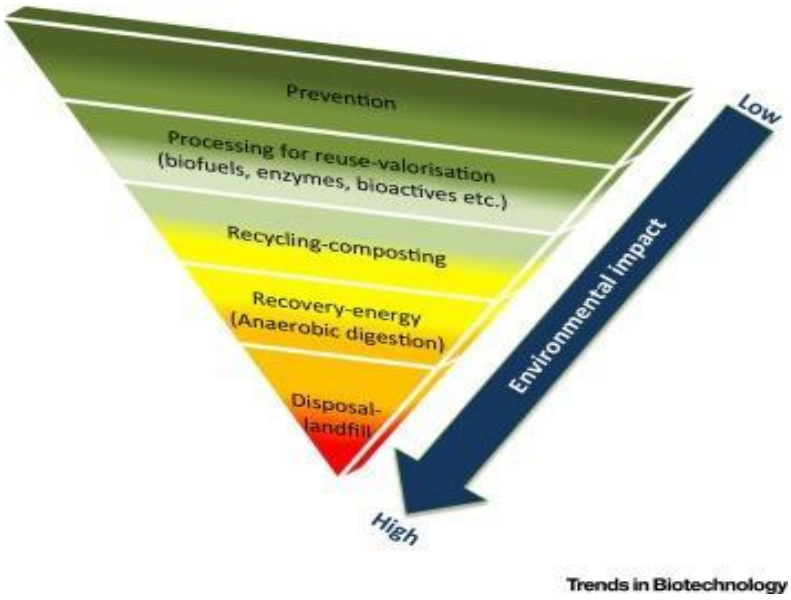

Figure 2: Environmental pyramid assessment impact (Lin et al., 2013)

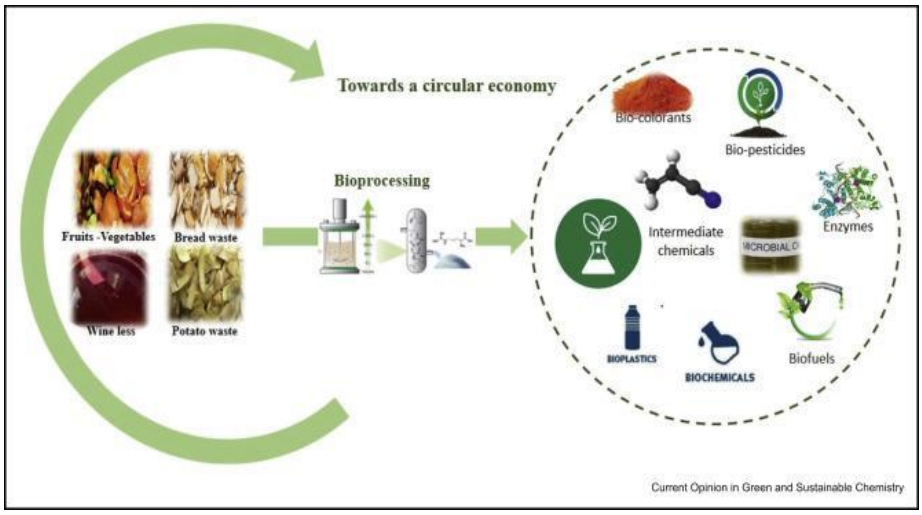

Figure 3: Bio-processing applied to food supply chain waste to obtain high value added products (Maina et al., 2017)

1.3 BIO-REFINERIES AND CIRCULAR BIO-ECONOMY

Bio-refineries are industrial platforms based on the use of waste biological resources to obtain a wide range of products such as bio-fuels, energy and fine chemicals and the recycling and re-use approach of waste biological resources, mainly biomass resources, is called **circular bio-economy (**Philp, 2017). The bio-refineries therefore represent the motor performers of circular bio-economy (Philp, 2017) and are based on four fundamental principles (fig. 4) (Escamilla Alvarado et al., 2017):

- principle of cascading;
- principle of sustainability;

- principle of non-conflict with food;
- principle of neutral carbon footprint.

The principle of cascading concerns the obtaining of a series of products from biomass starting from a network and cascade of processes. The principles of sustainability and non-conflict with food are very important and underline the fact that these processes use renewable raw materials and coming from agro-industrial by-products not in conflict with the food chain. The principle of the neutral carbon footprint is based on the fact that the carbon dioxide emitted goes to feed the growth of new biological material such as lingo-cellulosic biomass with the closing the of the cycle. These principles are interconnected and linked to that of sustainability (Escamilla Alvarado et al., 2017).

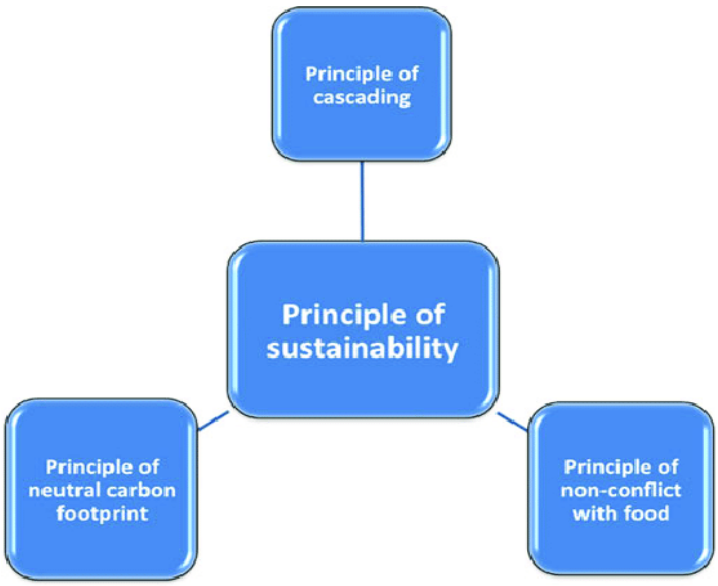

Figure 4: Principles used in the bio-refineries (Escamilla Alvarado et al., 2017)

The International Energy Agency has defined the bio-refinery as the sustainable processing of biomass to obtain a wide range of products such as bio-materials, chemicals and energy (bio-fuels, heat). The bio-refinery, in the circular approach uses all the components of biomass and from the processing of these it is able to obtain products with high added value (Manan et al., 2017). The circular bio-economy, through bio-refineries, has a dual function. On the one hand creates value for the sustainable use of biomass and on the other hand it produces a great variety of bio-based products such as bio-materials, bio-plastics, chemicals and bio-energy allowing them to embrace more production chains (de Jong et al., 2015).

1.4 CIRCULAR BIO-ECONOMY APPLIED TO THE WINE INDUSTRY

Among the activities of the food industry, the winemaking process generates a great variety of by-products that can be used in many fields (Lucarini et al., 2018). For example, grape seeds and pomace

represent the portion of winemaking waste with the highest concentration of bioactive compounds. Many studies have shown how grape seeds constitute the part of the fruit with the highest antioxidant activity followed by the skins and the pulp (Pastrana Bonilla et al., 2003). Grape seeds can therefore be used for the extraction of bioactive compounds and for having extracts, which can be used for cosmetic, nutraceutical and pharmaceutical purposes.

The disposal of the by-products of the wine industry produces environmental impacts, which can be determined by calculating the **carbon footprint** through the **LCA** (life Cycle Assessment) method. For example, according to some data deriving from the calculation of the carbon footprint of winemaking, the equivalent CO_2 emissions in 2016 were 834,300 tons for grape pomace and 185,400 for stems (Bevilacqua et al., 2017). The environmental impacts of the by-products of winemaking can be reduced by using these as secondary raw materials to be used in several production chains, thus avoiding disposal. In this way, it is also possible to apply a circular bio-economy approach to the wine industry (fig. 5).

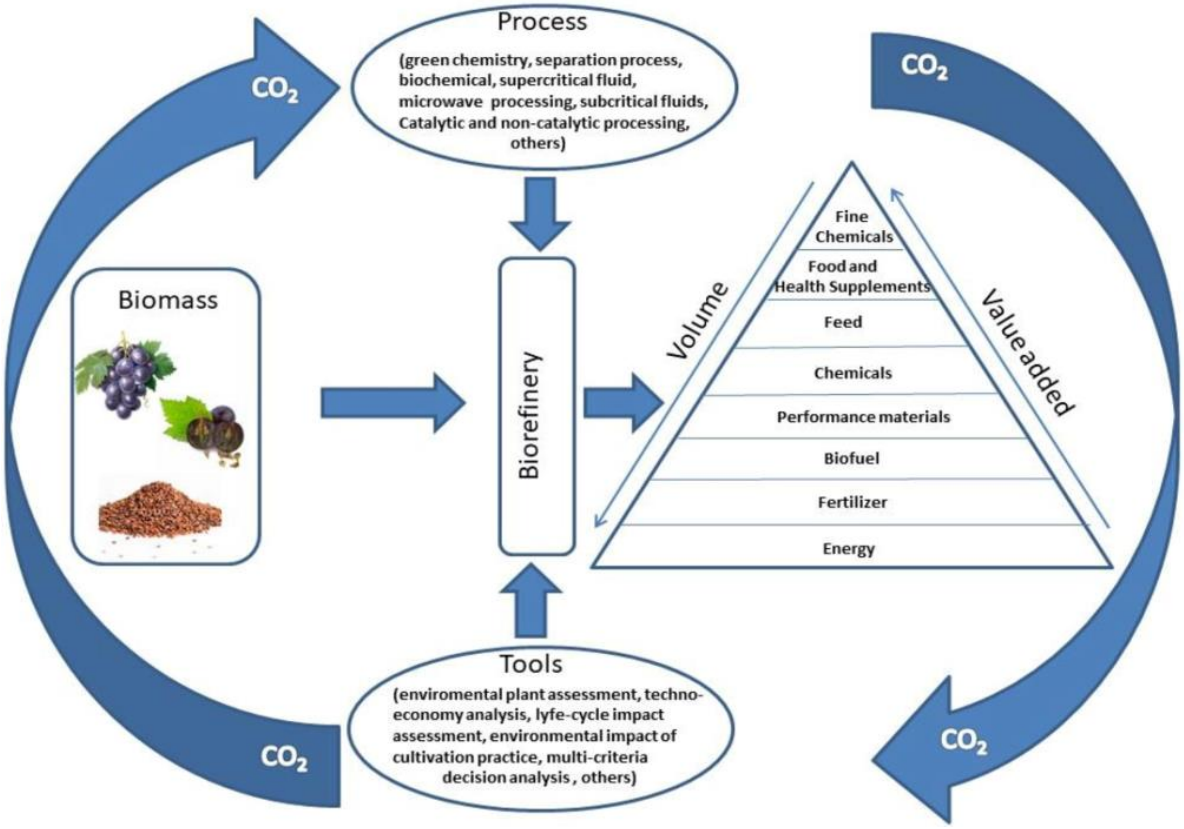

Figure 5: Circular Bio-Economy approach applied to the wine industry by-products (Lucarini et al., 2018)

From the point of view of the circular bio-economy approach applied to the wine industry, much importance has been given, as previously mentioned, to seeds and grape pomace due to high concentration of phenolic compounds (quercetin, kaempferol, monomeric flavan-3-ols, catechin, epicatechin and procyanidin dimers and trimers) with antioxidant activity. Many studies have indeed confirmed the beneficial effect on human health of seed and grape pomace extracts related to chemopreventive activity against different types of cancer and cardiovascular diseases. For the extraction of these compounds, methodologies are used such as extraction in the supercritical phase using CO_2 and ultrasounds. These techniques allow an increase in the number of extractable bioactive compounds and allow their stability (Lucarini et al., 2018). Microfiltration and nanofiltration techniques (fig. 6) have been recently used for the purification of bioactive compounds from aqueous or hydro-alcoholic extract of grape pomace. With regard to this we have an example of a bio-refinery, based on the recovery of bioactive compounds from the by-products of winemaking and located in Tuscany, which uses nanofiltration (Lucarini et al., 2018). The extraction of the compounds takes place through aqueous solvents and hydro-alcoholic mixtures and following this process there are various filtration steps. This allows avoiding the use of solvents in the purification and concentration phases by means of membrane technology and using filters of suitable diameter. Microfiltration produces a concentrate rich in colloidal matter, ultra-filtration a concentrate rich in polysaccharides and a nanofiltration a concentrate rich in polyphenolic compounds (Giacobbo et al., 2017).

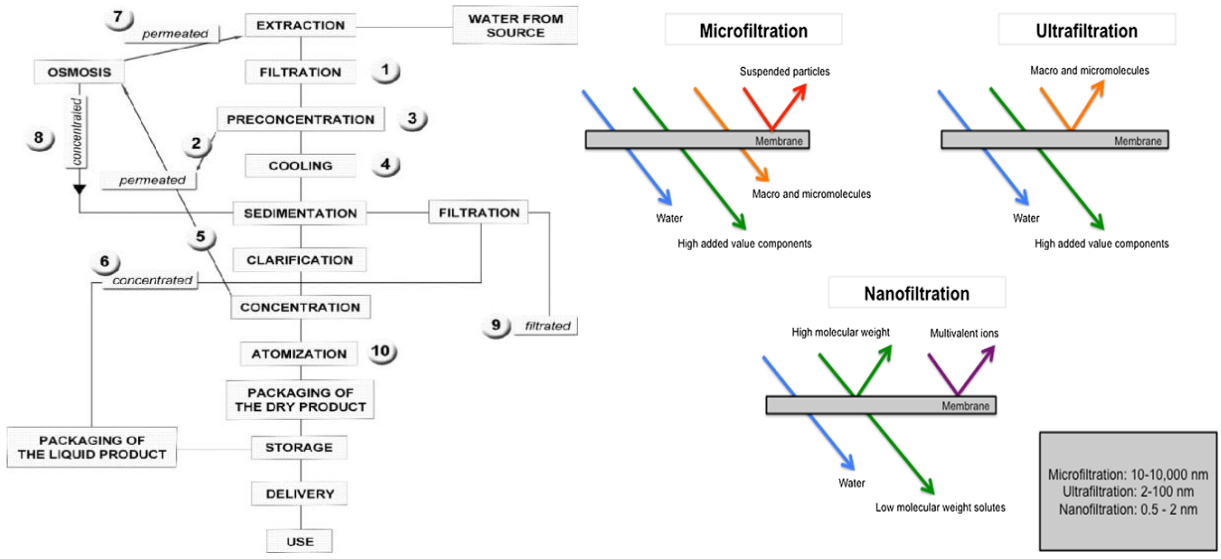

Figure 6: Diagram for extraction and purification for grape pomace (Lucarini et al., 2018) and steps of filtration

2. LIGNOCELLULOSIC BIOMASS

2.1 STRUCTURE OF LIGNOCELLULOSIC BIOMASS

Lignocellulosic biomass is a renewable and complex raw material composed of three biopolymers: cellulose, hemicellulose and lignin. It can be obtained from agro-industrial by-products, wood residues and organic waste (Brandt et al., 2013). Cellulose, hemicellulose and lignin represent the structural components of the lignocellulose cell wall fig. 7 and 8). The cellulose is composed of glucose units linked together by β-1, 4-glycosidic bonds. hemicellulose is a complex polymer consisting of pentoses such as xylose and arabinose, hexoses such as glucose, mannose and galactose and sugar acids (glucuronic and galacturonic acids) (Schutyser et al., 2018). The last structural component is lignin and it is formed by units of phenylpropanoids bound together by ether and carbon-carbon linkages (Madadi et al., 2017). In addition, lignin is covalently linked, through the ferulic acid units, to the hemicellulose with ester bonds (Brandt et al., 2013; Li et al., 2017).

In this complex structure lignin and hemicellulose cover the surface of cellulose, making it difficult to separate and use it.

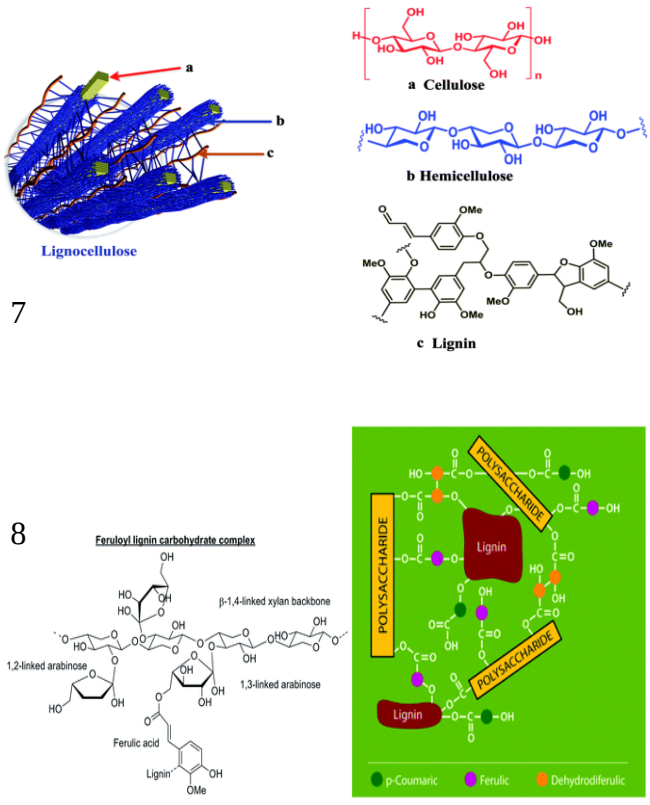

Figure 7 and 8: Structure of lignocellulosic biomass and linkages between lignin and hemicellulose (Brandt et al., 2013)

2.2 LIGNIN STRUCTURE

2.2.1 LIGNIN POLYMER STRUCTURE

After cellulose, lignin is the second most naturally occurring biopolymer. It is particularly present in the secondary walls of plant cells and gives biomass resistance to the chemical and biological degradation. This makes it insoluble in aqueous environment avoiding the entry of chemical and biological degrading agents.

In the walls of plants lignin forms the macromolecular complex with the carbohydrate components of hemicellulose called glycol-lignin, which improve the resistance of plant structures (Brandt et al., 2013).

Lignin is a heterogeneous polymer and has a complex macromolecular structure composed of phenylpropanoid monomers called monolignols (fig. 9). The monolignols present in lignin are: monolignol guaiacyl with one hydroxyl and one methoxyl group (G unit), monolignol syringyl with two methoxyl groups and one hydroxyl group (S unit) and monolignol 4-hydroxyphenyl (H unit). These are derived from the coniferyl, sinapyl and coumaryl alcohols respectively (Vanholme et al., 2010).

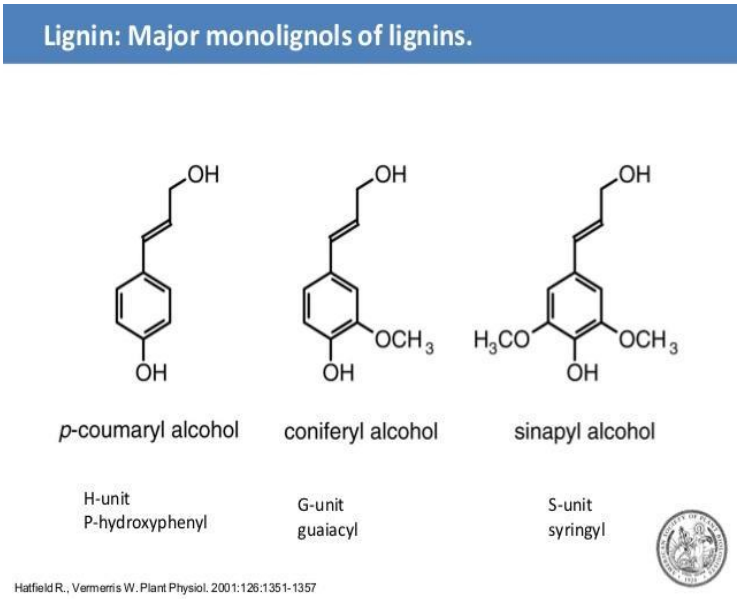

Figure 9: The major monolignols in lignin structure (Hatfield et al., 2001)

2.2.2 BIOSYNTHESIS OF LIGNIN

The monolignols are aromatic alcohols and are synthesised in the cytoplasm of the plant cell. Then these monomeric precursors are exposed near the cell wall where their polymerisation, through ether and C-C bonds, takes place. Finally, they are integrated into the plant cell wall as structural subunits of lignin (Vanholme et al., 2010). The monolignol precursors are derived from the phenylalanine and tyrosine amino-acids (Rinaldi et al., 2015) through a series of enzymatic reactions (fig. 10) catalysed by the following principal enzymes (Vanholme et al., 2010; Buiyan et al., 2008):

- phenylalanine ammonia-lyase (PAL) catalyzes the formation of cinnamic acid from the phenylalanine amino-acid;
- tyrosine ammonia-lyase (TAL) catalyzes the formation of *p*-coumaric acid from the tyrosine amino-acid;
- cinnamate 4-hydroxylase (C4H) converts the cinnamic acid into the *p*-coumaric acid;
- 4-coumarate- Coenzyme A ligase (4CL) converts the p-coumaric acid into the *p*-coumaroyl-Coa;
- cinnamoyl-Coa reductase (CCR) causes the conversion of the *p*-coumaroyl-Coa into the *p*-coumaryl aldehyde;
- cinnamyl alcohol dehydrogenase (CAH) catalyzes the formation of the monolignol *p*-coumaryl alcohol (H unit *p*-hydroxyphenyl of lignin structure) from the reduction of the *p*-coumaryl aldehyde;
- *p*-coumarate-3-hydroxylase (C3H) converts the p-coumaric acid into the caffeic acid;
- catechol-*O*-methyltransferase (COMT) causes the conversion of the ferulic acid from the caffeic acid;
- 4-coumarate-Coenzyme A ligase (4CL) converts the ferulic acid into the feruloyl-Coa;
- cinnamoyl-Coa reductase (CCR) catalyzes the formation of the coniferaldehyde;
- cinnamyl alcohol dehydrogenase (CAH) causes the conversion of the coniferaldehyde into the coniferyl alcohol (G unit guaiacyl of lignin structure);
- ferulate 5-hydroxylase (F5H) converts the coniferaldehyde and the coniferyl alcohol into the 5-hydroxy coniferaldehyde and 5-hydroxy coniferyl alcohol respectively;
- catechol-*O*-methyltransferase (COMT) causes the formation of the sinapaldehyde and sinapyl alcohol (S unit syringyl of lignin structure) from the 5-hydroxy coniferaldehyde and 5-hydroxy coniferyl alcohol respectively.

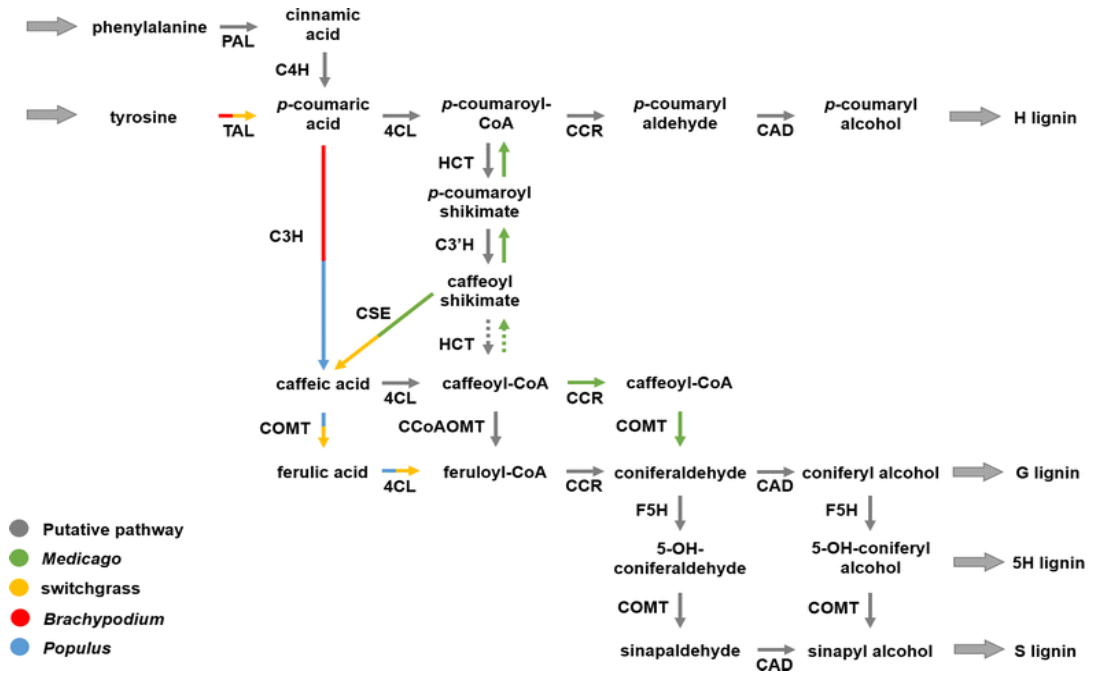

Figure 10: Enzymes involved in the biosynthetic pathways of lignin (Faraji et al., 2018)

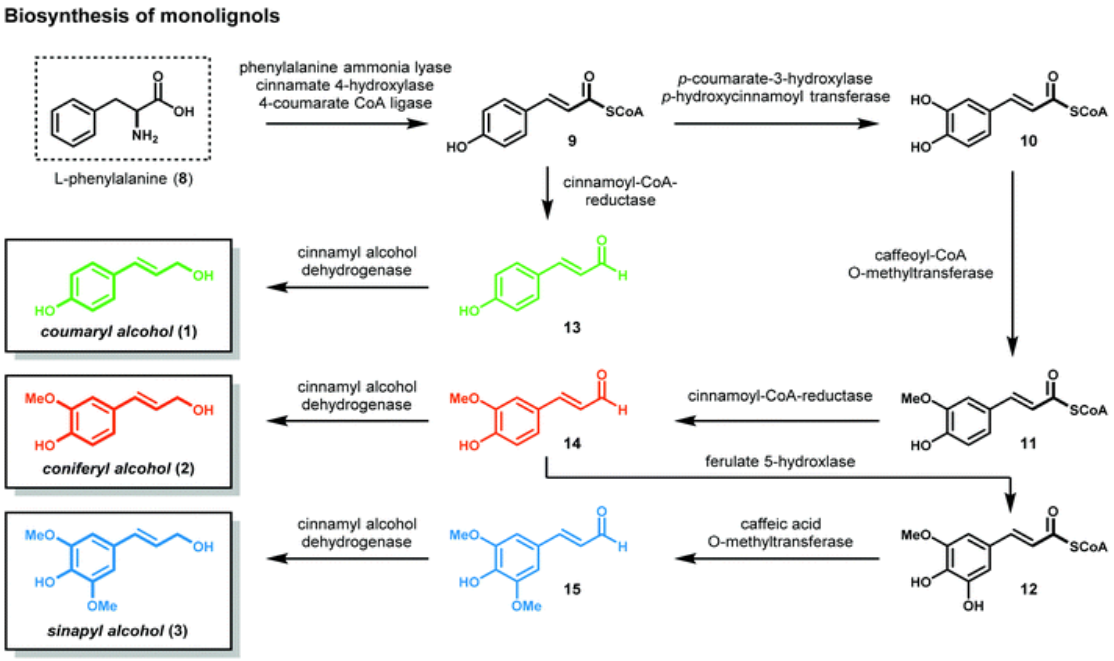

Figure 11: Mechanism of biosynthesis of monolignols (Karkas at al., 2016)

Once the monolignols have been synthesised they are transported out of the cytoplasm by the specific protein carriers (ABC protein) (Miao et al., 2010) and are subjected near plant cell wall (fig. 13) to an oxidative polymerisation (Karkas et al, 2016) process by the peroxidase enzymes and laccases with the formation of ether and C-C bonds (Vanholme et al., 2010). This is the radical polymerisation process

with the formation of phenoxy radical species from the monolignols coumaryl, coniferyl and sinapyl alcohols. The resulting radical compounds give rise to the coupling reactions radical-radical or a combinatorial radical reaction with the formation of the reactive quinone intermediates, consisting of several aromatic rings (Rinaldi et al., 2015). Subsequently these intermediates give rise to inter-molecular nucleophilic substitutions, coupling reactions with other monolignol radicals and intra-molecular cyclisations (fig. 12) to form the first substructures of the lignin polymer (Vanholme et al., 2010; Karkas et al., 2015); the substructures, which are formed from the first coupling reactions involving the cinnamyl compounds are dihydrobenzofuran or phenylcoumaran, β-β linkages in the resinol structure and β-O-4 linkages. The radical compounds involved in the oxidative coupling reactions are formed by the action of the various oxidoreductases called peroxidases. These are manganese-peroxidase (MnP), lignin-peroxidase (LiP) and versatile peroxidase (VP). Hydrogen peroxide required by peroxidases is produced by various enzymes as superoxide dismutase and aryl-alcohol oxidase. The substructures then are integrated in the plant cell wall where they will form the lignin complex structure.

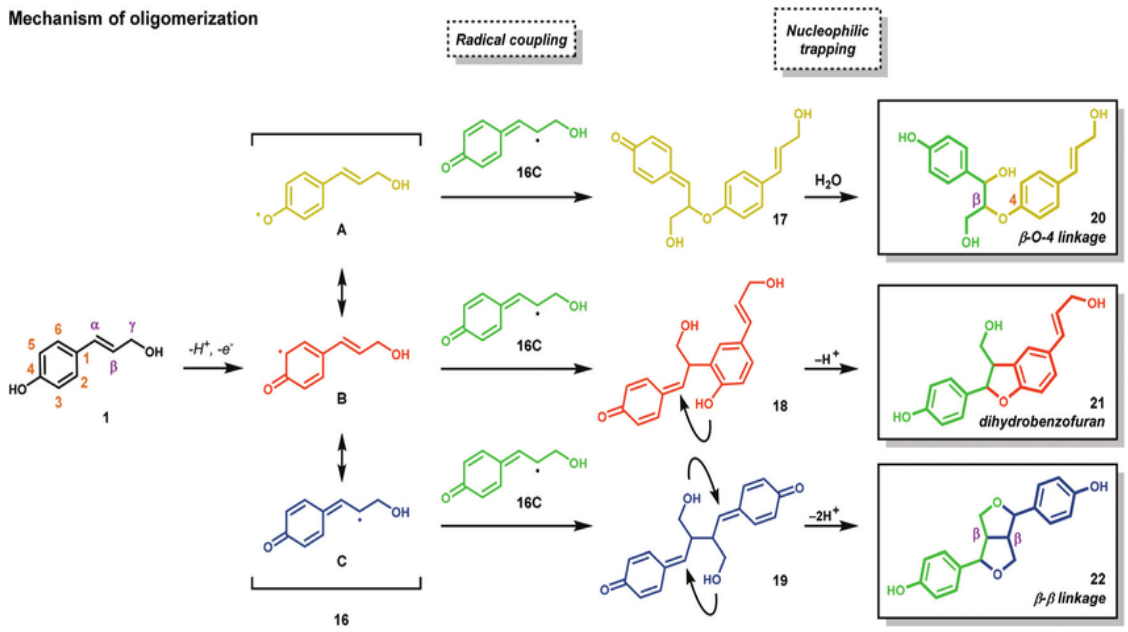

Figure 12: Mechanism of radical coupling and oxidative polymerisation in the lignin biosynthesis (Karkas et al., 2015)

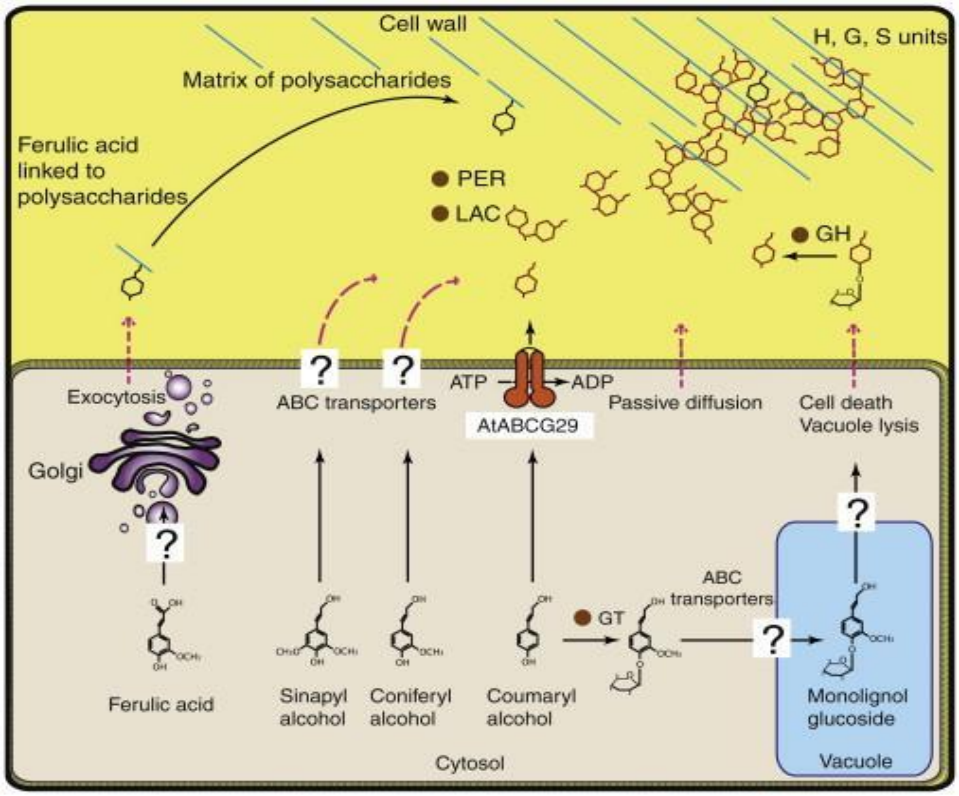

Figure 13: Mechanism of the cellular transport of the monolignols for the biosynthesis of lignin (Sibout et al., 2012).

The guaiacyl-, syringyl-, and hydroxyphenyl units are covalently linked with ether, ester and carbon-carbon bonds such as:

- β-aryl ether or β-*O*-4 bonds;
- α-aryl ether bonds or α-*O*-4 bonds;
- β-5' bonds;
- biphenyl bonds (5-5);
- diphenyl ether bonds (4-*O*-5);
- β-1 ether bonds;
- β-β aliphatic bonds.

In this way, sub-structures are created within the lignin structure. These consist of alkyl-aryl ethers, phenylcoumarans, resinols, dibenzodioxocins, biphenyls, diphenyl ethers, diarylpropanes, cinnamyl alcohols and *p*-hydroxybenzoates (fig. 14).

Other substructures are those created between lignin and hemicellulose by ester bonds.

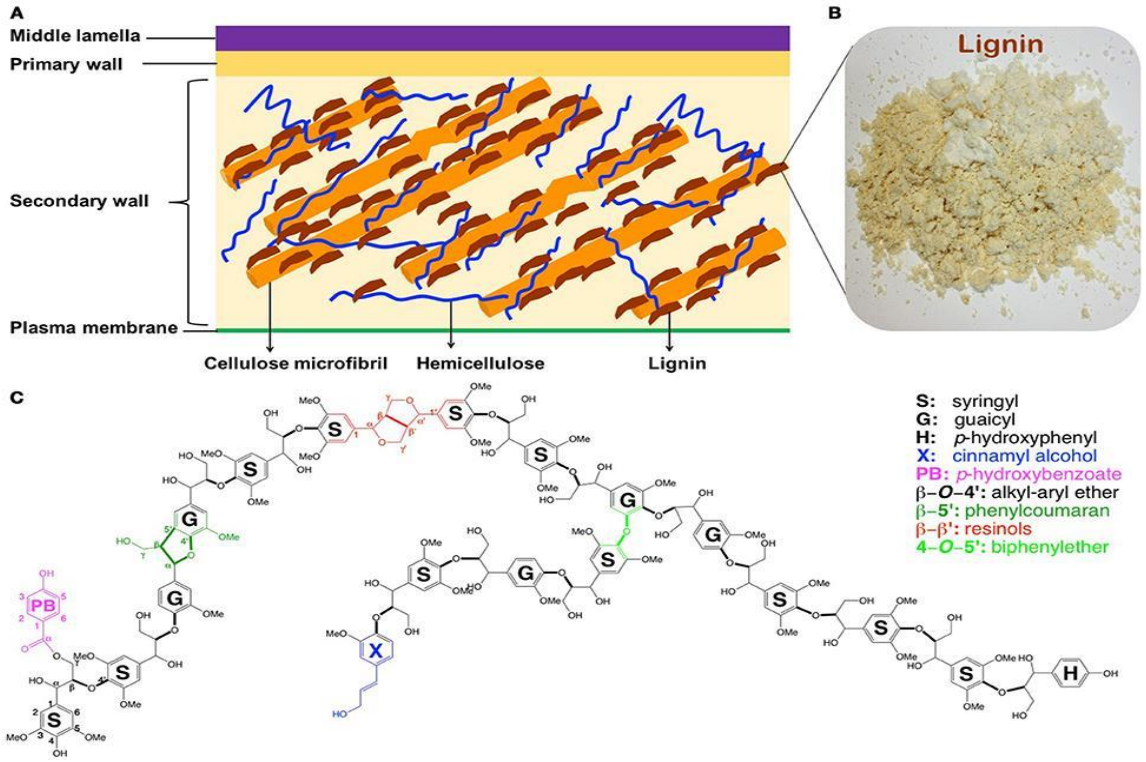

Figure 14: Lignin structure (Li et al., 2016)

2.2.3 POSSIBLE USES OF LIGNIN

Lignin is a versatile material for several applications in the bio-based industries and is an important resource of aromatic compounds. One of these concerns the splitting of lignin structure to obtain aromatic building blocks for fine chemistry such as vanillin, vanillic acid and eugenol (Fache et al., 2015). Today the potential of lignin as a resource of valuable aromatic compounds to produce biopolymers and for use in organic chemistry is largely unexploited (Sun et al., 2018).

Phenolic compounds and phenolic acids, which make up lignin, can be obtained from lignocellulosic biomass and from other agro-industrial by-products through the depolymerisation of lignin. These compounds can be used as such as building blocks for fine and pharmaceutical chemistry (fig. 15) or can be subjected to functionalisation to obtain a great variety of derivatives (fig. 16). The functionalisation can be chemical or enzymatic type and through it can be obtained compounds, which could find application in the chemical industry as intermediates for the synthesis of aromatic polymers (Delidvich et al., 2015; Upton et al., 2015) and bioactive compounds for pharmaceutical and cosmetic use (Sun et al., 2018).

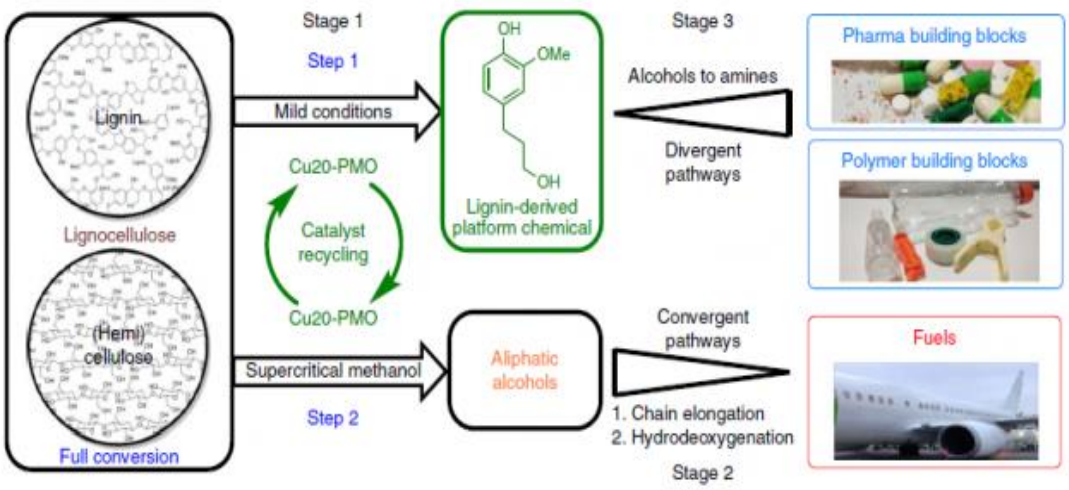

Figure 15: Conversion of lignocellulose into value-added chemicals (Sun et al., 2018)

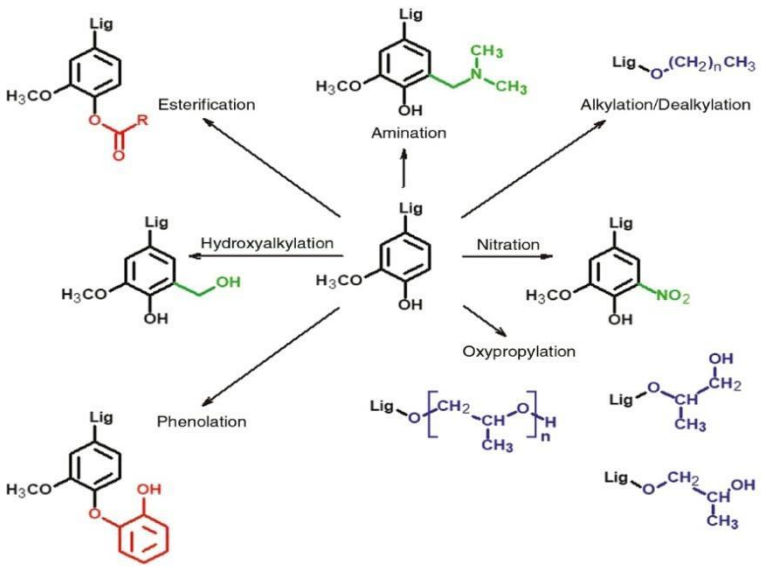

Figure 16: Introduction of functional groups (strategy of functionalisation) into aromatic compounds of lignin (Mimini et al., 2018)

2.3 STRUCTURE OF CELLULOSE AND HEMICELLULOSE IN LIGNOCELLULOSIC BIOMASS

2.3.1 STRUCTURE OF CELLULOSE AND HEMICELLULOSE

Cellulose is a linear polymer formed by glucose units linked together by β-1,4-glycosidic bonds and its content in the lignocellulosic biomass varies between 35 and 50% wt. The β configuration at anomeric carbon provides a conformation characterised by the presence of a network of intra and inter-molecular hydrogen bonds between the various polymer chains (fig. 17) (Coseri, 2017). This conformation also

allows the stabilisation of cellulose into crystalline fibrils (Brandt et al., 2013). Furthermore, the dense network of hydrogen bonds and Van Der Waals interactions between the various planes of the polymer chains are responsible for its insolubility in water and related solvents.

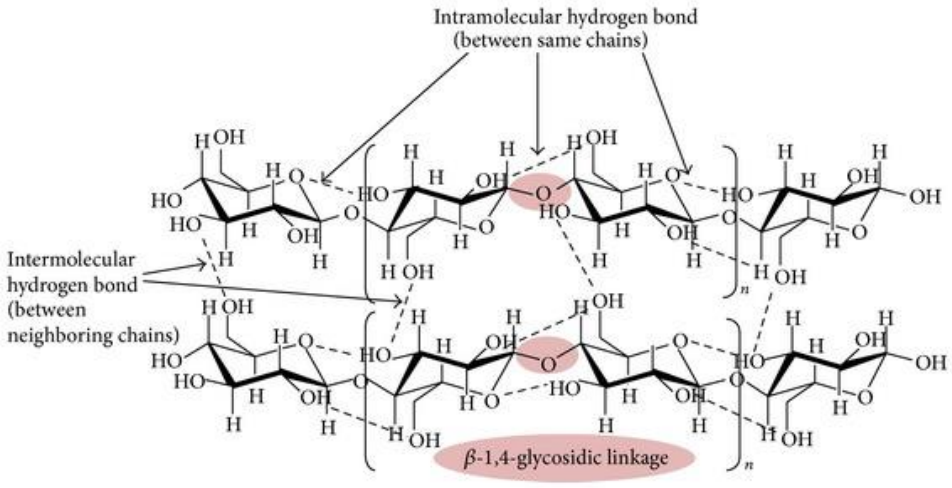

Figure 17: Structure of cellulose with intra-molecular and inter-molecular hydrogen bonds (Lee et al., 2014)

Hemicellulose is the second polysaccharide component of biomass and constitutes 25% of it. Unlike cellulose, it has a lower average molecular weight and a lower degree of polymerisation and is composed of pentose sugars (fig. 18) such as xylose and arabinose and hexose as glucose and mannose (Lee et al., 2014; Marriot et al., 2016). Furthermore, various functional groups can be linked in the hemicellulose chains such as acetyl, methyl, glucuronic and galacturonic acids and lignin phenolic acids (Brandt et al., 2013; Scheller et al., 2010). The hemicellulose is therefore characterised by a lower crystallinity than cellulose and is therefore more sensitive to depolymerisation. The hemicellulose covers the surface of the cellulose through non-covalent bonds and is combined with lignin (fig. 19) with the formation of the lignin-carbohydrate complexes involving ferulic and p-coumaric acids (Brandt et al., 2013; Scheller et al., 2010).

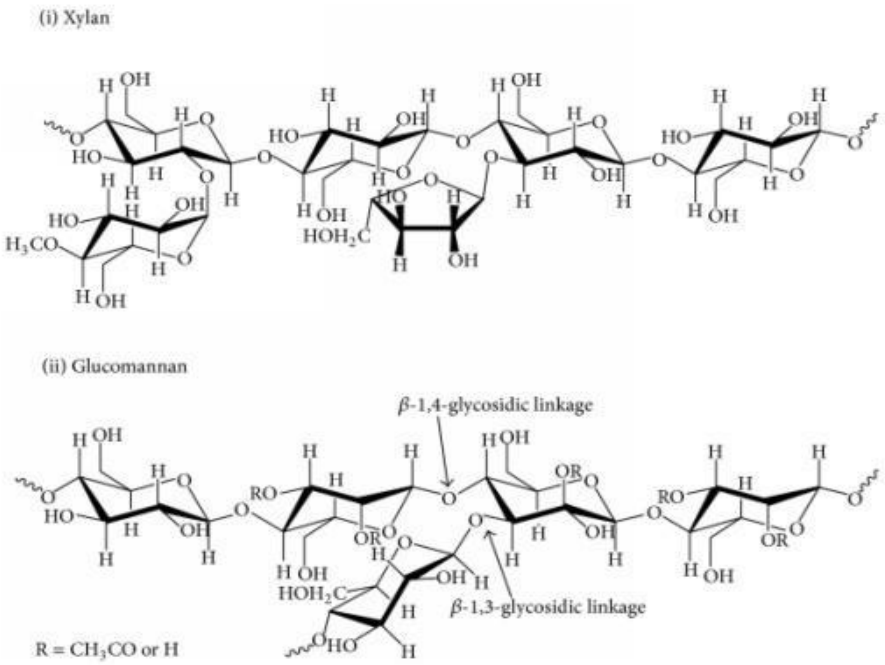

Figure 18: Structure of hemicellulose (Lee et al., 2014)

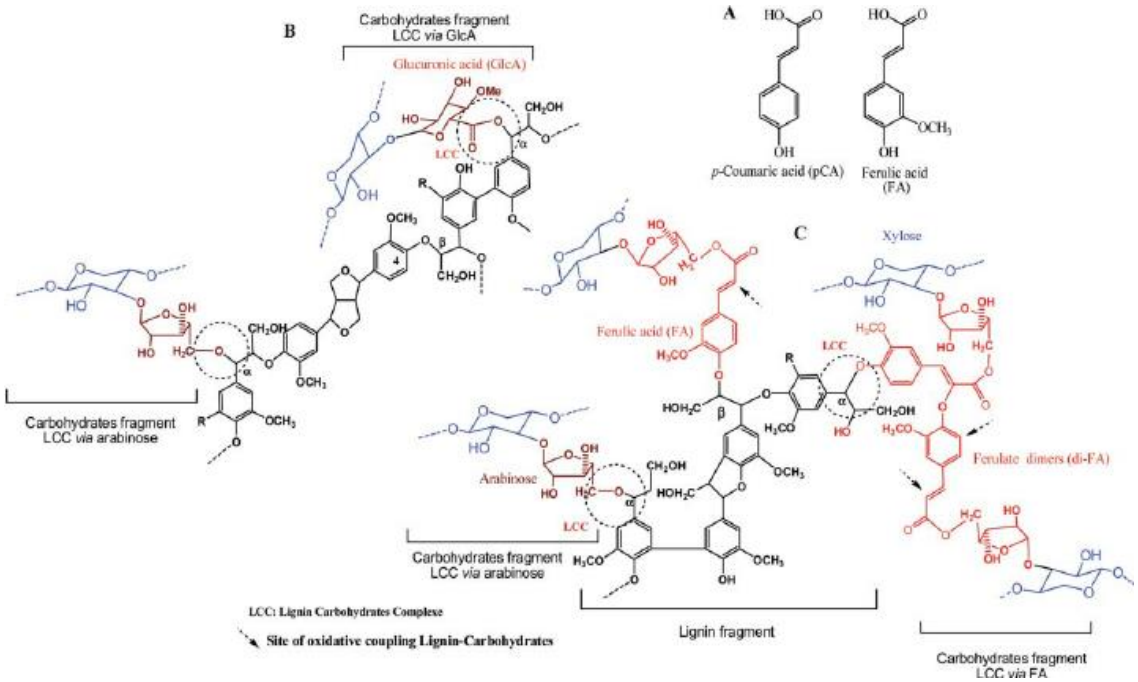

Figure 19: Structure of lignin-carbohydrate complex (Monlau et al., 2013)

2.3.2 POSSIBLE USES OF SUGARS OBTAINABLE FROM CELLULOSE AND HEMICELLULOSE

Hydrolysis of the cellulose and hemicellulose polysaccharides of biomass can lead to the release of monosaccharides mainly glucose and xylose. These can be used in microbial fermentations to obtain chemical products with high added value. One of this is bio-ethanol and it plays a very important role as a bio-fuel and in the bio-based industry (fig. 20) as a platform chemical for the synthesis of various and important chemical intermediates (Isikgor et al., 2015).

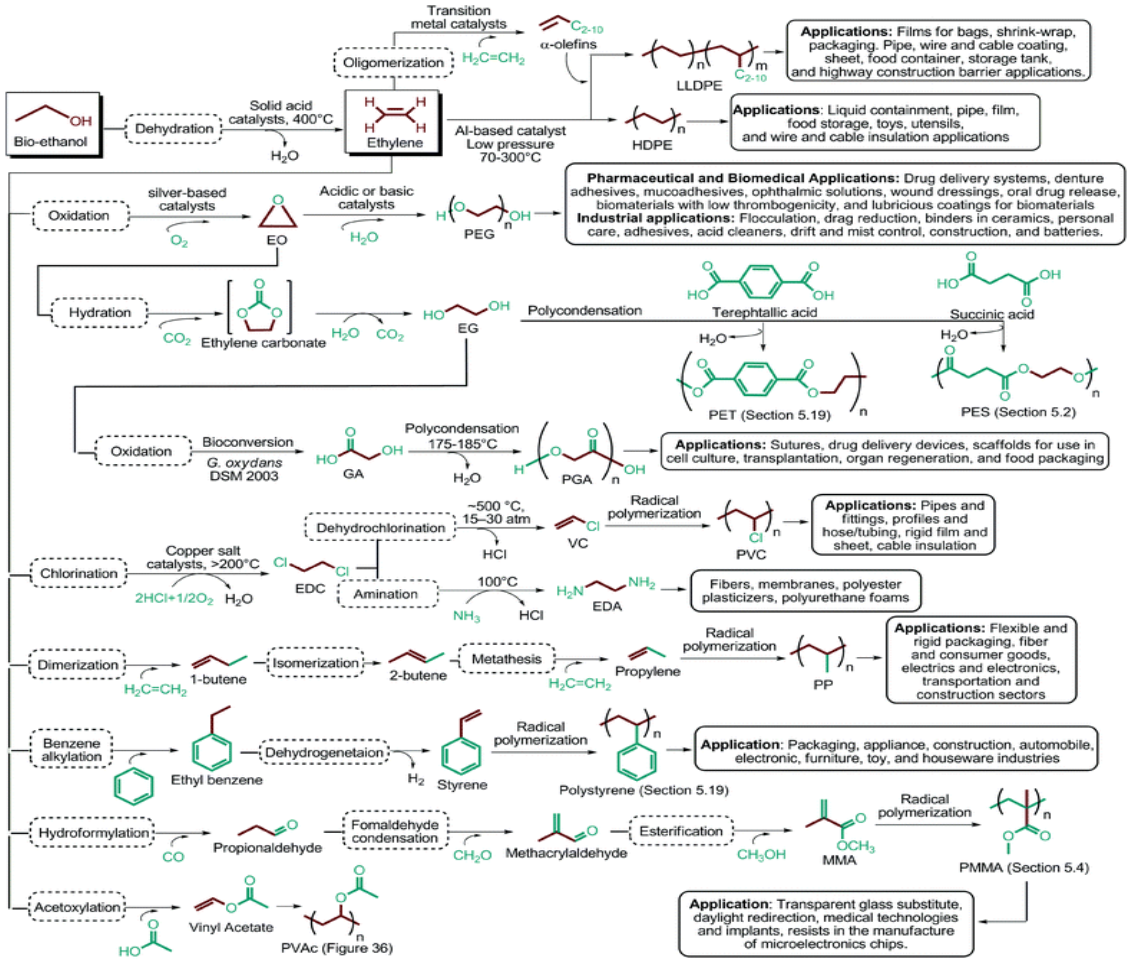

Figure 20: Bio-ethanol platform for the synthesis of monomers and related polymers (Isikigor et al., 2015)

Bio-ethanol is produced by fermentation from biomass using glucose. This can be achieved by fractionation of complex polysaccharides such as starch and cellulose, which are first subjected to a pretreatment process to obtain glucose (Rose at al., 2011). In the case of starch we have processes of liquefaction and saccharification in which glucose monomers are obtained with the addition of

enzymes. However, bio-ethanol can also be obtained from agro-industrial waste matrices that are not in competition with food production such as algae, agricultural and forestry residues.

Bio-ethanol turns out to be the key compound for the synthesis of ethylene in turn usable for the synthesis of a wide range of polymers of the chemical industry such as polyethylene, poly-(vinyl chloride), polystyrene and poly-(ethylene terephthalate) (de Jong et al., 2012). Moreover, the bio-ethylene is convertible into ethylene oxide, which in turn by means acid or basic catalysis can be used to obtain polyethylene glycol (PEG). This polymer has low toxicity and high solubility and it is widely used in pharmaceutical, biomedical and cosmetic sectors. Ethylene oxide is also an important intermediate for the synthesis of glycolic acid, starting from the oxidation of ethylene glycol obtained from the hydration of ethylene oxide. Glycolic acid provides poly-glycolic acid by polymerisation. Poly-glycolic acid is widely used together with poly-lactic acid in pharmaceutical and biomedical fields (Isikigor et al., 2015).

Another compound obtainable from the microbial fermentation of glucose is lactic acid, which can be used to make bio-plastics (fig. 21) based on its polymer, poly-lactic acid (Pleissner et al., 2016). Lactic acid is mostly used in the chemical industry of bio-plastics and as well as an additive in the cosmetic and food sectors (Diaz et al., 2018). Esterification of lactic acid with alcohols, principally with ethanol, leads to the formation of lactic acid esters (lactates), very promising as green and bio-based solvents in the chemical industry due to low vapour pressure, high boiling point and low toxicity (Gu et al., 2013). Furthermore lactic acid can be converted by dehydrating to acrylic acid, a key intermediate for the synthesis of poly-acrylates, and by hydrogenation to propylene glycol (Isikigor et al., 2015; Esposito et al., 2015).

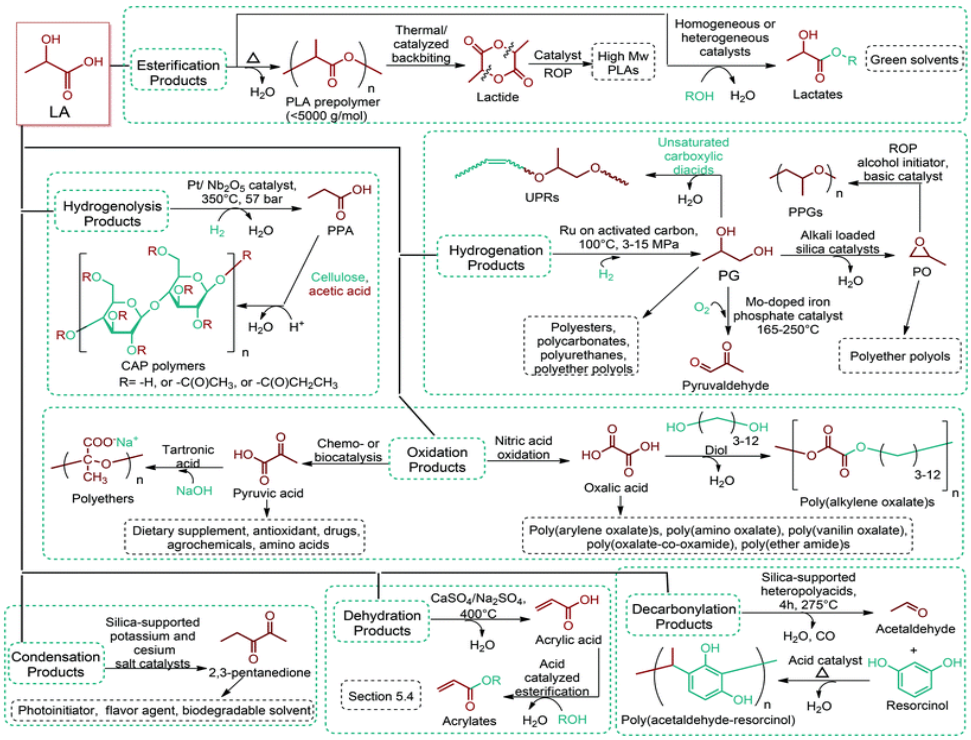

Figure 21: Lactic acid chemical platform (Isikigor et al., 2015)

Another interesting compound obtainable from the microbial fermentation of glucose is succinic acid, which can be used for the synthesis of polyesters and fine chemicals (fig. 22) such as 1,4-butanediol and 2-pyrrolidinone (Isikigor et al., 2015; Bechthold et al., 2008).

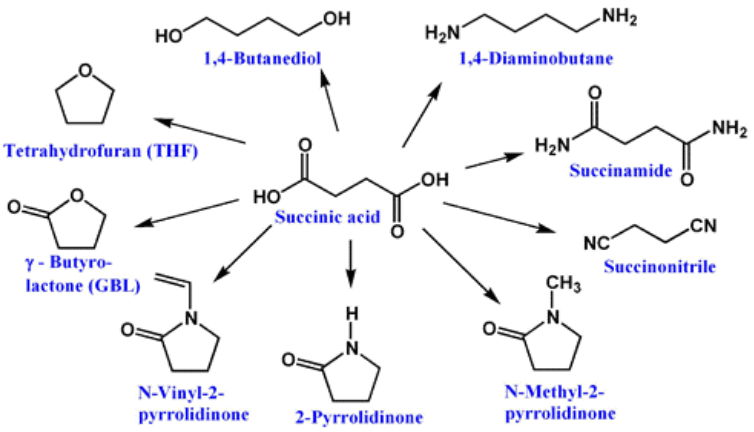

Figure 22: Succinic chemical platform (Isikigor et al., 2015)

2.4 STRUCTURAL SURVEY METHODS APPLIED TO LIGNOCELLULOSIC BIOMASS

A great variety of methods is used for the structural investigation of lignocellulosic biomass. Experimental techniques include methods based on mass spectrometry, nuclear magnetic resonance and infrared absorption spectroscopy. With these techniques it is possible to study the structure of lignocellulosic biomass from the point of view of its biopolymers (Lupoi et al., 2015).

2.4.1 MASS SPECTROMETRY METHODS

Mass spectrometry, in its numerous configurations, is used for the structural investigation of lignocellulose biopolymers. One of the most used for this purpose is the Matrix-Assisted Laser Desorption Ionisation coupled to Time of Flight analyzer. The MALDI ionizes the chemical compounds from a dry and crystalline matrix through a pulsed laser (fig. 23) and it is mainly used for the analysis of the complex solid mixtures of the polymers and biopolymers (Richel et al., 2012). This method consists in adsorption of the sample onto a solid matrix irradiated with a beam of laser light. This causes the surface heating and evaporation of organic molecules. Following this process, protonic transfer equilibriums occur between the analyte molecules and those of the matrix with the formation of protonated ions of the compounds of interest. These are then sent to the analyzer consisting of a time of flight (TOF). The matrix therefore plays a fundamental role in the ionisation of the analyte molecules through their protonation (Lupoi et al., 2015).

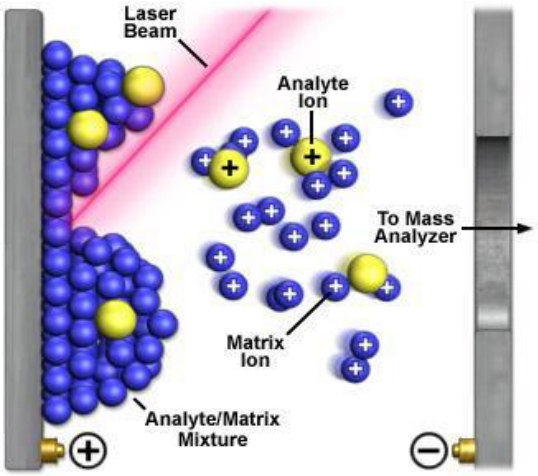

Figure 23: MALDI ion source in mass spectrometry

The MALDI allows identifying the structure of the lignin and therefore to establish, on the basis of this, the type of lignocelluloses used. Another technique of mass spectrometry, which allows the structure of lignin oligomers, is that with electrospray ionisation and hybrid analyzer quadrupole-time of Flight. In this case, the ions produced by the electrospray ionisation are analysed and separated by a quadrupole, fragmented by a collision cell and finally directed towards a time of flight analyzer (fig. 24).

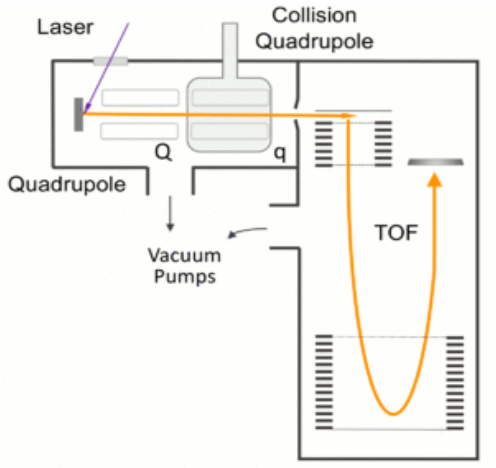

Figure 24: Hybrid system Quadrupole-Time of Flight in mass spectrometry

2.4.2 VIBRATIONAL SPECTROSCOPY FOR THE STRUCTURAL ANALYSIS OF LIGNOCELLULOSIC BIOMASS

Another technique widely used for the structural analysis of lignocelluloses is infrared absorption spectroscopy. This finds numerous applications for the simplicity in the preparation of the sample and for the rapidity in the analysis times. It is also a low cost and non-destructive technique, so that the sample can be used for the subsequent analysis after spectroscopic study (Lupoi et al., 2014). For lignocellulosic biomass, infrared spectroscopic analysis provides information on its structure especially in relation to the nature of functional groups (Traorè et al., 2016). Infrared molecular absorption spectroscopy is based on the energy-matter interaction and in particular on the absorption of infrared electromagnetic radiation by the functional groups of organic molecules. Following this interaction, there is an oscillation of the dipole moment of the chemical bond with consequent variation of its vibrational state and different functional groups give rise to different absorptions (Allison et al., 2011). Infrared consists of three regions classified according to wavelength range or to wavenumber (cm^{-1}): near infrared (12800-4000 cm^{-1}), mid infrared (4000-400 cm^{-1}) and far infrared (400-10 cm^{-1}). The region used for the structural analysis and identification of the fundamental vibrations of the functional groups is that of the mid infrared, while that of the near infrared provides information on the combinations of vibrations and therefore on the overtones. The components of an infrared absorption spectrometer (fig. 25) are the radiation source, the optical system formed by filters to select the wavelength range and lens to direct the light beam towards the sample, the container with the sample inside, the detector and finally a data processing unit (Xu et al., 2013).

Moreover, the infrared absorption spectroscopy can be coupled with microscopic techniques with obtaining imaging techniques with a higher resolution of the lignocellulosic biomass structure (Xu et al., 2013).

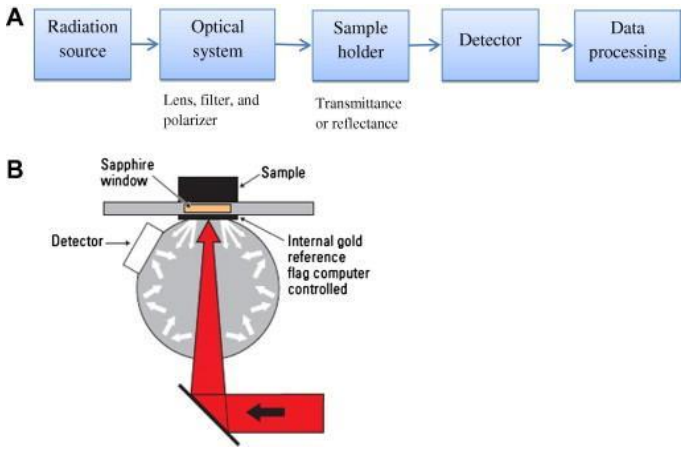

Figure 25: Components of an infrared absorption spectrometer (Xu et al., 2013)

Infrared molecular absorption spectroscopy is a rapid and non-destructive technique for the determination and identification of the functional groups of lignocelluloses biopolymers. This is done by studying the absorption bands in the infrared of these groups. In the preparation of the sample for this technique it is first necessary to proceed with its drying to avoid interferences due to the water absorption band and then to a reduction in the size of the material particles (Xu et al., 2013).

Infrared molecular absorption spectroscopy not only provides information on the fine structure of lignocelluloses, but based on this it can predict the most suitable pretreatment method (fig. 26).

Furthermore, the study of infrared absorption bands can be coupled to the use of chemometric techniques, which allow to reduce the large quantity of spectral data and to obtain a correlation between the spectral characteristics and the chemical structure (Xu et al., 2013).

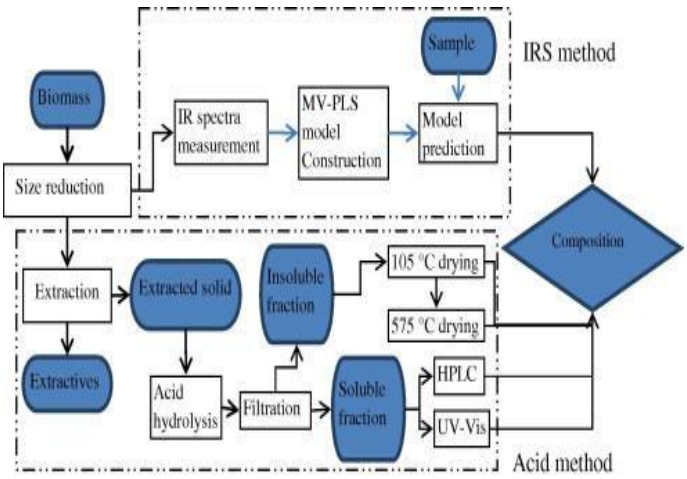

Figure 26: Scheme for the acquisition of IR spectra of lignocelluloses and comparison with the extraction method by acid hydrolysis (Xu et al., 2013)

3. METHODS OF PRETREATMENT OF LIGNOCELLULOSIC BIOMASS

3.1 DECONSTRUCTION OF LIGNOCELLULOSIC BIOMASS WITH PRETREATMENT

The lignocellulosic biomass is a complex material characterised by the presence of three biopolymers cellulose, hemicellulose and lignin, associated with each other. For its use it is therefore necessary a deconstruction (fig. 27) with the separation of these components and the breaking of their interactions (Chen et al., 2015). The different pretreatment methods allow breaking down the lignocellulosic biomass into its fundamental units and increasing the accessibility for the subsequent treatments on these bio-polymers (Kumar et al., 2009; Brandt et al., 2013; Madadi et al., 2017; Holm et al., 2011).

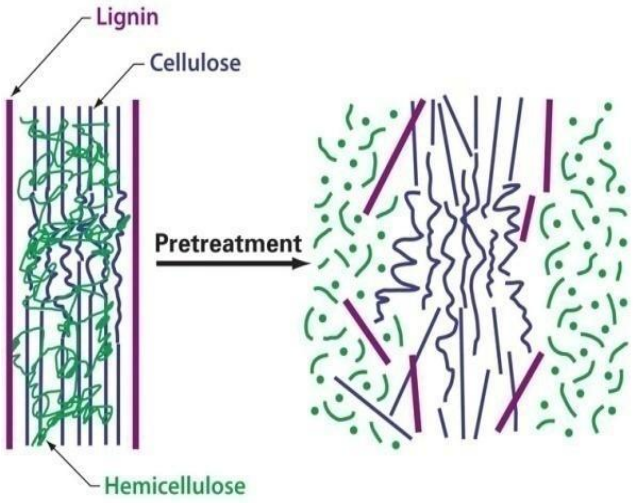

Figure 27: Deconstruction of lignocellulosic structure (Brandt et al., 2013)

3.1.1 CLASSIFICATION OF PRETREATMENT METHODS

The pretreatment methods can be divided into following categories (Silveira et al., 2015):

- physical pretreatments;
- chemical and bio-chemical pretreatments;
- physico-chemical pretreatments.

3.2 MILLING AND EFFECTS OF MILLING ON LIGNOCELLULOSE STRUCTURE

Milling falls into the category of physical pretreatment methods. It is a mechanical pretreatment method, which allows reducing the crystallinity of cellulose, to reduce the particle diameter and to increase the surface area for the subsequent treatments. This could lead to an improvement of the hydrolysis process of cellulose, hemicellulose and lignin. In the milling process, the lignocellulosic biomass is subjected to the following types of stresses: impact, compression, shearing and abrasion/attrition (fig. 28). These stresses are generated by the interaction between the grinder and the

material and are propagated through the structure of this, leading to different particles from the point of view of diameter, morphology and rheological properties. The propagation of mechanical stresses during milling can occur in two ways: intercellular and intracellular. In the first, the break occurs through the cells with the separation of the cells from each other; in the second the break occurs inside the cells (Mayer-Laigle et al., 2018).

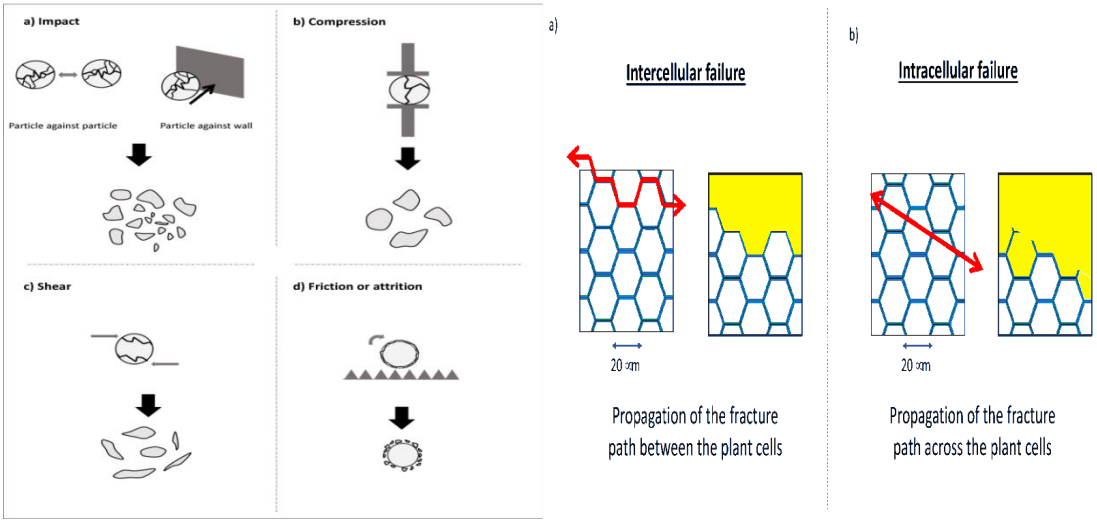

Figure 28: The main mechanical stresses in the milling process of biomass (Mayer-Laigle et al., 2018)

3.3 MICROWAVE AND SONICATION TECHNOLOGIES

Other physical pretreatment methods consist of the use of microwaves and sonication. The use of microwaves is based on electromagnetic radiation from the microwave region of the electromagnetic spectrum. The microwaves are non-ionising-radiations, which induce molecular rotations of the molecules of the material or of the solvent with heating of the sample. The heat generated breaks the lignocellulose structure with the separation of three biopolymers. The sonication is a recent physical technique in the pretreatment of lignocellulosic biomass. In this case, ultrasounds cause the formation of cavitation bubbles on (fig. 29) the surface of lignocellulosic biomass. When these structures collapse, it occurs the breakdown of the bonds between cellulose, hemicellulose and lignin (Silveira et al., 2015). The ultrasound process is mainly influenced by the ultrasonic frequency, the duration of the process, the geometry of the reactor and by the type of solvent used.

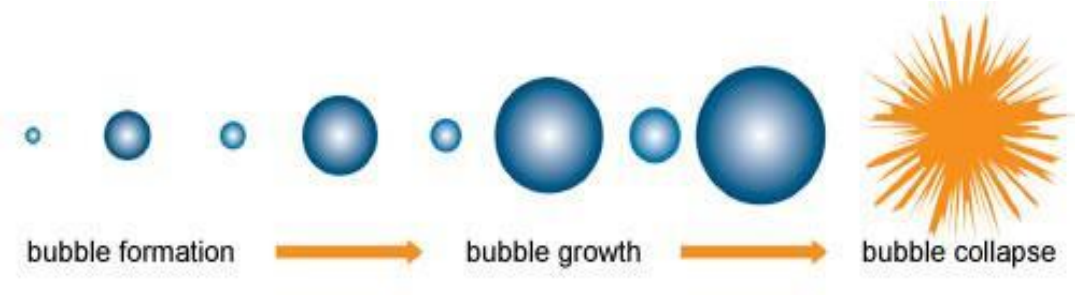

Figure 29: Mechanism of ultrasound process

3.4 PYROLYSIS AND PULSED ELECTRIC FIELDS

Further physical pretreatment methods are pyrolysis and pulsed electric fields (PEF). Pyrolysis is a pretreatment method, which consists in subjecting the lignocellulosic biomass to temperatures within the following range, 500-800 °C, in the absence of oxidizing agents. This process leads to the breaking of the lignocellulosic structure and the decomposition of cellulose and hemicellulose with the formation of end products such as gaseous substances and pyrolysis oil. The pretreatment with PEF is another physical process, which subjects the lignocellulosic biomass to electric fields with strong voltage and short duration. These cause the formation of pores on the surface of lignocellulosic biomass with the deconstruction of the bonds between three lignocellulosic biopolymers.

3.5 CHEMICAL PRETREATMENTS OF LIGNOCELLULOSIC BIOMASS

Chemical pretreatments include the use of both concentrated and dilute acids and bases and that of a new class of solvents called ionic liquids. The chemical pretreatment has the purpose of breaking the complex architecture of bonds between the biopolymers of lignocellulosic biomass (fig. 30) reducing the crystallinity of the cellulose and increasing the porosity of the material for the subsequent steps of depolymerisation (Lee et al., 2014).

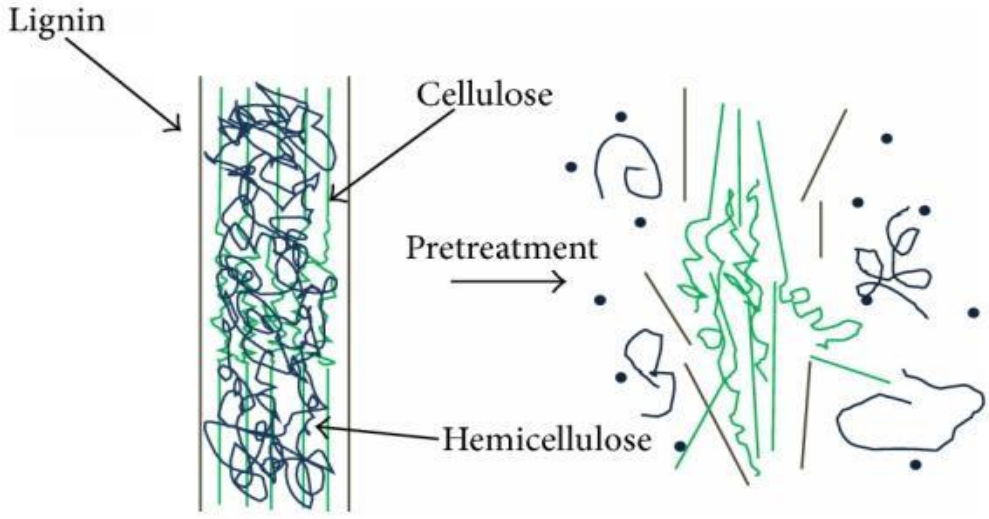

Figure 30: Deconstruction of lignocellulose into cellulose, hemicellulose and lignin (Lee et al., 2014)

3.5.1 USES OF ACIDS AND BASES

Acid pretreatment is a process in which the hydronium ions break the inter and intra-molecular bonds between cellulose, hemicellulose and lignin and for this purpose concentrated and dilute solutions of strong acids such as sulphuric acid and nitric acid are used (Brodeur et al., 2011; Hendriks et al., 2009). Since the concentrated solutions of acids are toxic, corrosive and dangerous in the hydrolysis process, it is preferred to use dilute solutions of sulphuric or nitric acid at a concentration between 2% and 3% (Lee et al., 2014). The alkaline treatment allows, through saponification, to break the ester bonds between lignin and hemicellulose leading to a partial solvatation of the hemicellulose. Furthermore, the degree of crystallinity and polymerisation of cellulose is also reduced (Lee et al., 2014).

3.5.2 IONIC LIQUIDS IN THE CHEMICAL PRETREATMENT OF LIGNOCELLULOSE

Ionic liquids constitute a new class of organic solvents and are formed by an organic cation and an inorganic anion (fig. 31). They are therefore salts, which exist in the liquid state even at moderately low temperatures. Ionic liquids have some interesting features such as low vapour pressure, good chemical and thermal stability and the possibility of solubilising many chemical compounds (Holm et al., 2011). For these properties they are classified as green solvents mainly by virtue of their low vapour pressure (Yoo et al., 2017). Cellulose and hemicellulose can be dissolved in ionic liquids through the formation of hydrogen bonds between the inorganic anion and the hydroxyl groups of the biopolymers (fig. 32). In this way the intra and inter-molecular hydrogen bond interactions between the various cellulose and hemicellulose chains are destroyed (Yoo et al., 2017).

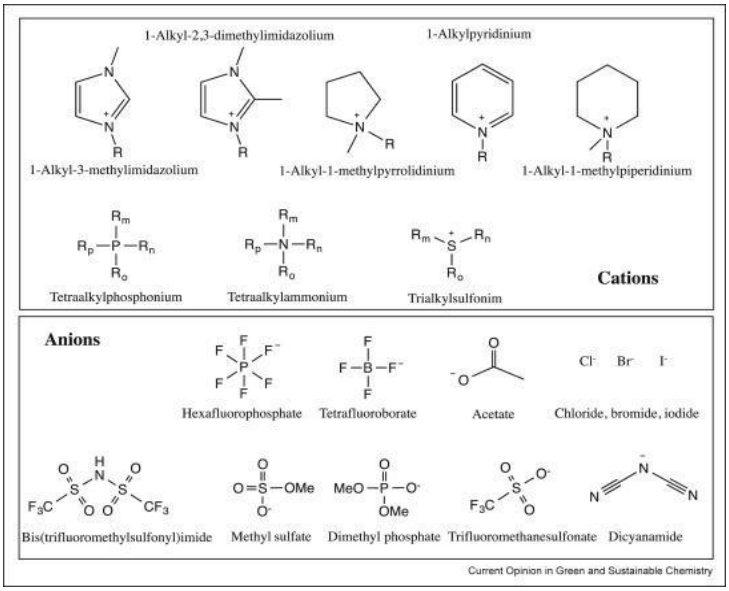

Figure 31: Structure of ionic liquids (Yoo et al., 2017)

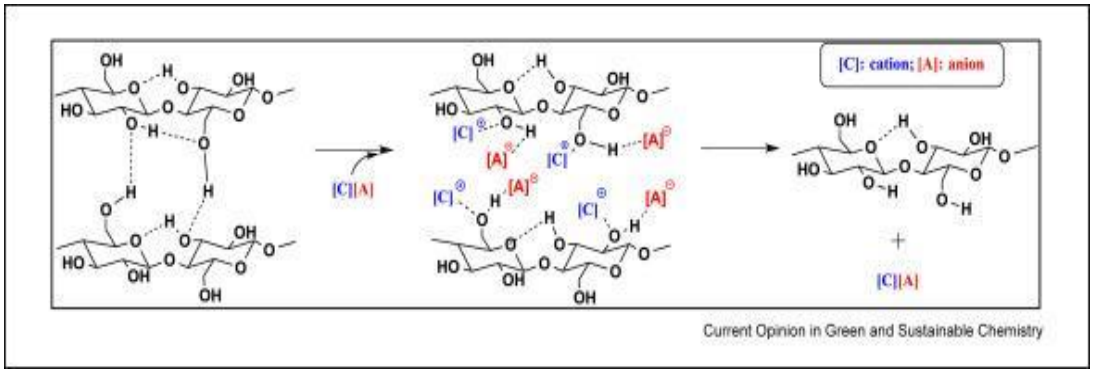

Figure 32: Mechanism of dissolution of cellulose in ionic liquids (Yoo et al., 2017)

The dissolution of cellulose and hemicellulose in ionic liquids leads to a breakdown of the interactions between three biopolymers and to an improvement in accessibility to the lignocellulose for subsequent depolymerisation treatments (Elgarbawy et al., 2016).

3.6 BIOTECHNOLOGICAL METHODS: ENZYMES IN THE PRETREATMENT OF LIGNOCELLULOSE

Biotechnological pretreatment methods are based on the use of biocatalysts, mainly enzymes, to conduct complex chemical reactions called bio-conversions. The bio-catalytic processes can be divided into three groups based on the type of biocatalyst used for the conversion (Sheldon et al., 2017):

- bio-catalysis conducted with cells;
- bio-catalysis based on the isolated enzymes;

- bio-catalysis with the immobilizer enzymes.

The bio-catalysis can be defined as the use of biological catalysts obtained from the fermentation technologies such as enzymes or cells (fig. 33) and since these bio-catalysts are produced from renewable resources and are bio-degradable the bio-catalysis strategies play a fundamental role in sustainable chemistry (Sheldon et al., 2017).

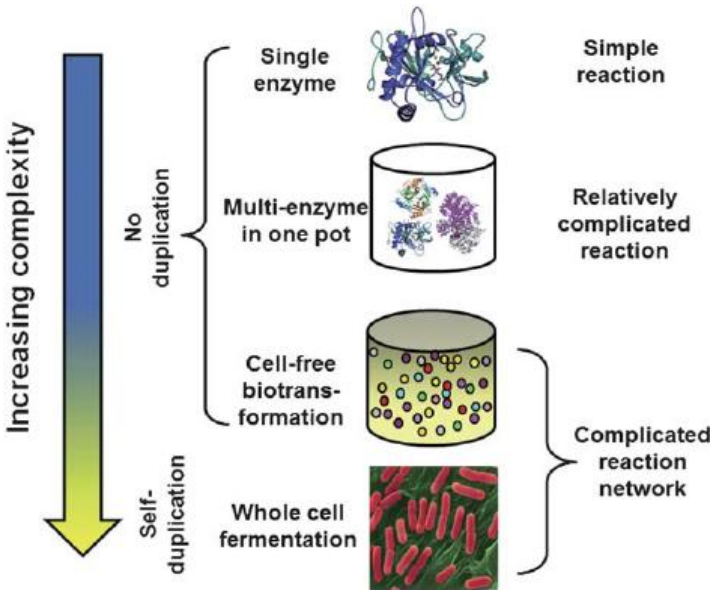

Figure 33: Bio-catalyst types with cells and enzymes

Enzymes play a fundamental role in the pretreatment and bioconversion processes of lignocellulosic biomass. They can be used individually or together with other enzymes to form the enzymatic cocktails. The main enzymes for the pretreatment of lignocellulosic biomass are cellulase, hemi-cellulase and laccase.

3.6.1 LACCASE ENZYME: STRUCTURE AND PROPERTIES

Laccases, benzenediol oxygen oxidoreductases, are dimeric or tetrameric glycoproteins consisting of three β-barrel sequential domains and belonging to the class of multi-copper oxidases (MCO) for the reduction of oxygen to water molecules (Riva et al., 2006). This enzyme contains four copper ions (fig. 34) having different spectroscopic characteristics and distributed in the following regions of the active site of laccase: one type 1 (CuT1) located in the third domain, one type 2 (CuT2) and binuclear type 3 (CuT3) placed between the first and the third domain (Kalia et al., 2014; Christopher et al., 2014). The one type 2 and two type 3 form a substructure called Tri-nuclear Cluster (Arora et al., 2010; Jones et al., 2015). The T1 Cu with trigonal planar geometry has two histidines, one methionine and one cysteine as ligands. The type-1 has an intense electronic absorption band at 600 nm, which is

responsible of the deep blue colour of laccase enzyme (Wong et al., 2009). The type 2 copper is coordinated by two histidines and water. The type 3 is made up of two copper ions each of which is coordinated by three histidines and a hydroxyl group and they are thus maintained in an anti-ferromagnetic position (Sergio Riva et al., 2006; Wong et al., 2009; Dwivedi et al., 2011; Jones et al., 2015).

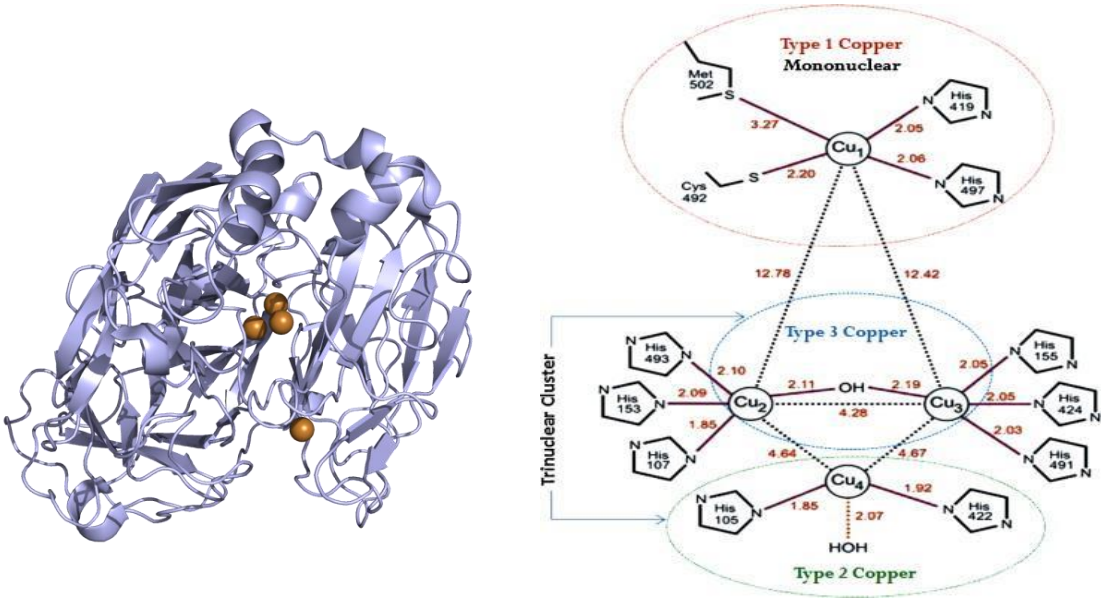

Figure 34: Crystal structure of laccase and active site with four copper ions (Dwivedi et al., 2011)

3.6.2 LACCASE ENZYME FOR THE DECONSTRUCTION OF LIGNOCELLULOSE

Laccases can be used to partially oxidize the monolignols of the lignin structure. The laccase enzyme extracts one electron at the time from the lignin substrates, bound to the substrate binding region near the type-1 Cu, and converts them in reactive phenoxy radical species, which can initiate the depolymerisation of lignin (fig. 36 and 37). After receiving four electrons from the four substrates, the enzyme transfers sequentially these electrons, through the His-Cys-His tri-peptide group, to the tri-nuclear cluster where molecular oxygen is reduced to two water molecules (Pardo et al., 2015; Sergio Riva et al., 2006).The main steps of laccase catalysis are (Arora et al., 2010; Jones et al., 2015):

1) the oxidation of the substrate at the type-1 Cu, which represents the primary electron acceptor in the laccase catalysed reaction, and the conversion of the enzyme to the reduced form;
2) internal electron transfer from the type-1 Cu to the tri-nuclear cluster with the type-3 Cu and type-2 Cu tri-nuclear cluster and binding of molecular oxygen to the tri-nuclear cluster of the active site;
3) reduction of oxygen to two water molecules at the tri-nuclear cluster and restoration of the oxidised form of the laccase.

The reduction of laccase enzyme can be considered the limiting stage of the reaction catalysed by the laccase and according to Marcus's theory of electronic transfer mechanism (Medina et al., 2013) the difference in redox potential between the active sub-site type-1 Cu and substrate determines the electron transfer flow (Giardina et al., 2010). In the reduction of laccase the three copper atoms in the tri-nuclear cluster are sequentially reduced through the oxidation of substrate with the electron transfer to the type 1 Cu. In the molecular mechanism of oxygen reduction to water, the first step is represented by the formation of peroxy intermediate (PI) with the two electron transfer from the type 1 Cu (Giardina et al., 2010; Guzik et al., 2014; Prajapati et al., 2018). Subsequently the peroxy intermediate is converted into the native intermediate through the transfer of two other electrons and thus the release of two water molecules is obtained (Guzik et al., 2014). In the oxygen reduction by laccase enzyme the first step, related to the formation of peroxy intermediate, is the determining step while the second with the reductive cleavage of the O-O bond is faster (Mollania et al., 2018).

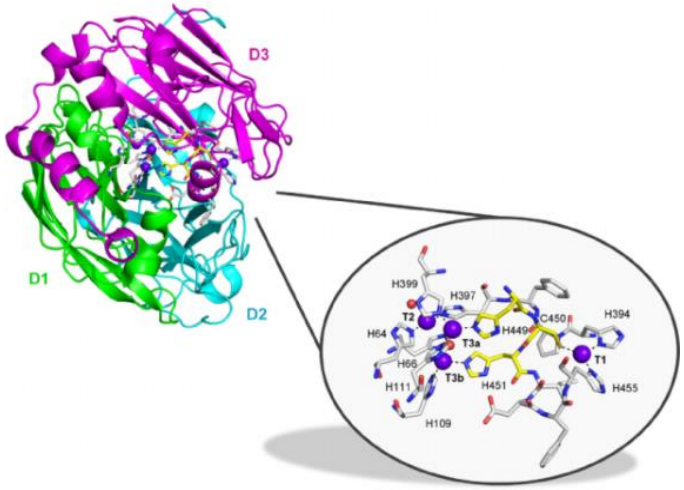

Figure 35: Structure of laccase with the active site with four copper ions

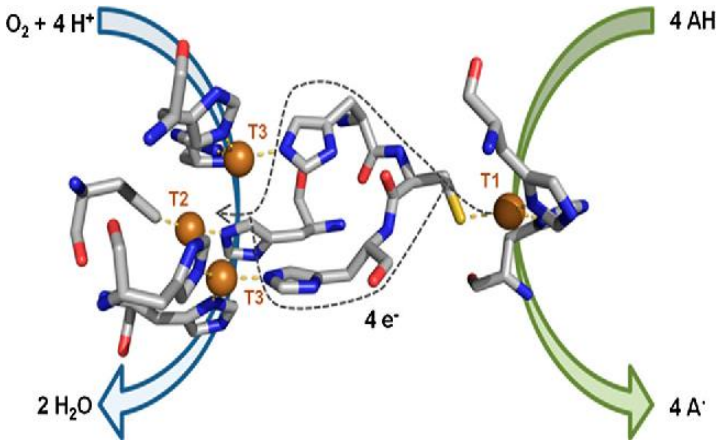

Figura 36: Electron transfer in the active site of laccase (Pardo et al., 2015)

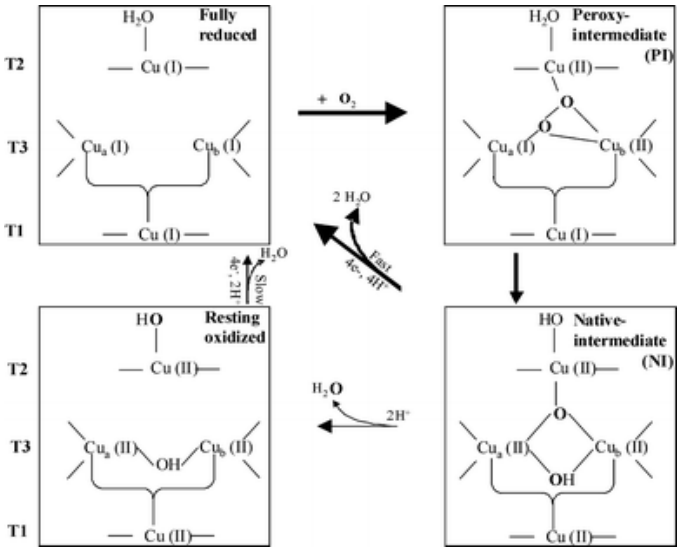

Figure 37: Oxido-reductive mechanism in laccase (Mollania et al., 2018)

3.6.3 GLYCOSIDE HYDROLYTIC ENZYMES FOR THE CELLULOSE AND HEMICELLULOSE CLEAVAGE

Cellulases and hemicellulases are involved in the hydrolysis of polysaccharides of lignocellulosic biomass, cellulose and hemicellulose, through the breakdown of β-1,4 glycosidic bonds. Cellulases and hemicellulases belong to the glycoside hydrolases (GHs) (Obeng et al., 2017) and they are divided into three categories (Juturu et al., 2014):

- β-1,4-Endoglucanase (EC 3.2.1.4);
- β-1,4-Exoglucanase (EC 3.2.1.91);
- β-Glucosidases(EC 3.2.1.21).

Endoglucanases (fig. 38) attack the internal portions in the amorphous regions of the cellulose chain of glucose, forming oligomer chains (Behera et al., 2017). Exoglucanases or cellobiohydrolases have greater affinity for the crystalline regions of the cellulose and produce more cellobiose and cello-oligomers from reducing and non-reducing ends of the oligosaccharide chain (Jorgensen et al., 2007; Saranraj et al., 2012; Juturu et al., 2014; Behera et al., 2017). β-Glucosidases have a rigid structure with the active site in a large cavity. This favours the interaction between the enzyme and substrate. These enzymes hydrolyze the soluble cellobiose and cello-oligomers into glucose. There is therefore for cellulose a cascade depolymerisation favoured by the synergism between the three categories of cellulases (Jorgensen et al., 2007; Obeng et al., 2017).

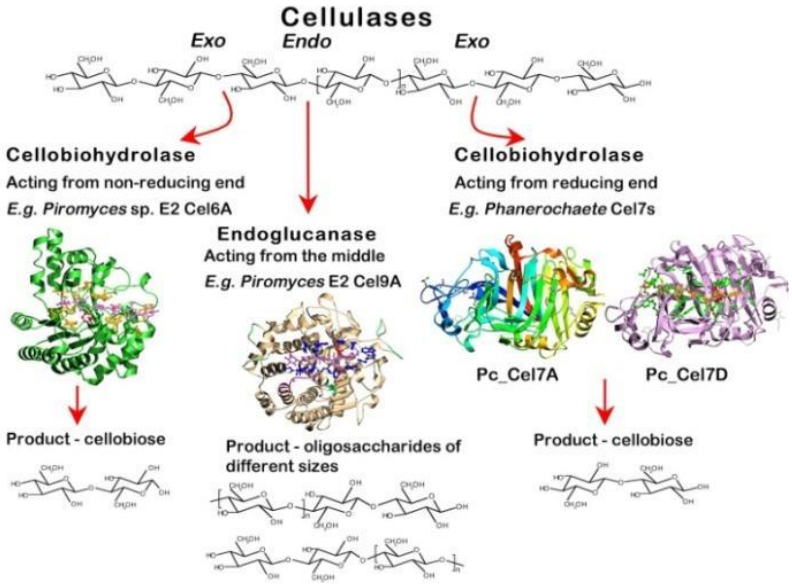

Figure 38: Structure and mechanism of cellulase enzymes

Cellulases are produced by a variety of microorganisms such as *Aspergillus niger*, *Trichoderma reesei* and *Cellulomonas flavigena*. Cellulases such as endoglucanases and cellobiohydrolases present in their structure (fig. 39) a catalytic domain responsible for the hydrolysis reaction and a binding domain called cellulose binding domain (CBD) (Jorgensen et al., 2007; Behera et al., 2017) belonging to the carbohydrate binding modules class (CBMs) (Saranraj et al., 2012). The latter does not exert any catalytic action, but favours the adsorption of the enzyme on the cellulose surface (Jorgensen et al., 2007). This improves the process of hydrolysis, preventing the enzyme from separating from the substrate after the splitting of a glycosidic bond and allowing it to move on the next. β-Glucosidases do not present this protein domain and therefore have low affinity for cellulose unlike endoglucanases and exoglucanases (Obeng et al., 2017)

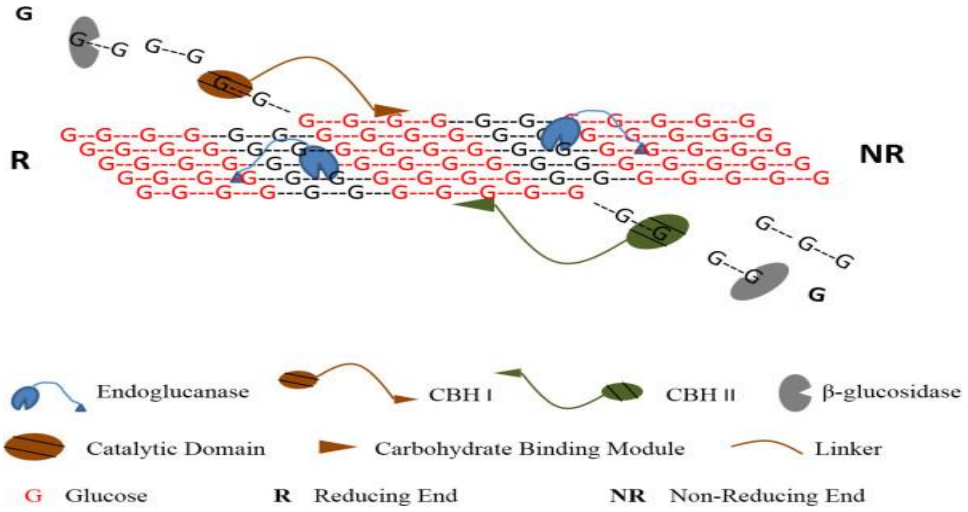

Figure 39: Mechanism of cellulase enzymes with catalytic domain and carbohydrate binding module

For their catalytic mechanism there are two important amino acid residues, one that acts as a donor of protons and another as a nucleophile (fig. 40). In the first step there is the protonation of the substrate and the formation of the intermediate glycosylated enzyme with the intervention of nucleophile residue. In the second step there is the deprotonation of a water molecule. This attacks the anomeric carbon of the glycosylated enzyme intermediate with the breaking of this complex and the restoration of the active site of enzyme. This leads to the cleavage of the glycosidic bonds (Paes et al., 2012).

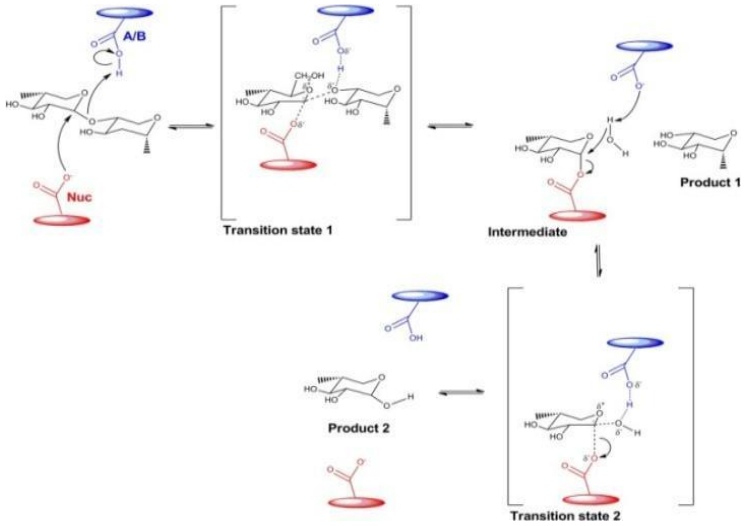

Figure 40: Catalytic enzymatic mechanism of the hydrolysis of cellulose (Paes et al., 2012)

The hemicelluloses are for the most part made up of xylose units and therefore the hemicellulolytic enzymes are subdivided into β-1,4-endoxylanases (EC 3.2.1.8) and β-1,4-xylosidases (EC 3.2.1.37)

(Polizeli et al., 2005; Walia et al., 2017). The first split the β-1,4-D-xylopyranosyl linkages of xylan chains, while the second hydrolyze the xylobiose and xylo-oligosaccharides forming xylose (Juturu et al.,2012). Furthermore the xylanase can be classified according to the nature of sugars released in:

- non arabinose liberating endoxylanases, which do not act on the arabinosyl units linked to the xylans and liberate xylobiose and xylose as major products;
- arabinose liberating endoxylanases, which act on the arabinosyl units linked to the xylans and liberate mainly arabinose, xylose and xylobiose;
- exo β-1,4-D-xylanases, which remove xylose units from non-reducing end of xylan chains;
- β-xylosidase, which hydrolyzes the xylobiose and xylooligosaccharides and liberates mainly xylose (Knob et al., 2010).

As cellulases, hemicellulases are modular proteins (fig. 41) with a catalytic domain and a carbohydrate binding module (CBM) (Jorgensen et al., 2007). The first is responsible for the hydrolysis of xylanic units to xylose. The second binds the carbohydrate, increasing the concentration of enzyme on the surface of substrate and protecting it from other degradations. For the catalytic mechanism two amino-acid residues of glutamic acid are probably involved in the catalytic domain (Paes et al., 2012).In the first step (glycosylation) the acid/base residue of the enzyme acts as an acid and protonates the substrate. At the same time another residue acts as a nucleophile and leads to the release of the leaving group and to the formation of an intermediate called the glycosyl enzyme with the break of β-1,4-glycosidic bond. In the second step (deglycosylation) the acid/base residue extracts a proton from a water molecule, which then attacks the anomeric carbon of the intermediate glycosyl enzyme (Collins et al., 2005). This leads to the restoration of the functional unit of the catalytic domain of the xylanase enzyme (Paes et al., 2012).

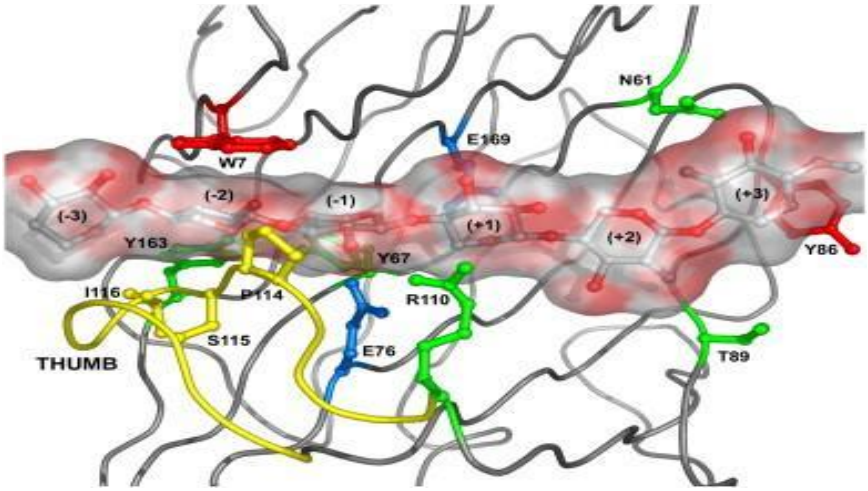

Figure 41: Xylanase binding module to a hemicellulose residue (Paes et al., 2012)

3.6.4 ADVANTAGES AND DISADVANTAGES IN THE USE OF ENZYMES

The use of enzymes in the bio-catalytic pretreatment of lignocellulosic biomass allows to obtain some advantages such as the use of safe processes and methodologies and the handling of catalysts, enzymes, renewable, safe and biodegradable (Sheldon et al.,2017). However, the production of enzymes, obtained by fermentation, is still too expensive and applicable in specialised structures. This still partially limits their use.

3.7 PRETREATMENT CHEMICAL-PHYSICAL METHODS

The chemical-physical pretreatment methods consist of a combination of chemical and physical means to obtain the deconstruction of lignocellulosic biomass. One of the best known methods is the steam explosion.

3.7.1 STEAM EXPLOSION PRETREATMENT

Steam explosion is the most used chemical-physical pretreatment method for lignocellulosic biomass. It is a combination of mechanical forces such as the high pressure generated inside the reactor and of chemical reactions such as the hydrolysis of acetyl groups of hemicellulose. In the steam explosion the lignocellulosic biomass is treated with saturated steam at high pressure (0.4-4.7 MPa) and at high temperatures (160-250 °C) (Brodeur et al., 2011; Chen et al., 2015).This causes the hydrolysis of hemicellulose with the release of xylo-oligosaccharides and monosaccharides such as glucose and xylose and it leads to an increase of accessibility to cellulose for enzymes. The stem explosion process can be divided into two parts:

- auto-hydrolysis step;
- explosion step.

In the auto-hydrolysis step hemicellulose is dissolved and there is a variation in the structure of lignin (Tomaso Pejo et al., 2011). In this process there is the release of acetic acid bound to the acetyl groups of hemicellulose and this catalyzes the hydrolysis of this biopolymer (Kumar at al., 2009). In the explosion step the complex structure of lignocellulosic biomass is disrupted (Chen et al., 2015). The steam explosion pretreatment produces the solubilisation of hemicellulose and a reorganisation of lignin structure (Romani et al., 2013) with the obtaining of two fraction products: an insoluble solid fraction with cellulose and lignin and a liquid fraction with sugars derived from the solubilisation of hemicellulose. In addition, steam explosion leads to a change in the degree of crystallinity of the cellulose (Alvira et al., 2016).The steam explosion (fig. 42) is formed by a steam generator connected to a reactor, in which the sample is subjected to treatment with saturated steam at high pressure and at high temperature. In this phase the process of hydrolysis of hemicellulose and the reorganisation of the

lignin structure are carried out. Later the lignocellulosic biomass inside the reactor is subjected to the depressurisation process with the breaking of the interactions between cellulose, hemicellulose and lignin. During depressurisation, the exploded material is removed from the reactor and recovered in the collection vessel (Jacquet et al., 2015).

The efficiency of the steam explosion can be described by the following equation:

$$\mathbf{Ro = t \times exp\ [(TH–TR)/\ \omega}$$

where Ro is the severity factor and measure the efficiency of the steam explosion process (Alvira et al., 2010). It depends on the reaction time t and exponentially on the difference between the hydrolysis time and base temperature established at 100 °C with the following law (**TH–TR)** (Ouyang et al., 2018). **Ω** is an experimental parameter and is worth 14.75 (Gelosia et al., 2017). Many studies have shown that the hydrolysis of hemicellulose is closely related to the residence time of lignocellulosic biomass in the reactor of steam explosion. The longer the residence time, the better the efficiency of the hemicellulose hydrolysis process will be (Jacquet et al., 2015). The hemicellulose hydrolysis products, mono and oligosaccharides, may also undergo condensation, fragmentation and dehydration reactions with the formation of furanic compounds, levulinic acid and formic acid. An increase in residence time of lignocellulosic material within the reactor leads to an increase of these degradation products. Therefore, greater severity conditions with increase in temperature and residence time lead to a strong degradation of hemicellulose, but also to the formation of its degradation products, which may show an inhibitory activity towards the subsequent fermentation steps.

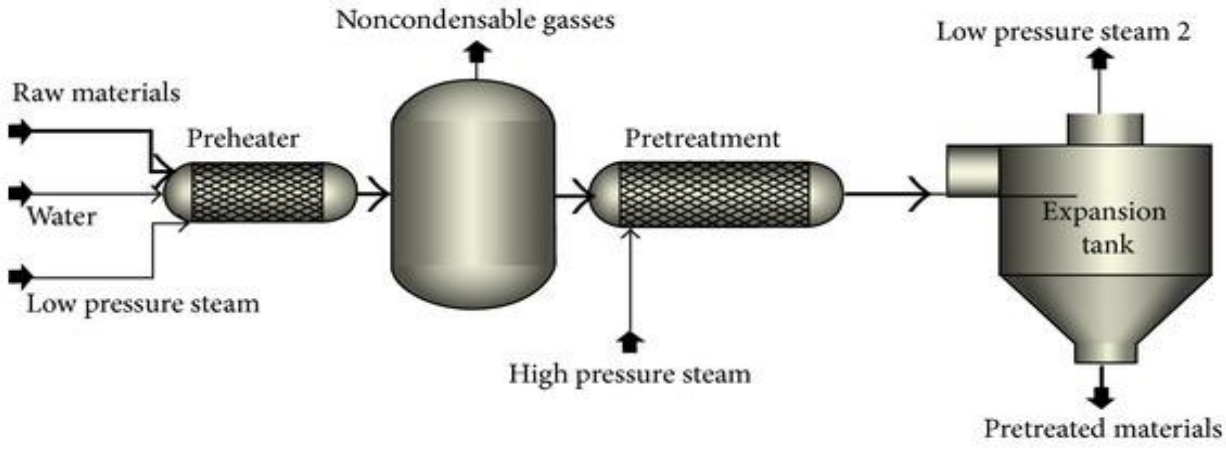

Figure 42: Description of the steam explosion reactor structure

4. EMERGING PRETREATMENT TECHNOLOGIES

4.1 ELECTROSTATIC SEPARATION TECHNOLOGY

Many methods for the pretreatment of lignocellulosic biomass are available based on the use of chemical-physical processes with high consumption of water, energy and solvents and generation of waste. Furthermore, in these steps the components of lignocelluloses could be degraded and purification operations for solvent removal are necessary. One of the most important challenges for next generation processes applied to lignocellulose biomass is to maintain the integrity of biopolymers and ensure sustainable fractionation with low consumption of energy and solvents. Electrostatic separation has emerged as an innovative and sustainable technique for the pretreatment and fractionation of lignocellulosic by-products of the food industry (Barakat et al., 2017).

4.1.1 PHYSICAL PRINCIPLES OF ELECTROSTATIC SEPARATION

Electrostatic separation is an innovative technology for the deconstruction and fractionation of lignocellulosic biomass and it is based on the different electrical conductivity and charge density of the particles in relation to their chemical-physical properties. In electrostatic separation (fig. 43 and 44) the particles, through a jet of compressed air, are conveyed towards a structure called charging line where they are charged by triboelectric effect. This phenomenon occurs through the impact between the particles and with the walls of the charging line (Mayer-Laigle et al., 2018).The charged particles are then sent into a separator with two high voltage electrodes and here the positively charged particles are separated from the negatively charged ones. Finally, two cyclones allow the recovery of the fractions. In more recent versions, the electrostatic separation can be coupled to ultrafine milling (Barakat et al., 2017).The conductivity of the particles depends on their chemical composition, their diameter, their morphology and their density. The triboelectric effect is governed by the surface properties of the particles and therefore by their tendency to accept or not electrons (Kdidi et al., 2018).Moreover, the electrostatic separation can be carried out in several stages increasing the separation efficiency. The following figures illustrate the mechanisms of electrostatic separation.

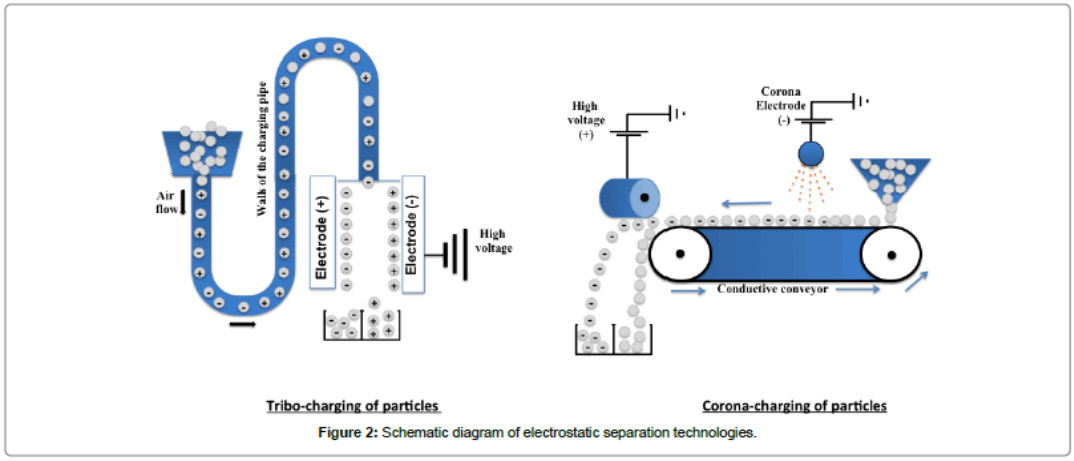

Figure 43: Mechanism of electrostatic separation (Barakat et al., 2017)

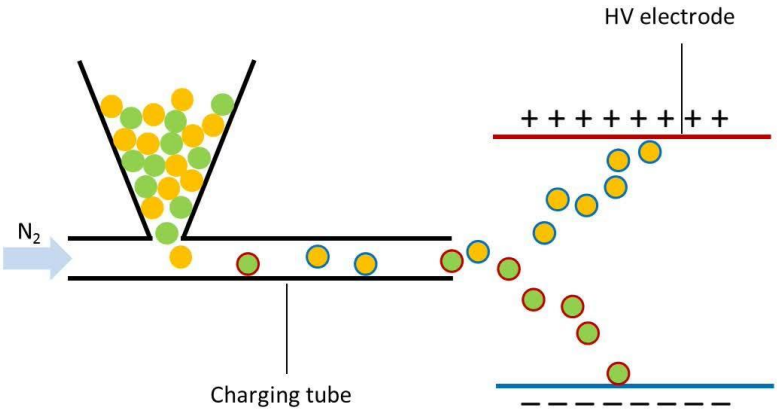

Figure 44: Mechanism of electrostatic separation with charging tube and two electrodes

4.1.2 APPLICATION OF ELECTROSTATIC SEPARATION TO THE PRETREATMENT PROCESS

Given the complexity of the lignocellulosic biomass with its three bio-polymers interacting with each other, it is very useful to find an easy pretreatment system that allows in a single step the de-structuring and the fractionation of this. The electrostatic separation, easily coupled to the ultrafine milling (fig. 45), could allow the fractionation of this complex matrix once it is deconstructed by the ultrafine mechanical bathing. In some electrostatic separations carried out on lignocellulosic biomass of various matrices a presence of cellulose was found in positively charged fractions and of hemicellulose and lignin in those negatively charged (Barakat et al., 2014).

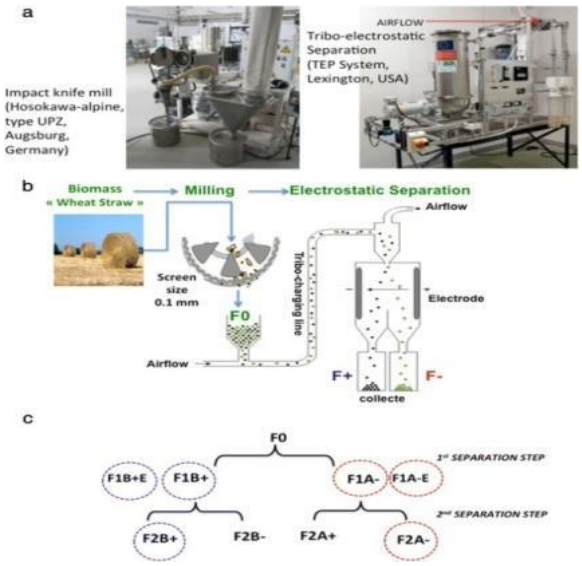

Figure 45: Electrostatic separation applied to lignocellulosic biomass (Barakatt et al., 2014)

4.1.3 ADVANTAGES OF ELECTROSTATIC SEPARATION TECHNOLOGY

The electrostatic separation technology allows the separation of the components of the lignocellulosic complex matrix with the following advantages (Barakatt et al., 2014; Barakatt et al., 2017):

1. absence of use and consumption of solvents and water;
2. possibility of not using chemical and biochemical catalysts;
3. absence of purification steps;
4. possibility of repeating the electrostatic separations to increase the efficiency of splitting;
5. low energy consumption;
6. high speed of fractionation;
7. reduced waiting times;
8. possibility of coupling with ultrafine milling and size separation;
9. reduced degradation of the biopolymers of lignocellulosic biomass;
10. ease of use on an industrial scale.

The figure below represents a pilot plant of electrostatic separation.

Figure 46: Electrostatic separation pilot plant

5. DISTILLATION

5.1 THEORY AND PRINCIPLES OF DISTILLATION

Distillation is one of the main physical techniques for separating chemical compounds. It is based on the evaporation of the liquid phase containing these components and on the subsequent condensation step for cooling. The principle behind the separative distillation process is the different volatility of the compounds. Compounds with greater volatility will pass more easily to the vapour phase than to those with a lower vapour pressure (D'Ischia., 2002). In chemistry the process of distillation can be used to separate mixtures of liquid compounds, isolate a product of a reaction and eliminate a solvent from a solution. The main distillation categories are:

- simple distillation;
- fractional distillation.

In simple distillation the condensation takes place near the evaporation site, while in the fractionated one between the two sites a column is placed to increase the separation efficiency. The two processes can take place at atmospheric pressure or under vacuum (D'Ischia., 2002).

In simple distillation (fig. 47) the product of the separation process, the distillate is obtained by means of a single evaporation-condensation step. The apparatus for simple distillation consists of the following units:

- distillation flask, in which the sample is vaporised;
- the refrigerating conduit (condenser) for the condensation process;
- the collection flask (receiving flask) for the recovery of distillate.

The heating of the liquid inside the distillation flask can take place by means of a water bath for liquids with high vapour tensions or with an oil bath with low vapour pressures.

The figure below represents a simple distillation apparatus.

In fractional distillation we have a fractionation column or concentration column between or the evaporation and condensation sites. In this, multiple liquid-vapour equilibriums are established due to the continuous condensations and evaporation, coming from the distillation flask. The fractional distillation proceeds through reflux with continuous recondensation of the steam and its re-immission in the distillation cycle. This strongly increases the separation efficiency since there are a series of distillation cycles in a single operation. The various evaporation cycles continuously enrich the vapour of volatile compounds, while those with low pressures will tend to return to the distillation flask. The fractionation column must be perfectly vertical and the separating power is maximum in adiabatic conditions of heat exchange between liquid and vapour. A very important parameter to measure the efficiency of the column separating power is the number of theoretical plates. The theoretical plate

corresponds to the portion of column, in which a condition of thermodynamic equilibrium is established between liquid and vapour. The greater the number of theoretical plates the greater the separation efficiency (D'Ischia., 2002).

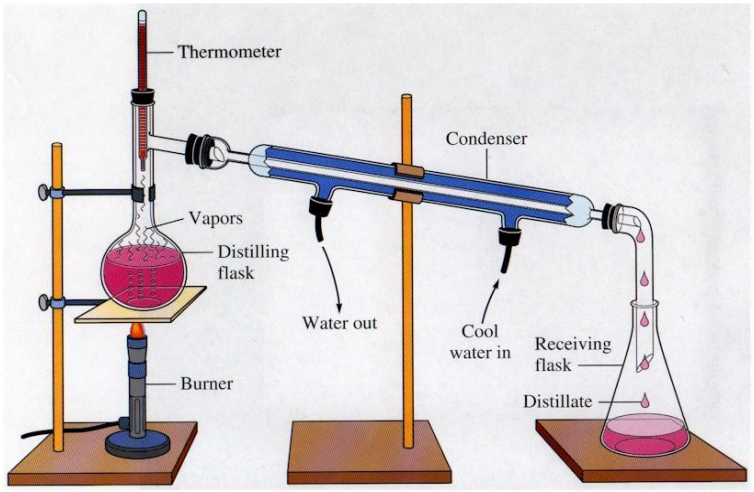

Figure 47: Simple distillation apparatus

The factors that affect the efficiency of the separation process are as follows:

- column length;
- thermal conductivity of the column packing;
- surface area of the column portions.

The distillation column consists of an external body, a reboiler, the plates, the condenser and the reflux case. The reboiler is responsible for the production of steam at the base of the column and can be internal or external to it. At the base of the plates of the column there are multiple equilibriums liquid-vapour. For distillation columns there are different types of plates such as bell, valves and perforated plates. The bell plates (fig. 48) have great operational flexibility, but are not very suitable for mixtures containing compounds having rather similar volatilities.

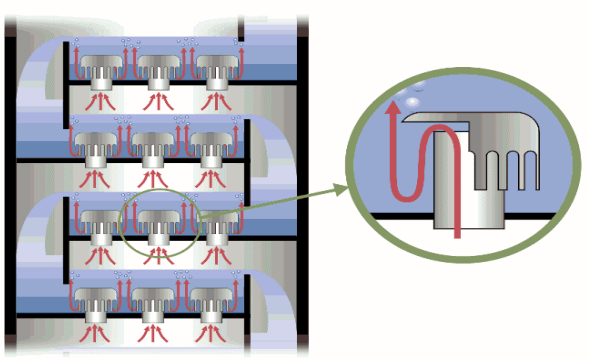

Figure 48: Bell-shaped plates in a section of distillation column

In the valve plates (fig. 49) these open up through the pressure generated by the rising steam. They can be fixed or mobile and yet they do not work well if the vapour pressure is low so that they cannot be opened.

Figure 49: Valve plates for the distillation column

In the perforated plates (fig. 50) the descent of the liquid and the rising of the steam take place through small holes made on the surface of these plates.

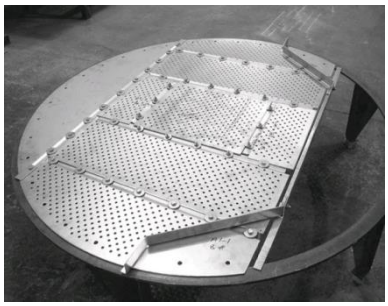

Figure 50: Perforated plates for the distillation column

The flows inside the distillation column (fig. 51) take place in the following ways: entraining, weeping and flooding. The entraining starts when the kinetic energy of the gas is such as to move drops of liquid

from one plate to the one above the column. The weeping instead occurs when the potential energy of the liquid is greater than that of the gas with displacement of the drops of liquid from a plate to the one below. When the volume of the reflux is insufficient, the flooding of the affected plate can occur with subsequent extension to the entire column.

The longer the column, the more the number of theoretical plates grows. By increasing the thermal conductivity of the column packing material and the surface area of the column portions, the liquid-vapour equilibriums in the various parts of the column grow (D'Ischia., 2002).

In fractional distillation the heating speed plays a very important role, which must be gradual and not too rapid to avoid a decrease in the separative process.

Thanks to the good separation potential, fractional distillation is very well applied to the purification of alcoholic mixtures.

The figure below illustrates the layout of the fractional distillation apparatus.

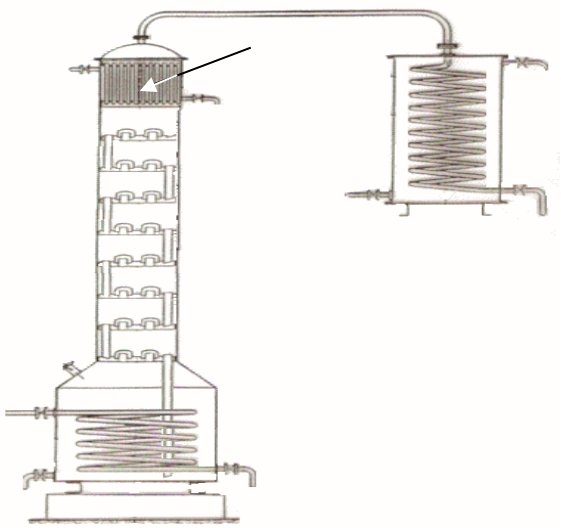

Figure 51: Fractional distillation applied to the separation of alcoholic mixture

5.2 DISTILLATION TECHNIQUES APPLIED TO THE WINE INDUSTRY

Distillation is applied in the wine industry to extract the volatile fraction and concentrate the alcohol fraction from grape pomace, separated from the must or wine at the end of alcoholic fermentation. The distillate obtained is called grappa. In this process the grape pomace is first separated from the must and then stored in special containers. Here the grape pomace becomes the substrate for microbial fermentations by yeasts with the activation of metabolic pathways, which lead to the biosynthesis of ethanol and minor compounds such as ethyl esters, acetates and higher alcohols responsible for the

aroma of distillates. Through distillation we can obtain the extraction of these volatile fractions and then concentrate the alcohol fraction.

The production of neutral alcohol generally takes place by fermentation and subsequent step of purification. The fermentation mixture, commonly called beer, also contains other volatile compounds often referred to as congeners (methanol, long chain alcohols and acids, esters and aldehydes). The separation of ethanol from these compounds takes place in multistage distillation columns based on the different volatility of the substances contained in the fermentation mixture (Decloux et al., 2005). In the field of distillation chemistry in order to characterize the volatility of a compound as a function of the alcoholic concentration of the liquid, a parameter called purification constant K is used. It is defined as the ratio between the concentration of the congener in the vapour phase and that in the liquid phase with reference to alcohol solutions.

$$K = \frac{Concentration\ of\ congener\ in\ the\ vapour\ phase}{Concentration\ of\ congener\ in\ the\ liquid\ phase}$$

A purification constant > 1 indicates that the congener is more volatile than ethanol. In the multi-stage distillation (fig. 52) the mixture is introduced in the upper part of the column and here it undergoes to the multiple liquid-vapour balance with reflux formation at the head of the column. The steam flow then feeds the rectification column, which processes the reflux with a stripping part called Lutter column. From the processing of the condensate we have the fraction of the head of the column, the intermediate product recovered corresponding to some plates under the head of the column and the fraction of the lower level of the column just above the entry point of the steam. The latter contains amyl alcohols and long chain esters soluble in ethanol and it is separated from the other fractions with the addition of water and subsequent decantation. From this step the lighter organic fraction is obtained and this constitutes the fusel oils, which are stored separately in the column oil recovery.

Subsequently there is the purification of the intermediate through another series of columns. This is first introduced into the purification column (extractive distillation column) where it is diluted with a stream of water injected at the head of the column. The partially purified residue is sent to a second purification column (rectifier column) with the removal of the other congeners. Subsequently the product deriving from this operation is sent to the demethylation column where ethanol is extracted at the base of the column with the removal of methanol and other congeners. At the end of the distillation apparatus there is a concentration column, which receives the flows coming from the two purification columns and concentrates the congeners.

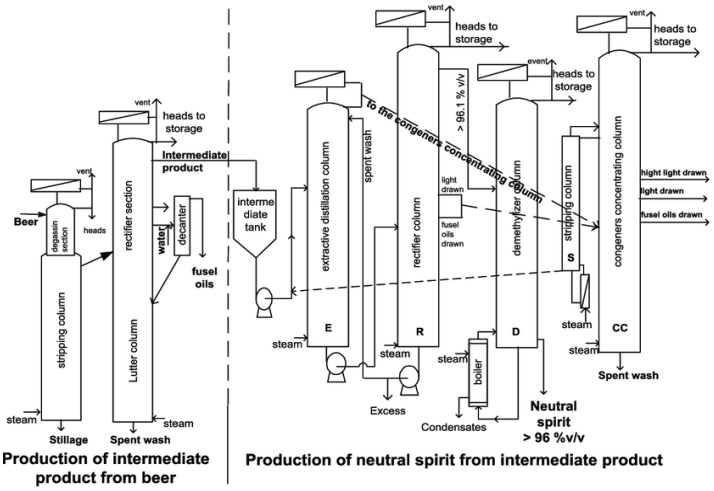

Figure 52: Distillation plant for the production of neutral alcohol from grape pomace

In the oenological distillation plant the grape pomace is conveyed in the fractional distillation column and here the alcoholic fraction, rich in ethanol, is removed and sent to the base of concentration column. The products of the fractional distillation column head are sent to the purification column for the recovery of alcohols. From the concentration column we have two different types of vapour streams, the ethanol rich fractions and the concentration tails. Of these fractions, the former are sent to the hydro-columns and the latter to the oil recovery column. In the hydro-column, the fraction corresponding to the reflux is removed from time to time, while the fractions at the head of column are periodically added to the concentration tails and then go to the oil recovery column. In the same hydro-column the fraction of lightening of the oils coming from the oil recovery column is also sent. From the oil recovery column different oil fractions are obtained, which are sent together in the decanter. The most interesting fractions for the recovery of compounds of interest from the food and energy point of view are represented by the heads of the hydro column, by the tails concentration and by the oils fractions coming from the recovery oil column.

Figure 53: Typical pilot distillation plant

5.3 MAIN BY-PRODUCTS OF DISTILLATION IN WINE INDUSTRY

The main distillation waste products consist of the heads of the hydro-columns, the concentration tails and the oily fractions separated during the distillation process. The heads, depending on the starting water-alcohol mixture, and tails can be a source of interesting compounds such as esters and methanol. The oily fractions are particularly rich in higher alcohols and esters of long chain acids, which can be used as aromas in the cosmetic industry. These fractions have long been neglected, but being rich in such compounds they can be very interesting in view of new circular economy strategies applied to the wine industry.

In fact, as regards the state of the art of circular economy strategies applied to the grape pomace (fig. 54), these are predominantly addressed to the extraction of polyphenolic molecules, to obtaining energy through production of biogas and biopolymers such as polyhydroxyalkanoates by microbial fermentation (Martinez et al., 2016).

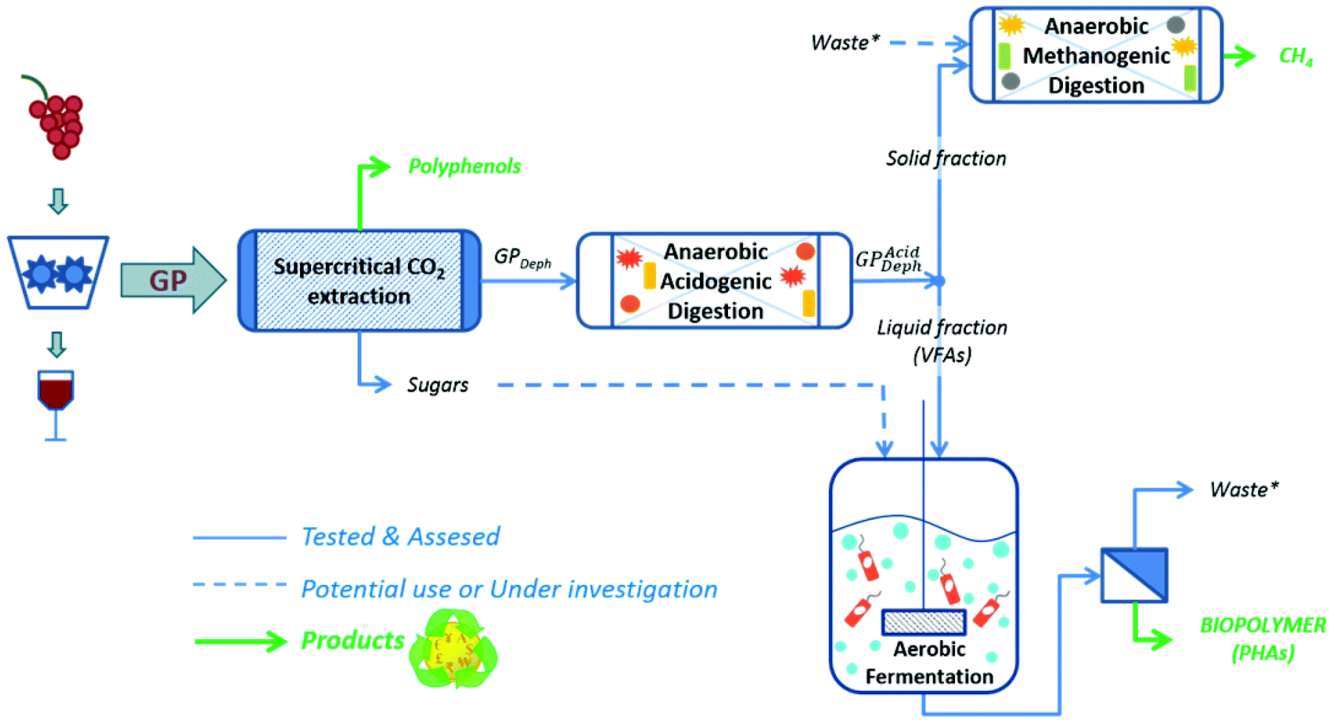

Figure 54: Main circular bio-economic strategies applied to the valorisation of grape pomace (Martinez et al., 2016)

The extraction of polyphenolic compounds allows to obtain extracts with positive effects on human health to be used in food, nutraceutical and pharmaceutical sectors. The obtaining biogas from anaerobic digestion of grape skins extraction residues and biopolymers from aerobic fermentation allows it to be exploited from an energy and chemistry point of view of polymers (Martinez et al., 2016).

6. RECOVERY OF COMPOUNDS WITH HIGH ADDED VALUE FROM THE BY-PRODUCTS OF OENOLOGICAL DISTILLATION

6.1 VOLATILE COMPOUNDS IN WINE

The aroma of wine is the result of a complex interaction between numerous volatile compounds, which may depend on the grape variety used or may bio-synthesised by yeasts during alcoholic fermentation or post-fermentation (fig. 55). During alcoholic fermentation yeasts can use amino-acids according to different metabolic pathways and the most important aromatic compounds biosynthesised from amino-acids are represented by the higher alcohols and by the esters associated with them (Sumby et al., 2010).

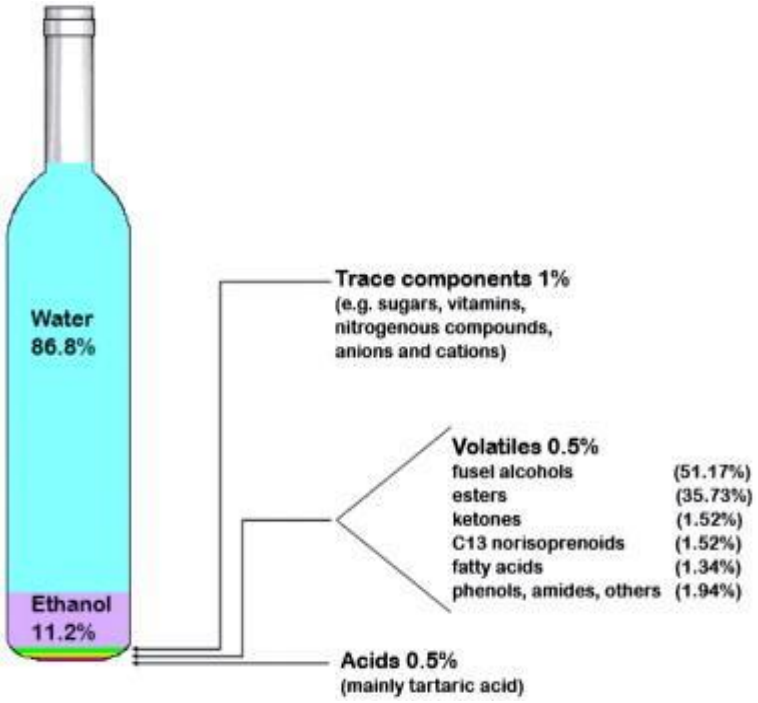

Figure 55: Main aromatic compounds in wines (Sumby et al, 2009)

6.1.1 BIOSYNTHESIS OF VOLATILE COMPOUNDS IN WINES AND DISTILLATES

The process by which amino-acids are catabolised to higher alcohols is known as the Ehrlich's reaction (fig. 56) and mainly involves the amino-acids valine, leucine, isoleucine and phenylalanine. The first step consists in a transamination in which α-keto acid is formed. This undergoes a decarboxylation to give and aldehyde. The aldehyde is then reduced through the NADH-dependent pathway to give the corresponding higher alcohol or oxidised to give the corresponding carboxylic acid (Styger et al., 2011; Belda et al., 2017).

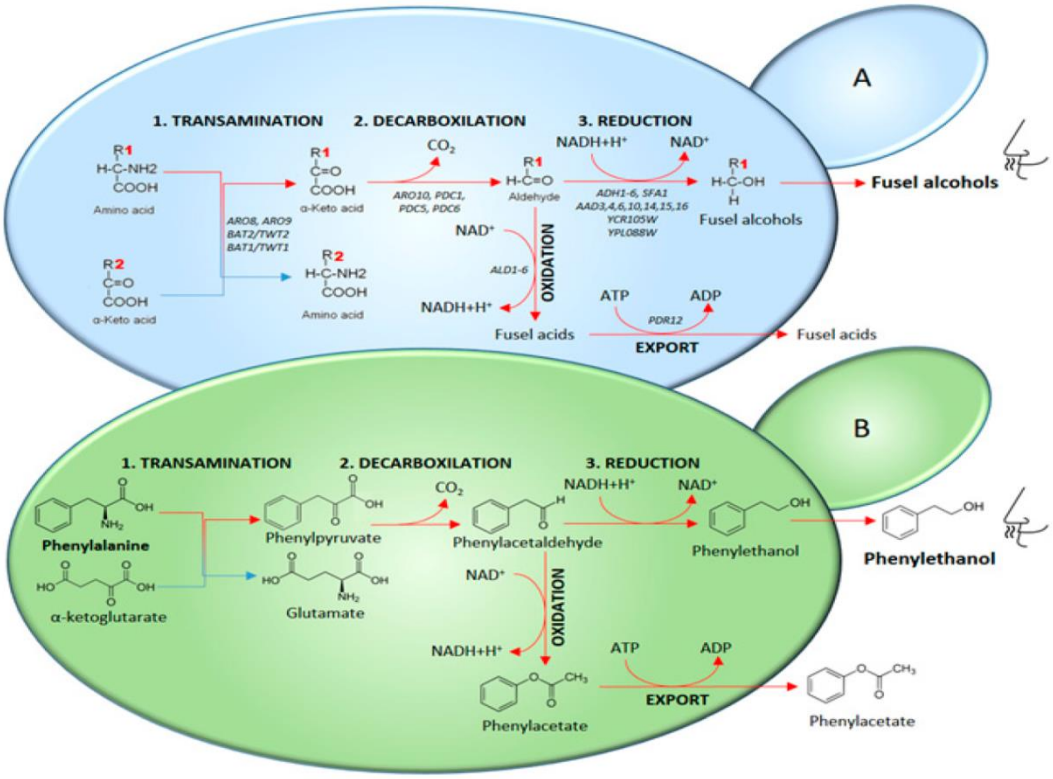

Figure 56: The Ehrlich's reaction pathway with the catabolism of aromatic and branched-chain amino-acids (Belda et al., 2017)

With this process is formed from the leucine the isoamyl alcohol, from the valine isobutanol, from the isoleucine the amyl alcohol and from the phenylalanine the phenyl ethanol (fig. 57). Moreover, in the course of this metabolic pathway there also the formation of acetates such as isoamyl acetate, ethyl acetate by conversion of pyruvate and volatile fatty acids, involved in the biosynthesis of ethyl esters(Styger et al., 2011; Belda et al., 2017).

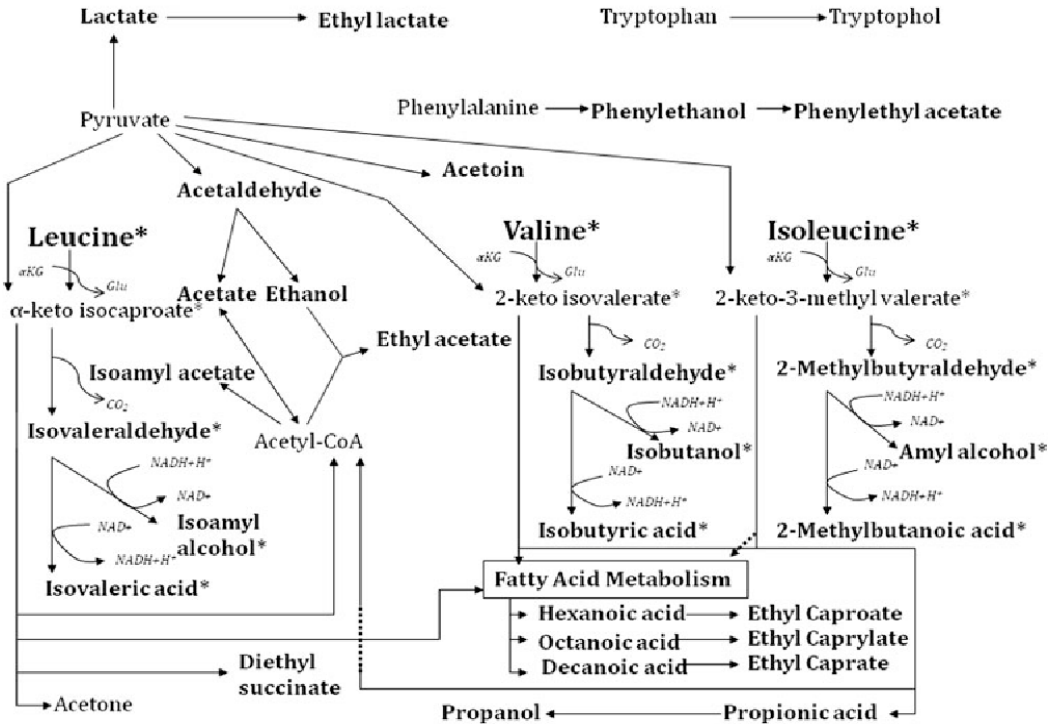

Figure 57: Ehrlich pathway complex reactions (Styger et al., 2011)

Another very important class of volatile compounds responsible for the aroma of wines and distillates is ethyl esters. Esters are organic compounds, which originate by reaction between an acid and alcohol. Their enzymatic formation starts with the activation of carboxylic acid with coenzyme A and with the formation of acyl coenzyme A, catalysed by the acyl coenzyme A synthetase (Styger et al., 2011).Subsequently, there is the alcoholysis of the acyl coenzyme A with the formation of the ester and restoration of coenzyme A. In this way, we have the biosynthesis of ethyl esters such as ethyl hexanoate, ethyl octanoate and ethyl decanoate (Sumby et al., 2010).

The other group of esters, represented by acetates, is always biosynthesised by the reaction of acyl coenzyme A (fig. 58) with the alcohols deriving from the catabolism of amino-acids during Ehrlich pathway. Compounds like isoamyl acetate and hexyl acetate are formed during this way (Sumby et al., 2010). The following figure illustrates the esterification with coenzyme A intervention.

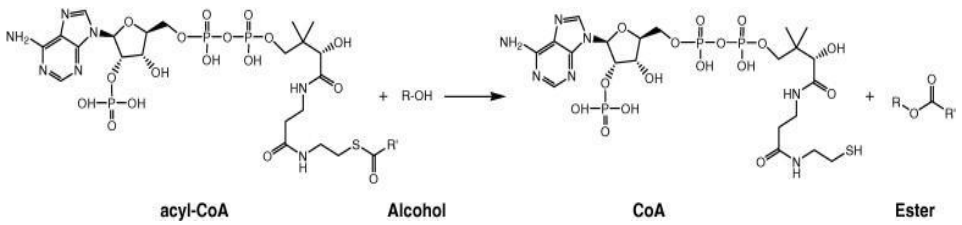

Figure 58: Formation of esters by yeasts biosynthesis in wine and distillates (Sumby et al., 2010)

6.1.2 ANALYTICAL DETERMINATION OF VOLATILE COMPOUNDS IN WINES AND DISTILLATES

An enormous variety of sophisticated analytical techniques are used in oenology to study the complex of metabolites present in wines and distillates. The most used are represented by chromatographic systems, liquid chromatography and gas chromatography, coupled to mass spectrometry. Mass spectrometry is one of the main instrumental analytical techniques used for the identification of unknown compounds from a given matrix. It is based on the ionisation of compounds in gas or liquid phase. A typical mass spectrometer consists of an ion source to produce the ions of analytes of interest, a mass analyzer, which separates the ions and measures the mass-charge ratio (m/z) and a detector to register the ions at each m/z ratio. The ionisation sources most commonly used in mass spectrometry are represented by the electrospray ionisation (ESI) and by electron impact ionisation (EI) (Lei et al., 2011). The electro-spray (fig. 59) method ionizes the analytes from an aqueous solution and for this it can be coupled with the liquid chromatography systems. In the ESI technique the solution of the analytes of interest for the liquid chromatography reaches the end of a capillary. This is maintained at some electric potential and the high electric field leads to the formation of a surface charge on the liquid containing the analytes. The solution undergoes an atomisation process, through the electrostatic repulsion of charged particles and the nitrogen conveying, with the formation of a spray of charged droplets (Kebarle et al., 1993; De Hofmann et al., 1997). The charged droplets undergo evaporation of the solvent with increasing charge density until the ions are released from the droplets (Kebarle et al., 1993). These are then sent to the analyzer for the separation (Alanon et al., 2015). The following figure illustrates the electrospray ionisation.

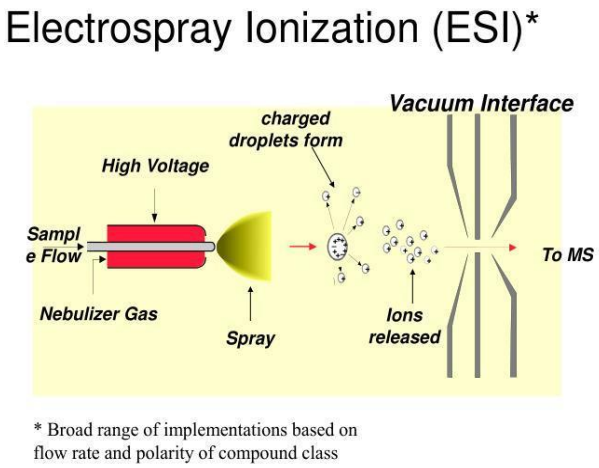

Figure 59: Mechanism of electrospray ionisation

The **electron impact ionisation (fig. 60)** involves the use of an electron beam, produced by an incandescent filament generally of tungsten. This electron beam repeatedly hits the molecules of the analyte in the gas phase. Thus molecular ions and their fragment ions characteristic of the chemical species of interest are generated (De Hofmann et al., 1997). These can be identified through the use of specific libraries of compounds. The figure below shows the electron impact for the ionisation of organic compounds.

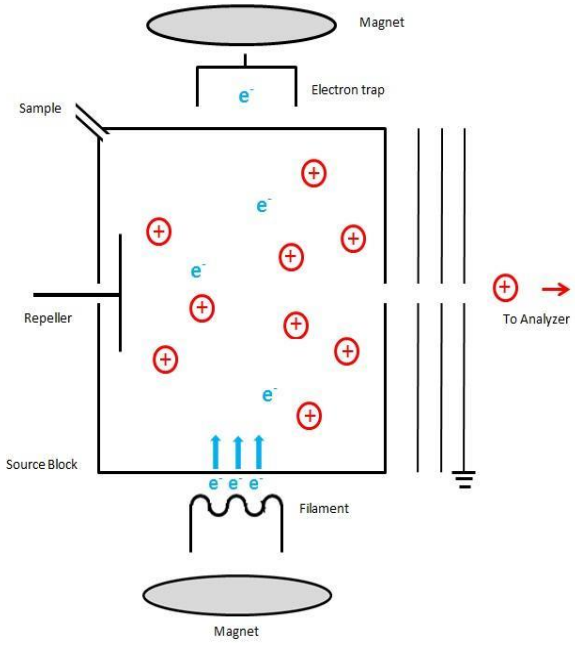

Figure 60: Electron impact mechanism

The main mass analyzers can be classified in this way:

1. ion trap (IT);
2. time of flight (TOF);
3. quadrupole;
4. orbitrap.

These analyzers in the mass spectrometer configuration can be stand alone or can be coupled. The coupling may concern two or more analyzers of the same type or two or more different analyzers (hybrid analyzers) and give rise to tandem mass spectrometry. The principal mass spectrometry techniques are:

1. triple quadrupole;
2. ion trap;
3. time of flight-time of flight (TOF-TOF);
4. quadrupole-time of flight (Q-TOF).

The quadrupole (fig. 61) is the one of the simplest and most versatile mass spectrometry analyzers. It is made up of four metal bars arranged parallel to each other and crossed by an electric current generated by a radiofrequency. In this way a magnetic field is generated and this allows the ions from the source to move inside the quadrupole. According to the voltage applied, the ions with a determined m/z ratio will cross the quadrupole, while the others with different values will be diverted and will not go. The quadrupole then acts as a filter and by adjusting the electric potential generated by the radiofrequency it is possible to monitor ions with a determined m/z ratio (De Hofmann et al., 1997). The single quadrupole can be used in two ways: Scan mode and SIM (Single Ion Monitoring). In the first method the spectra are acquired continuously by repeatedly varying the voltage, while in the second the quadrupole electric potential is chosen to monitor ions with a determined m/z ratio. The figure below shows the mechanism of single quadrupole analyzer for mass spectrometry.

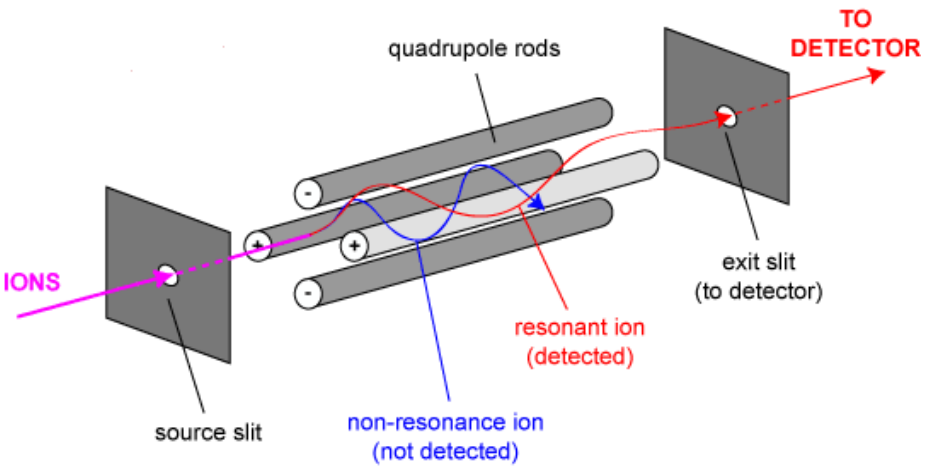

Figure 61: Quadrupole analyzer in the mass spectrometry

The main chromatographic systems coupled to mass spectrometry for the determination of wine metabolites are represented by gas chromatography-mass spectrometry **(GC-MS)** and by liquid chromatography-mass spectrometry **(LC-MS)** (Dettmer et al., 2007). The **GC-MS** combines the separation of compounds of interest in the transport gaseous phase, based on their different interaction with the stationary phase, with their identification by electronic impact mass spectrometry. The separation of the ions is allowed by a quadrupole. Thus the spectral fingerprinting of the samples is obtained. The **GC-MS** is particularly used for the qualitative and quantitative determination of volatile and semi-volatile compounds also through previous extraction step in solid phase and micro-extraction (Dettmer et al., 2007). The **LC-MS** combines the separation of compounds in the liquid phase, based on their different interaction with the stationary phase, with their identification by electrospray ionisation. This technique operates at lower temperatures than GC-MS and provides a large range of

metabolites. The separation of the ions obtained by electro-ionisation can take place by means of quadrupole analyzers, time of flight **(TOF)** or ion trap **(IT)** (Alanon et al., 2015).

In the ion trap analyzers (fig. 62) the ions are captured within a structure called an ion trap and undergo several fragmentations. The ion trap consists of three electrodes: a ring electrode in the middle, which replaces two of the bars of the linear quadrupole and the two ion inlet and outlet electrodes called end caps. The end caps are electrically connected and an electric potential is developed between theme and the ring electrode. By applying to the annular electrode a given electric field, various ions are trapped inside it and exerting a compression effect on them. Initially, the entire ion range is trapped inside the quadrupole ion trap (De Hofmann et al., 1997). Then with the transmission of radiofrequency pulses there is the generation of an electric field between the ring electrode and the end-caps and the intensity is such as to cause the sequential expulsion of ions as a function of their mass-to charge ratio. This property is called mass selection due to instability. A CID (collision induced dissociation) collision cell can then be inserted in the quadrupole ion trap. In the ion trap with CID for the tandem mass spectrometry the ions are stored in this cylindrical structure and those with a particular m/z ratio are fragmented by the collision with a gas (helium or nitrogen). The fragments are then scanned in succession to generate the tandem mass spectrum. The following figure shows the mechanism of ion trap mass analyzer.

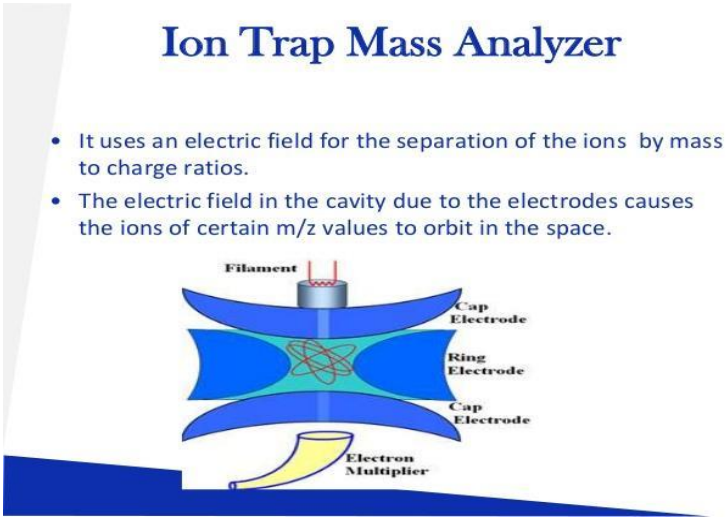

Figure 62: Structure and mechanism of ion trap analyzer in mass spectrometry

In the time of flight (fig. 63) the ions are accelerated with high kinetic energy and separated along the flight tube according to their different speed. This depends on their mass to charge ratio so that ions with a lower m/z ratio will travel faster the time of flight. It consists of a metal tube maintained at a certain potential to accelerate the ions coming from source. The fundamental physical principle of the time of flight is that ions having the same charge have equal kinetic energy, but velocity depending on

their mass. For these ions having a low m/z ratio will reach the detector first, while those with high m/z ratio value will come out later from the flight tube (De Hofmann et al., 1997). This is done in the linear mode of the time of flight, which however, provides a modest resolution. This problem is overcome with the reflectron procedure in which a ring ion mirror reflects the ions to the detector. Those that show a greater affinity with it will travel a greater path along the flight tube than the less interacting ones. In this way a higher resolution is obtained, in terms of spectral separation, for the ions having similar m/z ratios. The following figure illustrates the time of flight analyzer.

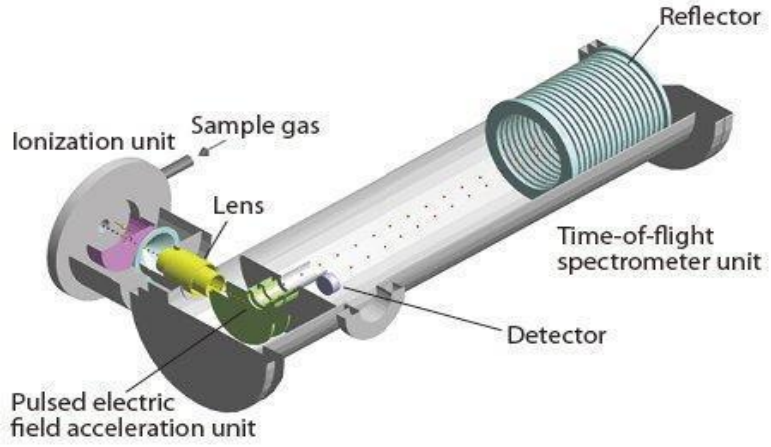

Figure 63: Time of Flight (TOF) analyzer in mass spectrometry

6.1.3 POSSIBLE USES IN THE FIELD OF AROMA CHEMISTRY AND IN THE ENERGY SECTOR

The volatile compounds, which constitute the flavours and fragrances, are obtained by chemical synthesis, through the extraction from raw materials of animal or vegetable origin or with the use of microorganisms by fermentation techniques. Based on this consideration, flavours and fragrances can be divided into natural, obtained by extraction form natural raw materials or by biotechnological methods, and synthetic, obtained by chemical synthesis (fig. 64). These compounds can find many applications in food, cosmetic and pharmaceutical sectors. The world demand for aromas and fragrances is estimated at around 20 billion dollars/year (Gupta et al., 2015). In particular among the most interesting volatile compounds, responsible for many sensory notes and object of enormous interest for the flavours and fragrances industry, we find esters such as ethyl acetate and, iso-butyrate and ethyl hexanoate and alcohols such as phenyl-ethanol. Esters are widely used in food and cosmetic sectors (Gupta et al., 2015).

Among the methods previously mentioned for the production of flavours and fragrances, including esters and alcohols, the chemical synthesis is not often safe and eco-friendly and extraction from natural sources is rather long and difficult due to the enormous presence of interfering chemical species in various matrices. Recently, microbial biotechnology strategies have been introduced. These use

microorganisms or enzymes as biocatalysts for the biosynthesis of flavours, but they are very still expensive to be fully applied on an industrial scale (Sciubba., 2009).

The approach of obtaining such compounds from food industry waste matrices offers several opportunities. On the one hand it make it possible to recover a waste matrix, avoiding disposal problems and on the other hand to obtain compounds, which can be used as flavours and fragrances and can be classified as natural aromas (de Oliveira Felipe et al., 2017; Saffarionpour et al., 2018). In particular from the waste fractions of the distillation of the wine industry it is possible to recover esters such as ethyl acetate, isoamyl acetate, ethyl laurate and ethyl octanoate usable as flavours in the cosmetic and food fields. The following figure illustrates the classification of flavours.

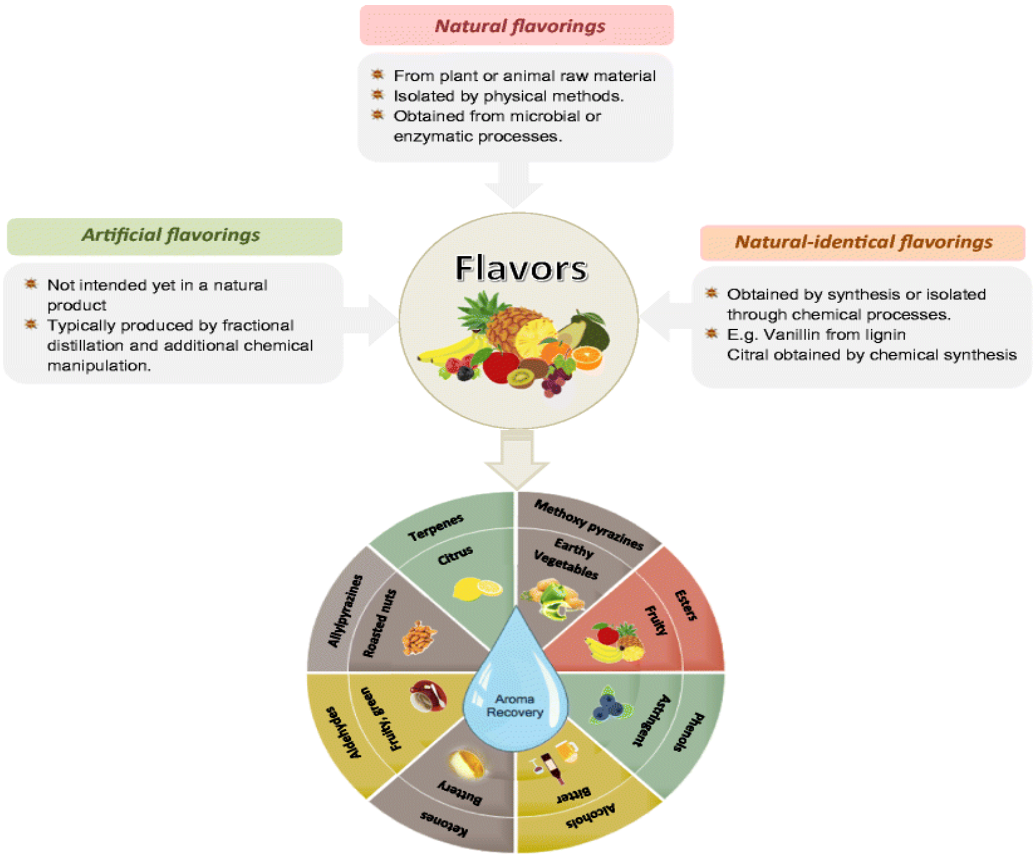

Figure 64: Classification of flavours (Saffarionpur et al., 2018)

Another interesting product, recoverable from the waste fractions of the distillation of the wine industry, is methanol. Methanol derives from the hydrolysis of the pectins contained in the grape pomace. Pectins are heteropolysaccharides formed mainly of galacturonic acid esterified with methanol and from the hydrolysis of this bond we have the liberation of it. This alcohol and its solutions can be used as reducing agents in the fuel cells. The fuel cell is an electrochemical energy converter, in which a fuel and an oxidant react, in correspondence of two electrodes separated by a membrane, for the conversion of chemical energy into electrical energy (Bahrami et al., 2013). In the direct methanol fuel

cells **(DMFC)** methanol and water are oxidised in the anode layer of the cell and release electrons (fig. 65). These will be transported through an external circuit to the cathode, where oxygen is reduced to water (Li et al., 2013). The direct methanol fuel cell is composed of five porous layers:

1. anode gas diffusion layer;
2. anode catalyst layer;
3. polymer electrolyte membrane;
4. cathode catalyst layer;
5. cathode gas diffusion layer

The fuel passes from the anode diffusion layer to the catalyst-containing layer. During the oxidation-reduction reaction, the methanol solution produces carbon dioxide, electrons and protons. The electrons will then reach the cathode by flowing through an external circuit and will go to reduce the oxygen to water. The figure below shows the structure of a typical methanol fuel cell (Bahrami et al., 2013).
The use of alcoholic bio-blends deriving from the alcoholic distillation supply chain can constitute an ecological alternative to the use of methanol alone.

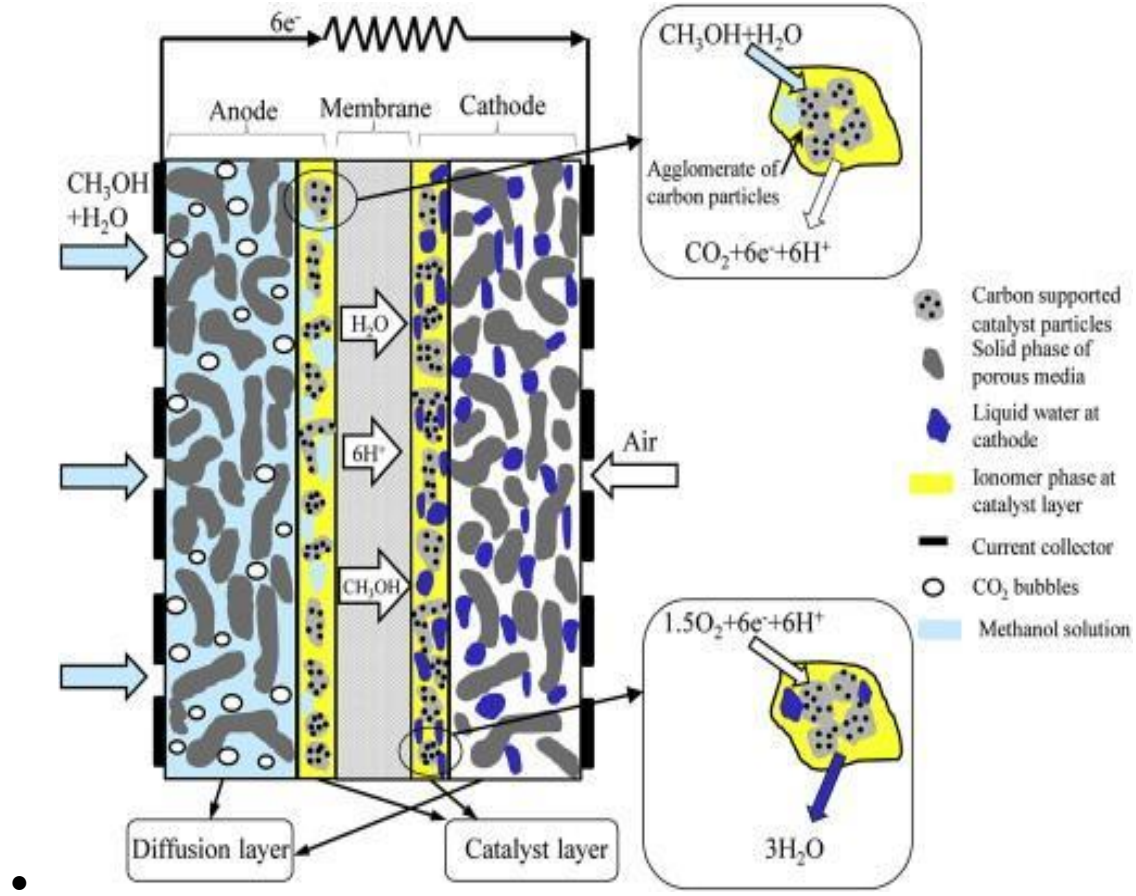

Figure 65: Representation of a direct methanol fuel cell (Bahrami et al., 2013)

AIM OF THE WORK

The purpose of this thesis work is to find alternative solutions for the enhancement of some by-products of the wine industry, which are still scarcely considered. Among them, grape stalks, which are made up of lignocellulosic biomass, could represent a source of biopolymers for the realisation of bio-composite materials. A cutting-edge technology consisting in an electrostatic separation is explored to verify the possibility to disassemble the different bio-polymers (lignin, cellulose, or hemicellulose). The different fraction are analysed to verify the concentration of simple sugars and phenolic compounds. The formation of furanic compounds deriving from sugars is also considered for their potential use as building blocks in fine chemistry.

Other interesting by-products are represented by those of distillation, mainly distillation heads, tails, and fusel oil fractions. These can be a source of interesting compounds from the standpoint of the chemistry of aromas due to the presence of esters and long chain alcohols, and from the energy standpoint due the presence of methanol. These by-products are mainly re-used for energy purposes by combustion and therefore without careful valorisation. The study aims to verify the possibility to use alcoholic phlegms resulting from distillation of the so-called “beer” obtained from the alcoholic fermentation of mash of different origin on the fuel cell technology. These fractions obtained from the distillation are rich of ethanol and methanol, but also higher alcohols, fusel oils, esters, aldehydes, and other minor compounds of yeast metabolism. Fuels with this complexity of composition have never been explored on fuel cells and they can give results very different from the expected one from the use of pure compounds such as methanol or ethanol as usually carried out.

7. MATERIALS AND METHODS

7.1 Chemicals

Absolute ethyl alcohol, acetic acid, acetic anhydride, acetoin, acetone, amyl alcohol, benzyl alcohol, butanoic acid, 1-butanol, 2-butanol, cellulase, ethyl acetate, ethyl decanoate, ethyl dodecanoate, ethyl hexanoate, ethyl isobutyrate, ethyl lactate, ethyl valerate, Folin-Ciocalteu reagent, furfural, gallic acid, glucose, hemicellulase, 1-hexanol, hexyl acetate, hydroxymethylfurfural, isoamyl acetate, isoamyl alcohol, isobutyl alcohol, laccase, limonene, methanol, 2-octanol, phenylethyl alcohol, 1-propanol, sulphuric acid, xylose were purchased from Sigma−Aldrich (Milan, Italy). Geniosil GF 31 3-methacryloxypropyltrimethoxysilane from Wacker Chemical Corporation (Milan, Italy). Deionized water was obtained through an Elix^{3UV} purification system (Merck Millipore, Milan, Italy).

7.2 DISTILLATION FRACTIONS

7.2.1. CLASSIFICATION OF THE DISTILLATION FRACTIONS

The distillations fractions of interest were supplied by the distillation company Caviro S.p.A. based in Faenza (Emilia-Romagna) and were classified as follows:

- distillation heads and tails deriving from the lees;
- distillation heads and tails deriving from the grape pomace;
- demethylation column reflux fraction fraction;
- epuration column recycling fraction;
- fraction containing fusel oils in the upper and lower phases.

These fractions were stored at room temperature in glass bottles in a place with low humidity and away from heat sources.

7.2.2. ANALYSIS OF THE DISTILLATION FRACTIONS

The distillation fractions were analysed by gas chromatography coupled to mass spectrometry prior the addition of the internal standard to the samples and preparation of a pure reference standard solution of known concentration, containing the compounds of interest.

7.2.3. PREPARATION OF THE DISTILLATION FRACTIONS SAMPLES ANG GC-MS ANALYSIS

The internal standard method consists in adding a compound, not present in the sample of interest, to a known concentration with behaviour similar to the analytes of interest. The signal of the internal

standard undergoes the same alteration as that of the analytes of interest and their relationship is independent of the sample and constant. A good internal standard must have the following characteristics:

- chemical-physical properties similar to the analytes of interest;
- must be separable from the other components of the sample;
- must not be present in the sample of interest;
- must not give rise to chemical reactions and interferences in the sample;
- must be miscible with the solvent used for the analysis.

As an internal standard, 2-octanol was chosen. A solution of internal standard 2-octanol was prepared at a concentration of 100.000 ppm. This solution was then added to the various distillation fractions as follows: 100 µL of the internal standard solution are introduced into a 5 mL flask and brought it to volume with the sample of interest. In this way the following solutions have been prepared:

- 5 mL of heads and tails lees with 2-octanol;
- 5 mL of heads and tails grape pomace with 2-octanol;
- 5 mL of demethylation column reflux fraction with 2-octanol;
- 5 mL of epuration column recycling fraction with 2-octanol;
- 5 mL of the upper phase of fusel oil fraction with 2-octanol;
- 5 mL of the lower phase of fusel oil fraction with 2-octanol.

A volume of 1 µL of each of these solutions was injected into a gas chromatograph Hewlett-Packard (HP) 6890 series instrument (Hewlett-Packard Waldbronn, Germany) with a split/splitless injection port coupled with a mass spectrometer instrument HP 5973 Mass Selective Detector (Hewlett-Packard Waldbronn, Germany), equipped with a capillary column Stabilwax-DA (Restek, Milan, Italy) 30 m, having an internal diameter of 0.25 mm and film thickness of 0.25 um. The oven temperature was set at 45 °C, and increased at 4.25 °C/min up to 230 °C and then held for 20 min, and finally increased at 15.00 °C/min up to 245 °C and then held for 10 min (74.53 total min of analysis). The injection was performed in split mode at 240 °C (split ratio of 20:1), the temperature of the transfer line was set at 240 °C. The carrier gas was ultrapure helium (constant flow rate 1 mL/min). The molecular fragmentation was obtained by electron ionization (EI). The data were obtained in full-scan mode and the mass to charge ratio (m/z) was recorded between 30 and 350 at 70 eV.

Chromatograms were acquired and processed using the software Enhanced Chem Station (G1701AA Version A.03.00, Hewlett Packard). Peaks were identified by comparing retention times and mass spectra of pure standards and by the library NIST Databases for GC/MS (Agilent Technologies).

Quantification was performed using the internal standard method. Peak integration was followed by the application of the following formula:

$$\frac{Compound\ area\ x\ (sample\ of\ interest)}{Internal\ standard\ area\ (sample\ of\ interest)}$$

Each sample was thrice analyzed following the same procedure.

7.2.4. PREPARATION OF THE STANDARD SOLUTIONS

In order to quantify the volatile molecules present in the various distillation fractions, standard solutions of 5 mL of these compounds were prepared at a concentration of 100.000 ppm as follows: 500 µL of the standard compound of interest are introduced into a 5 mL flask. This will be brought up to volume with ethanol. The standard solutions of the following compounds were thus obtained:

- Acetone;
- Isobutyl acetate;
- Ethyl acetate;
- Isoamyl acetate;
- Hexyl acetate;
- Acetic acid;
- Butanoic acid;
- Methanol;
- 1-Butanol;
- 2-Butanol;
- Propanol;
- 1-Hexanol;
- Isobutyl alcohol;
- Amyl alcohol;
- Isoamyl alcohol;
- Phenylethyl alcohol;
- Benzyl alcohol;
- Furfuryl alcohol;
- 2-Octanol (internal standard);
- Acetoin;
- Ethyl lactate;
- Ethyl isobutyrate;
- Ethyl valerate;
- Ethyl hexanoate;
- Ethyl octanoate;
- Ethyl decanoate;
- Ethyl dodecanoate;
- Limonene.

These standard solutions were then used for the preparation of a solution mixture of such compounds at a concentration of 2000 ppm as follows: 100 µL of each standard solution are placed in a 5 mL flask and this is then brought with ethanol.

7.2.5. CALCULATION OF THE RESPONSE FACTOR AND DETERMINATION OF THE ANALYTES CONCENTRATION

A volume of 1 µL of the mixture standard solution was injected into GC-MS (gas-chromatography coupled to mass spectrometry). The areas of the standard solution mixture compounds are thus determined. The response factor K was then calculated for each compound of the standard solution mixture, through two replicates of GC-MS analysis of this solution, with the following formula:

$$\mathbf{K} = \frac{Standard\ area\ x\ (standard\ mixture)}{Internal\ standard\ area\ (standard\ mixture)} \times \frac{Internal\ standard\ concentration}{Standard\ x\ concentration}$$

With the response factor is then possible to calculate the unknown **Cx** concentration of each analyte in the sample with the following equation:

$$\mathbf{Cx} = \frac{Compund\ area\ x\ (sampe\ of\ interest)}{Internal\ standard\ area\ (sample\ of\ interest)} \times \frac{Internal\ standard\ concentration}{K}$$

7.2.6. DETERMINATION OF THE ALCOHOL BY VOLUME OF THE DISTILLATION FRACTIONS

Of each distillation fraction the alcoholic strength was determined by gas chromatography coupled with mass spectrometry and the internal standard method was used. Acetone was chosen as the internal standard. For this reason two standard solutions of ethanol/acetone were prepared at a concentration of 10000 and 5000 ppm. These standard solutions were subjected to GC-MS analysis for the determination of the areas and therefore for the calculation of the response factor **K** with the following equation:

$$\mathbf{K} = \frac{Standard\ area\ of\ ethanol}{Internal\ standard\ area\ (acetone)}$$

Subsequently, the internal standard acetone was added to the various distillation fractions as follows: for each distillation fraction 100 mL of solution at a concentration of 5000 ppm were prepared, adding 500 µL of the fraction of interest and 500 µL of internal standard acetone and then bringing to volume with the distilled water. Thus the following solutions have been prepared with the internal standard:

- heads and tails lees 5000 ppm with acetone;
- heads and tails grape pomace with acetone;
- demethylation column reflux fraction with acetone;
- epuration column recycling fraction with acetone;
- upper phase amyl oil fraction with acetone;
- lower phase amyl oil fraction with acetone.

A volume of 1 µL of each of these solutions was injected into GC-MS for the calculation of ethanol and acetone area in the fraction of interest. Thus the alcoholic degree was calculated with the following relation:

$$\textbf{Alcohol by volume} = \frac{Area\ ethanol\ (fraction\ of\ interest)}{Area\ internal\ standard\ (acetone)} \times \frac{Internal\ standard\ volume}{K}$$

7.3. DETERMINATION OF THE CHEMICAL PROFILE OF THE DISTILLATION FRACTIONS USED FOR ELECTRICITY PRODUCTION IN THE FUEL CELL TECHNOLOGY

In this study, four different fractions discharged from a distillation plant for the production of neutral ethanol were tested: grape pomace heads and tails (HTG), lees heads and tails (HTL), epuration waste (EW), and demethylation waste (DW). These fractions had high ethanol content (around 70%) and methanol below 5% (table composizione delle frazioni).

The instrumentation used includes an direct methanol fuel cell (DMFC; F111, Fuel Cell Store, College Station, Texas, USA) that works with dominant methanol solutions (3% w/w). The membrane used is of the PEM type, made of Nafion and uses a Pt-Rd binary catalyst on a carbon support with an active surface of 2.25 cm^2. To measure and graph current and voltage, a data logger to set the voltage and a multimeter to measure the current passing through the circuit were placed in series with the cell. The circuit thus assembles requires that the data logger defines the desired load (through the use of an internal variable-value resistor), the cell is the current generator and the multimeter measures the current passing. The power generator in this case was sized for power up to 10mW.

About 1.5 g (exactly weighed) of each diluted fraction was introduced into the chamber of the DMFC. For each test, it was expected that the instrumentation would return to normal conditions. After each test, the cell was rinsed with distilled water and then with 1%-sulphuric acid to regenerate the membrane. The tests were carried out in a random order to avoid as much as possible a contamination from the previous sample, thus obtaining false results. The solutions used for the realisation of the different compositions were the same for each of the samples.

A different experiment was performed using the same fractions. After setting a steady electric potential and, as a consequence, a variable resistance, the reaction started once all the cables were connected and the value of current intensity was registered. The experiment was stopped when the current intensity was halved, regardless of the total time of the experiment, and the final net weight of the residual sample was measured.

All the fractions, such as and after the DMFC reaction, were analysed with GC-MS. A volume of 1 µL of each sample was injected into a gas chromatograph Hewlett-Packard (HP) 6890 series instrument (Hewlett-Packard Waldbronn, Germany), equipped with a capillary column Stabilwax-DA (Restek, Milan, Italy) 30 m, having an internal diameter of 0.25 mm and film thickness of 0.25 um. The oven temperature was set at 45 °C, and increased at 4.25 °C/min up to 66 °C and then held for 1.00 min, and finally increased at 8.00 °C/min up to 120 °C and then held for 5.00 min (17.69 total min of analysis). The injection was performed in split mode at 240 °C (split ratio of 20:1), the temperature of the transfer line was set at 240 °C. The carrier gas was ultrapure helium (constant flow rate 1 mL/min). The molecular fragmentation was obtained by electron ionization (EI). The data were obtained in full-scan mode and the mass to charge ratio (*m*/*z*) was recorded between 30 and 350 at 70 eV.

Chromatograms were acquired and processed using the software Enhanced Chem Station (G1701AA Version A.03.00, Hewlett Packard). Peaks were identified by comparing retention times and mass spectra of pure standards and by the library NIST Databases for GC/MS (Agilent Technologies). Quantification was performed using the internal standard method. Two different internal standard were added (3-methyl-1-pentanol 20 µL at 10,000 ppm and propionic acid 20 µL at 100,000 ppm). Each sample was thrice analyzed following the same procedure.

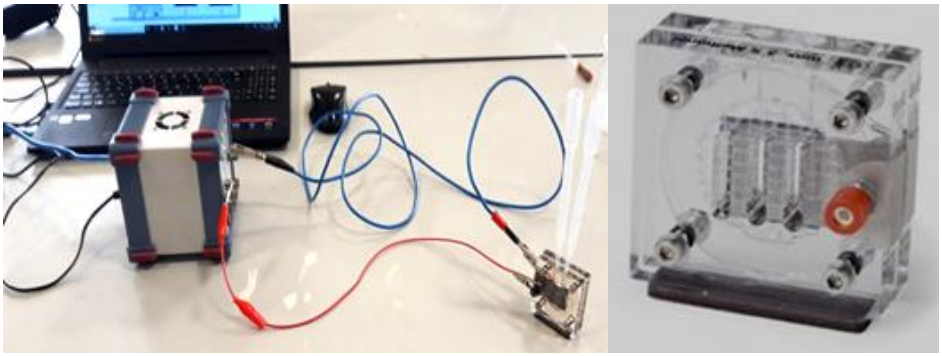

7.3.1. DETERMINATION OF RELATIONSHIP OF VOLTAGE, CURRENT INTENSITY AND APPARENT POWER DURING DMFC EXPERIMENTS

All the distillation fractions diluted with deionised water to 3% w/w of ethanol content were used in a different DMFC experiment letting the voltage (V) varying and by measuring the current intensity (mA) and apparent power (mW). Measurements were made using Pragma Industries Software (Biarritz, France).

7.4. GRAPE STALKS

7.4.1. PRETREATMENT OF THE GRAPE STALKS

The grape stalks, obtained from some wine companies, were first cleaned to remove residues of grape skins and grape seeds and then oven-dried at 65 °C up to constant weight (fig. 7.1). This process was carried out to remove water and prevent degradation reactions.

Figure 7.1: Oven for drying grape stalks

Subsequently, the dried grape stalks were subjected to milling in order to considerably reduce the dimensions of the material. A fine powder is thus obtained with a high surface area, thus facilitating the subsequent treatments of the material. The powder was then sieved in order to separate the finest fractions from the coarsest ones. For this purpose, sieves with the following meshes were used:

- 63 µm;
- 212 µm;
- 500 µm;
- 850 µm.

The various sieves were stacked in decreasing order of mesh size. The powder was placed on the first sieve with a mesh size of 850 µm and through a vibratory movement the various fractions separated and settled down on different levels according to the particle size (fig 7.2).

Figure 7.2: Separation of powder with the sieving equipment into its granulometric fractions

The fractions of the powder taken into consideration for subsequent treatments were the following:

- the finest fraction with a size less than 63 µm (285.40 g);
- the fraction with a size between 212 and 63 µm (285.61 g).

These fractions were then stored in sealed containers at room temperature.

7.4.2. ACETYLATION AND SILYLATION OF GRAPE STALKS POWDER

7.4.2.1. ACETYLATION

The fraction with a size between 63 and 212 µm was subjected to acetylation reaction (fig 7.3). The reaction consisted of the following steps (Hussain et al., 2004):

- 20 g of the powder were weighed and washed with 200 mL of hot water, thrice brought to boiling. The recovered material was subjected to centrifugation and oven dried at 105 °C for 24 h;
- the dried material was then treated with 200 mL of acetic anhydride and 20 mL of pyridine into a reaction flask connected to a refrigerant and immersed in a silicone oil bath under continuous stirring for about 3 h at 160 °C;

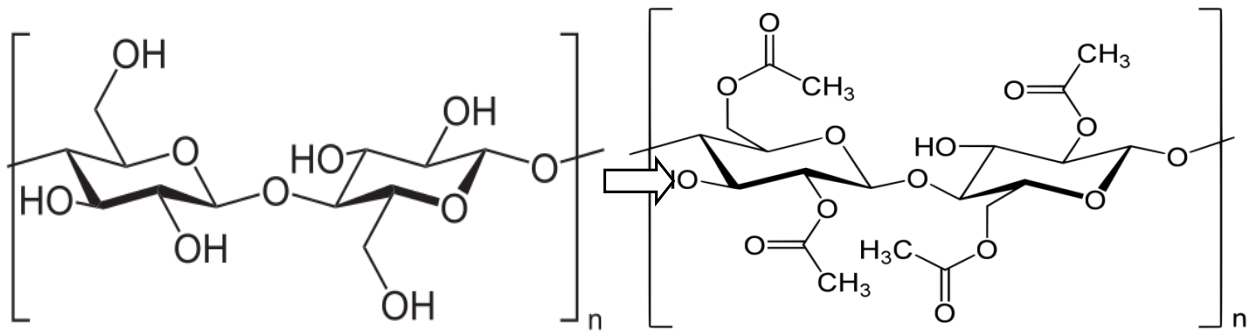

Figure 7.3: Conversion of cellulose into acetylated derivative

- the material was finally filtered by a Bückner apparatus and thrice washed with 30 mL of ethanol to remove the reagents. The recovered solid residue was then oven dried for two days at 65 °C.

The acetylation reaction was then carried out again with a higher amount of grape stalks powder with a size ranging from 212 to 63 µm. An aliquot of 50 g of this powder was weighed and introduced into a 1-L reaction flask together with 500 mL of acetic anhydride and 50 mL of pyridine. The reaction and the separation of the solid residue was carried out under the same conditions previously described.

7.4.2.2. SILYLATION

The silylation of the grape stalks powder with a size between 63 and 212 µm was carried out using 3-methacriloxypropyltrimethoxysilane (3-MPS) as derivatising agent (Fig. 7.4).

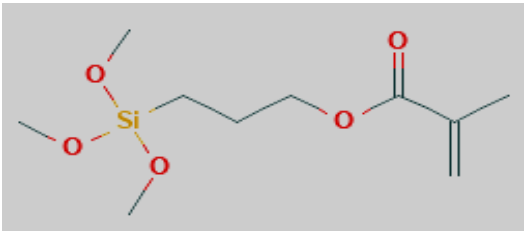

Figure 7.4: Structure of 3-methacriloxypropyltrimethoxysilane

3-MPS is usually used as a coupling reagent to modify the lignocellulose surface by forming C-O-Si ester bonds. The grape stalk powder (25.00 g) with a particle size between 63 and 212 µm was first dispersed in toluene (25.00 g) and then 3-MPS (24.84 g) was added (Brostow et al., 2016). The reaction mixture contained in a 250-mL reaction flask was then placed inside a reflux apparatus at 100 °C for 3 h under continuous stirring. The sample was then washed with toluene and dried over a

Bückner funnel. At the end of this treatment, the solid residue was placed into a porcelain tray and oven dried at 70 °C for 24 h.

Apparent density of the three samples (grape stalk powder such as, acetylated powder, and silylated powder) was carried out in two replicates. Colour measurements were carried out using a tristimulus reflectance colorimeter (Chroma Meter CR-400; Konica Minolta B.S. Italia S.p.A., Milan, Italy) set on the CIE standard illuminant D65. Brightness (L*), redness (a*), and yellowness (b*) were assessed by CIE tristimulus coordinates (McLaren, 1976). The three fractions were subjected to Fourier-transform infrared spectroscopic (FT-IR, Vertex 70, Bruker, Milan, Italy) to confirm the presence of the functional groups deriving from the derivatising reactions, and to compare the untreated material with the treated ones.

7.4.3. TESTS FOR THE REALISATION OF BIO-COMPOSITES

For the production of bio-composites, various tests were carried out using polybutylene succinate (PBS) as biopolymer (fig 7.5) and the three fractions of grape stalks powders as filler.

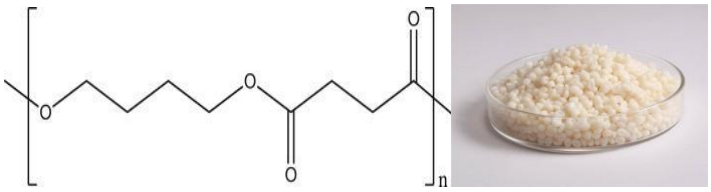

Figure 7.5: Structure and physical appearance of polybutylene succinate (PBS)

An aliquot of 150 grams of PBS and 1.5 grams of paraffin oil are weighed and mixed together. Each sample of grape stalk powder (15 g) was added and the whole content was properly mixed. Four samples were obtained using:

- grape stalk powder such as;
- acetylated powder;
- silylated powder;
- silylated powder *in situ*.

The mixture obtained was then extruded after purging the twin-screw extruder (fig. 7.6) (557 Rheomex, Haake S.r.l., Rezzato BS, Italy) with pure PBS.

Figure 7.6: Extruder equipment

The extruded materials were collected in a coil, then granulated and the yields were calculated.
The four granulates obtained were processed by injection moulding (fig 7.7) (MegaTech Tecnica DueBi injection moulding machine, Fabriano AN, Italy) in order to obtain tests for the mechanical and physico-chemical characterisation of the obtained bio-composites.

Figure 7.7: Injection moulding equipment

Colour measurements were made on the obtained bio-composites with the colorimeter and the granules of these are characterised by FT-IR spectroscopy.
Mechanical tests on the specimens were carried out through a dynamometer (5567 Instron, Pianezza TO, Italy).

7.5. ELECTROSTATIC SEPARATION OF GRAPE STALK POWDER

The finest fraction of grape stalk powder with an average particle size of less than 63 μm was subjected to electrostatic separation. A mass of 247.8 g of powder was introduced into a pilot electrostatic separator (TEP System, Tribo Flow Separations, Lexington, USA). The duration of the separation process was 10 min, while additional 10 min were set for the maximum recovery of the product.

The feeding system of the separator operated at 150 rpm. The particles in the F0 fraction (Fig. 7.8) were conveyed by compressed air along a charging line where they were charged by the tribo-electricity effect, both by impacting each other and impacting against the walls of the charging line. Subsequently, the charged particles passed through a separation chamber containing two high voltage electrodes (10000 V) where the positively charged particles are separated from the negatively charged ones. Two jars were located underneath the electrodes to gather the particles dropping into. Four fractions were obtained at:

2 electrodes (positive and negative);

2 jars (positive and negative).

Most of the powder of the two jars were pooled together (145.5 g) and subjected again to electrostatic separation, thus obtaining four fractions more.

1 control + 4 fractions from I separation + 4 fractions from II separation = 9 factions.

The particle size of the nine fractions was analyzed by laser granulometry (Maystersizer 2000; Malvern Instrument, Malvern, U.K.), the colour was measured by a tristimulus colorimeter and the morphology of the material was explored through a fluorescence microscope(Eclipse mod. 80i, Nikon instruments).

7.5.1. EXTRACTION TESTS ON GRAPE STALKS POWDER

The nine fractions deriving from the electrostatic separation treatment were subjected to a 2-step extraction with water followed by 2% sulphuric acid. Each sample (500 mg) was first extracted through three repeated cycles at 100 °C for 2 h, occasionally shaking, with deionised water. After each extraction the samples were centrifuged (DHLC-6632, Remi Electrotechnik, Vasai, India), the supernatants were recovered and the °Bx were measured to evaluate the rate of soluble solids extracted during each cycle. Finally, the residue was recovered using a Buchner funnel, while the supernatants were pooled together. The former was oven dried at 50 °C and its yield was calculated. Each solid residue was then added with 2% sulphuric acid, using a solid to solvent ratio 1:10, and extracted through three repeated cycles at 121 °C for 2 h with occasional shaking. The samples

were subjected to centrifugation at 2800 rpm for 15 min and the residue was recovered through Buchner funnel, while the supernatants were pooled together. The residue was oven dried at 50 °C and its yield was measured. The imbibition ratio (i.r.), defined as "mL of water imbibed per g of stalks" was calculated (Spigno et al., 2014).

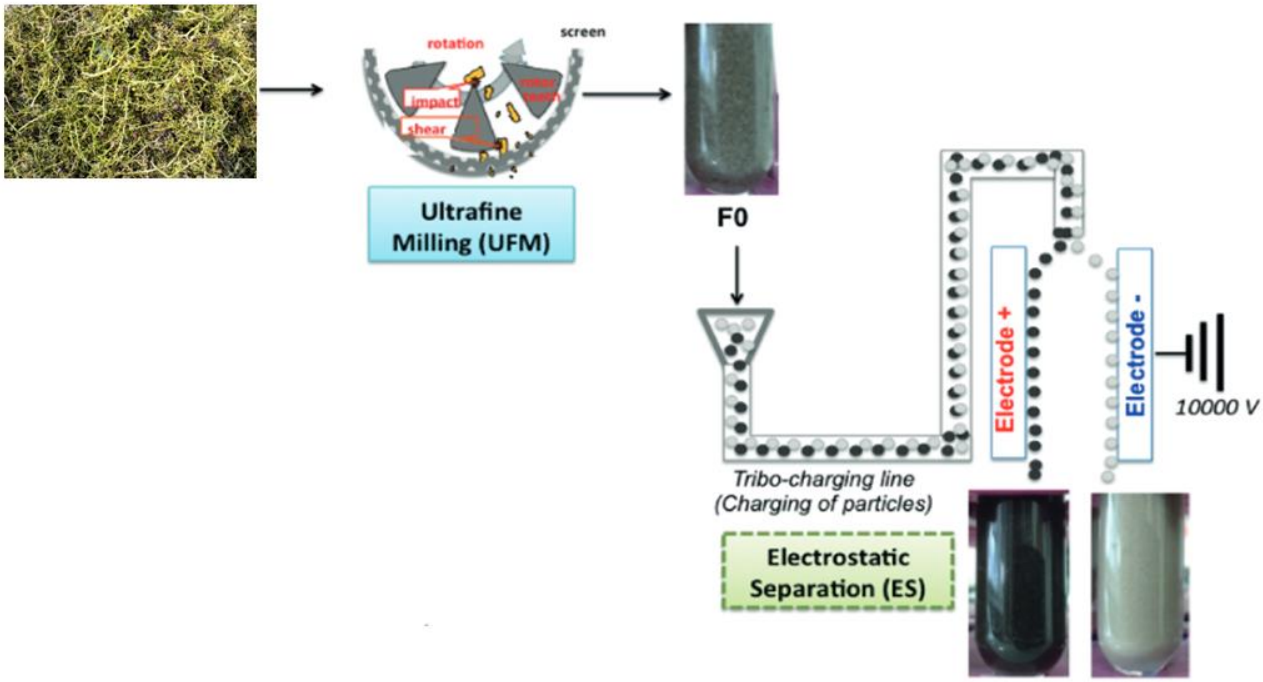

Figure 7.8: Electrostatic separation of grape stalks powder

7.5.2. HPLC DETERMINATION OF SUGARS AND FURANIC COMPOUNDS

The supernatants obtained from the extractions with both aqueous and acid extractions were then used for HPLC determination of sugars and furanic compounds. Each sample was analysed through a HPLC system (PU 4180, Jasco Europe Srl, Cremella, LC, Italy) equipped with a Rezex™ OOH-Monosaccharide H+ (Phenomenex, Bologna, Italy), 300 × 7.8 mm. The isocratic separation of sugars and furanic compounds was performed at 30 °C, using a mobile phase of sulphuric acid solution (pH 1.30) pumped into the column with a flow rate of 0.6 mL/min. The quantification of sugars was carried out with a refractive index detector (RI 4030, Jasco) and furanic compounds were quantified using an UV/Vis detector (UV4070, Jasco) at a wavelength of 280 nm. The identification of the analytes was performed by comparing the retention times of the peaks with pure reference standards. Quantification was carried out through the external standard calibration method.

7.5.3. COLOUR DETERMINATION

Spectrophotometric read of the wavelength at 440 nm was carried out on the undiluted aqueous and acid extracts and normalised by the specific sample weight. For the acid extracts the sulphuric acid solution at 2% p/v was used as blank solution (Spigno et al., 2014).

7.6. BIOCATALYTIC TREATMENT OF THE GRAPE STALKS POWDER

Grape stalks powder oven dried at 60 °C was also subjected to bio-catalytic treatment with different kinds of enzymes:

- laccase;
- hemicellulase;
- cellulase.

The powder was suspended in a citrate buffer and treated with different combination of enzymes at 45 °C, under continuous stirring. During the trials, the following combinations of enzymes were used for the treatment of lignocelluloses, by varying the enzymes concentration, expressed in units of enzymatic activity (U):

Laccase 25 U

- 100 mg of substrate with the addition of citrate buffer 975 µL and laccase 25 µL with enzymatic reaction times 24 h and 48 h. These samples were then diluted appropriately with water with a ratio 1:20 for the determination of absorbance with UV/VIS spectroscopy.

Laccase 50 U

- 100 mg of substrate with the addition of citrate buffer 950 µL and laccase 50 µL with enzymatic reaction times 24 h and 48 h. These samples were diluted with a ratio 1:40.

Laccase 100 U

- 100 mg of substrate with the addition of citrate buffer 900 µL and laccase 100 µL with enzymatic reaction times 24 h and 48 h. These samples were diluted with a ratio 1:100

The laccase enzyme was then combined with hemicellulase and cellulase. The following samples were prepared with laccase 100 U-hemicellulase 100 U

- 100 mg of substrate with the addition of citrate buffer 800 µL, laccase 100 µL and hemicellulase 100 µL with enzymatic reaction times 24 h and 48 h. These samples were diluted with a ratio 1:100 for the determination of absorbance at 280 nm and with a ratio 1:500 for the determination of absorbance at 500 nm (Molisch assay).

A similar procedure was carried out with laccase 100 U-hemicellulase 200 U

- 100 mg of substrate with the addition of citrate buffer 700 µL, laccase 100 µL and hemicellulase 200 µL with enzymatic reaction times of 24 h and 48 h. These samples were

diluted with a ratio 1:100 for the determination of absorbance at 280 nm and with a ratio 1:500 for the determination of absorbance at 500 nm (Molisch assay).

The following samples were prepared for the laccase 100 U-cellulase 100 U and laccase 100U-cellulase 200 U, respectively:

- 100 mg of substrate with the addition of citrate buffer 800 µL, laccase 100 µL and cellulase 100 µL with reaction times of 24 h and 48 h;
- 100 mg of substrate with the addition of citrate buffer 700 µL, laccase 100 µL and cellulase 200 µL with reaction times of 24 h and 48 h.

All these samples were diluted with a 1:100 ratio to determine the absorbance at 280 nm and with a ratio of 1:500 for that one at 500 nm (Molisch assay).

Finally, a combination of all three enzymes was used. The following samples were prepared for the laccase 100 U-hemicellulase 200 U-cellulase 100 U and laccase 100 U-hemicellulase 200 U-cellulase 200 U, respectively:

- 100 mg of substrate with the addition of citrate buffer 600 µL, laccase 100 µL, hemicellulase 200 µL, and cellulase 100 µL with reaction times of 24 h and 48 h;
- 100 mg of substrate with the addition of citrate buffer 500 µL, laccase 100 µL, hemicellulase 200 µL and cellulase 200 µL with reaction times of 24 h and 48 h.

The samples were then diluted with a 1:50 ratio to determine the absorbance at 280 nm and 1:1000 to determine that at 500 nm (Molisch assay).

Aside from the samples containing the enzymes, blank samples were prepared at times 24 h and 48 h using 100 mg of powder suspended in citrate buffer, but without adding the enzymes. For these samples dilutions with 1:10 and 1:20 ratios were adopted for the determination of absorbances at 280 and 500 nm (Molisch assay).

After the enzymatic reaction, the samples were subjected to centrifugation at 2000 rpm with the separation of the solid residue from the supernatant. The evaluation of absorbance at a wavelength of 280 nm was then performed on the supernatant with the UV/vis spectrophotometer for a qualitative evaluation of the presence of phenolic compounds.

The qualitative carbohydrate evaluation of monosaccharides and oligomers derived from the bio-catalytic cleavage of cellulose and hemicellulose was carried out using phenol/sulphuric acid colorimetric method (Molisch assay; Levine, 1930), consisting of the addition of 100 µL of phenol 5% and 1 mL of conc. sulphuric acid to the enzymatic extract. The absorbance was then evaluated at 500 nm. In this reaction, sulphuric acid causes the degradation of sugar to furfural, which, in turn, reacts with phenol to give an adduct that shows its maximum absorption at 500 nm.

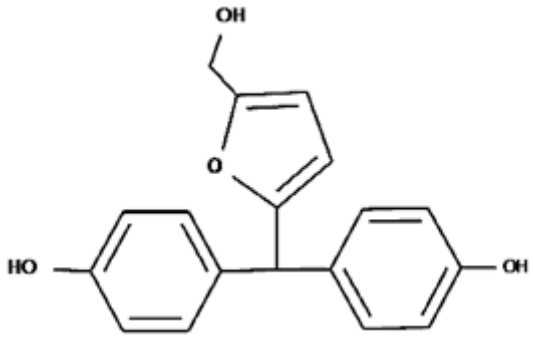

Figure 7.9: Adduct deriving from the phenol/sulphuric acid assay for carbohydrates

7.7. STATISTICAL ANALYSIS

Univariate analyses were carried. Differences among varieties were assessed by analysis of variance (one-way ANOVA) based on three replicates for each sample, after the verification of the normal distribution of the data set. When a significant effect (at least $P \leq 0.05$) was shown, comparative analyses were carried out by the post hoc Tukey's multiple comparison test. All tests were performed with Statistica v8.0 software (Stat 180 Soft Inc., Tulsa, OK).

8. RESULTS AND DISCUSSION

8.1. GC-MS ANALYSIS OF DISTILLATION FRACTIONS

The results of the GC-MS analyses on the distillation fractions are shown in table 8.1, together with the alcohol by volume (ABV) of each sample. Heads and tails deriving from grape pomace (HT G) showed very high concentration of methanol (around 38 g/L) with an alcohol by volume around 75%. However, epuration waste (EW), demethylation waste (DW), and lees head and tails (HT L) had high values of alcohol by volume, as well. All these samples showed promising characteristics for fuel cell applications.

In the upper lipophilic phase of the fusel oil fraction, high concentrations of medium-chain esters and alcohols were observed. These volatile compounds can find interesting applications in flavour industries.

	HT G	**DW**	**EW**	**HT L**	**Fusel oils (upper phase)**	**Fusel oils (lower phase)**
	mg/L	**mg/L**	**mg/L**	**mg/L**	**mg/L**	**mg/L**
Acetone	833	n.d.	17	12	14	19
Ethyl acetate	7899	47	5908	7272	40715	1385
Methanol	**38254**	**8337**	518	4527	2025	2960
Isobutyl acetate	31	n.d.	56	n.d.	100	7
2-Butanol	8116	52	19208	16005	26623	10435
1-Propanol	3887	n.d.	3560	6227	13421	56746
Ethyl isobutyrate	31	5	14	15	303	22
Ethyl valerate	138	n.d.	71	86	4020	106
Isobutyl alcohol	1078	2	n.d.		11265	2510
Isoamyl acetate	37	n.d.	261	70	1312	33
1-Butanol	26	n.d.	49	182	3341	1025
1-Pentanol	n.d.	n.d.	5	n.d.	1604	229
Isoamyl alcohol	149	8	995	735	73177	14229
Ethyl hexanoate	13	n.d.	108	64	4311	51
Hexyl acetate	n.d.	n.d.	3	n.d.	151	n.d.

Ethyl lactate	n.d.	n.d.	20	n.d.	6079	3627
1-Hexanol	n.d.	1	41	1	11829	1083
Ethyl octanoate	n.d.	1	247	3	15338	264
Acetic acid	928	n.d.	80	37	722	526
Acetoin	1058	n.d.	n.d.	n.d.	n.d.	228
Butanoic acid	47	n.d.	8	n.d.	4065	1038
Furfuryl alcohol	n.d.	n.d.	n.d.	n.d.	n.d.	n.d.
Ethyl decanoate	n.d.	n.d.	295	n.d.	36685	541
Phenethyl alcohol	n.d.	n.d.	1	n.d.	197	27
Benzyl alcohol	n.d.	n.d.	n.d.	n.d.	n.d.	n.d.
Ethyl dodecanoate	n.d.	n.d.	84	n.d.	18191	198
Alcohol by Volume (%)	**75**	**74**	**82**	**74**	**25**	**66**

Table 8.1: Results of the GC-MS analyses on the distillation fractions. HT G: grape pomace heads and tails; DW: demethylation waste; EW: epuration waste; HT L: lees head and tails; n.d.: not detected.

In the table 8.1 the concentrations of volatile congeners of all the distillation fractions are showed. The highest concentration of methanol (table 8.1 in bold) was found in the heads and tails deriving from the pomace (HT G), due to the high action of the pectinolytic enzymes on the pectines, followed by the demethylation column fraction (DW). Fusel oils, which have volatility lower than methanol and ethanol, tended to remain below the head of the distillation column and are removed by addition of water and subsequent settling process (Decloux et al., 2005).

8.1.1. ELECTROCHEMICAL MEASUREMENTS ON THE DISTILLATION FRACTIONS

The results of the four fractions are reported in Fig. 8.1, where the voltage (V) is reported as a function of the current (mA), in Fig. 8.2 the power (mW) is reported as a function of the voltage (V), and finally in Fig. 8.3 the power (mW) is reported as a function of the current (mA).

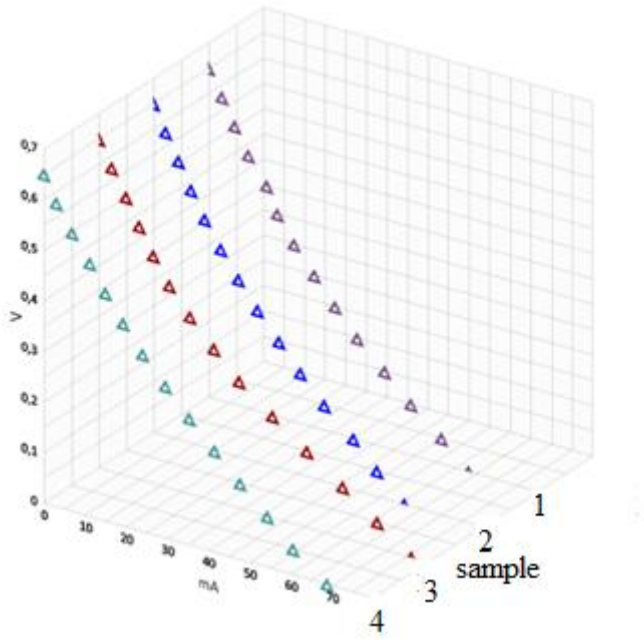

Figure 8.1: Current (mA) and voltage (V) variation in the fuel cell loaded with the 4 fractions.

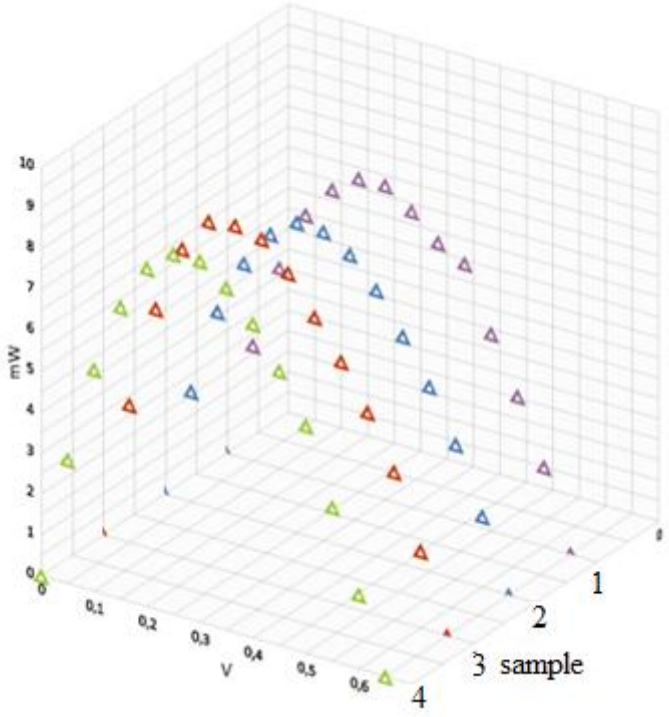

Figure 8.2: Voltage (V) and power (mW) variation in the fuel cell loaded with the four fractions

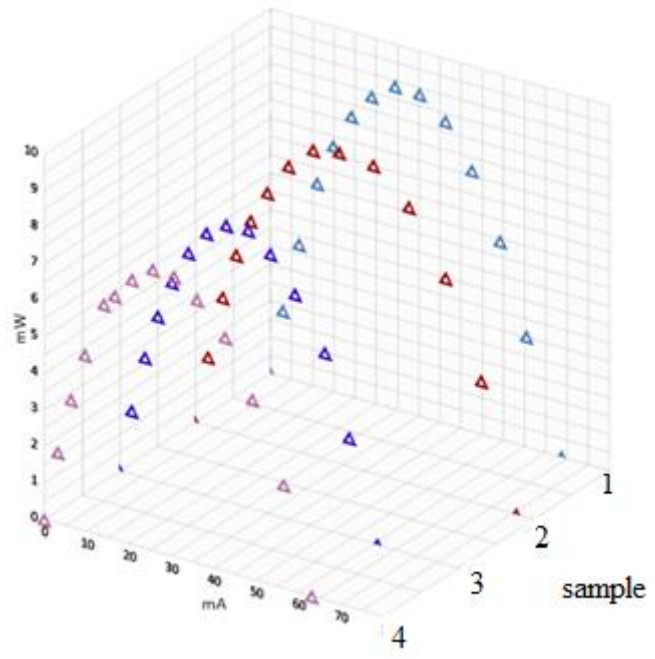

Figure 8.3: Current (mA) and power (mW) variation in the fuel cell loaded with the four fractions.

All the samples were able of releasing a measurable energy quantity. However, preventive trials with lab mixture of MeOH and EtOH (Fig. 8.4 and 8.5) showed that even a small amount of ethanol, added to the solution, was able to significantly lower the result. An EtOH content of 28% (case B tables 8.2 and 8.3) caused a decrease in power obtained on average 70.3% lower. Higher EtOH concentrations were less disrupting (Fig. 8.4 and 8.5). It was not possible to notice the same decrease by considering compositions B and F (tables 8.2 and 8.3), or any other solution, as extremes.

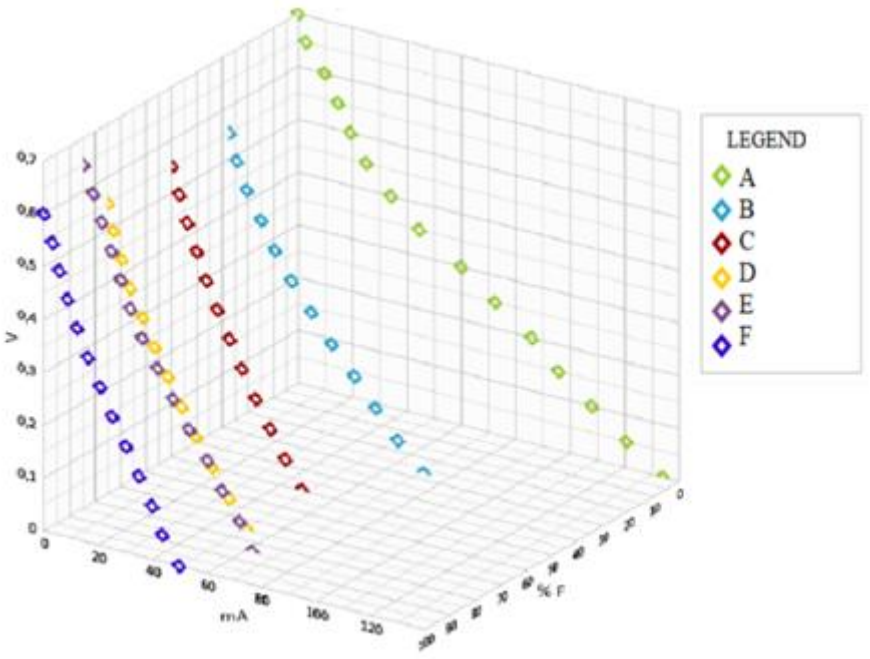

Figure 8.4: Current (mA) resulting from lab solutions of MeOH and EtOH.

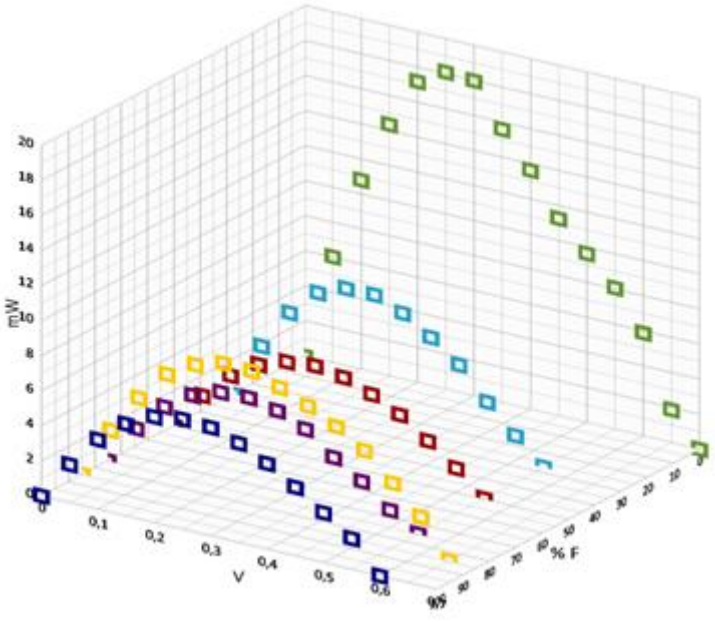

Figure 8.5: Tensions (V) resulting from lab solutions of MeOH and EtOH.

%EtOH %MeOH	0% 3.101%	0.894% 2.261%	1.635% 1.564%	2.464% 0.786%	2.784% 0.485%	3.291% 0%
V	mA (A)	mA (B)	mA (C)	mA (D)	mA (E)	mA (F)
0.00	134.08	71.55	47.73	51.00	61.98	49.68
0.05	120.53	61.90	41.60	44.28	57.33	43.48
0.10	107.93	53.83	36.03	38.20	50.98	39.73
0.15	95.63	46.03	30.75	32.35	45.55	34.95
0.20	85.85	37.63	25.70	27.05	38.78	30.15
0.25	72.38	30.20	21.15	21.93	32.85	25.10
0.30	59.93	22.93	16.73	17.05	27.20	20.63
0.35	44.55	16.80	12.65	12.73	21.65	16.20
0.40	34.08	11.73	9.10	8.03	17.30	12.23
0.45	25.03	6.55	5.63	4.95	13.68	8.70
0.50	19.28	2.83	2.70	1.95	10.28	5.68
0.55	14.65	0.00	0.00	0.00	6.68	3.18
0.60	9.78	/	/	/	3.55	0.00
0.65	2.88	/	/	/	0.00	/
0.70	0.00	/	/	/	/	/

Table 8.2: Composition (MeOH and EtOH) and measured mA at different voltages.

%EtOH %MeOH	0% 3.101%	0.894% 2.261%	1.635% 1.564%	2.464% 0.786%	2.784% 0.485%	3.291% 0%
V	mW (A)	mW (B)	mW (C)	mW (D)	mW (E)	mW (F)
0.00	0.00	0.00	0.00	0.00	0.00	0.00
0.05	6.03	3.10	2.08	2.21	2.87	2.17
0.10	10.79	5.38	3.60	3.82	5.10	3.97
0.15	14.34	6.90	4.61	4.85	6.83	5.24
0.20	17.17	7.53	5.14	5.41	7.76	6.03
0.25	18.09	7.55	5.29	5.48	8.21	6.28
0.30	17.98	6.88	5.02	5.12	8.16	6.19
0.35	15.59	5.88	4.43	4.45	7.58	5.67
0.40	13.63	4.69	3.64	3.21	6.92	4.89
0.45	11.26	2.95	2.53	2.23	6.15	3.92
0.50	9.64	1.41	1.35	0.97	5.14	2.84

0.55	8.06	0.00	0.00	0.00	3.67	1.75
0.60	5.87	/	/	/	2.13	0.00
0.65	1.87	/	/	/	0.00	/
0.70	0.00	/	/	/	/	/

Table 8.3: Composition (MeOH and EtOH) and calculated mW at different voltages.

As a matter of fact, ethanol and very likely also the other volatile congeners penalised the energy yield as already reported in literature (Leo et al., 2013). This result in the first place may seem daunting compared to the results of a pure MeOH supply (Fig. 8.6). However, these mixtures for a distillery are almost worthless wastes and there is a real profitable possibility to be exploited directly where they are produced with no cost for transport and negligible storage costs. Moreover, there is also the possibility to a further MeOH purification for fuel cell exploitation, diluting the fraction with water thus separating soluble alcohol from the rest of volatile congeners. The fractionation of the diluted alcoholic fraction could be quite easy.

For each distillation fraction, electrochemical measurements were performed for the determination of the electric current intensity and the apparent power at different voltages (table 8.4). HT G, HT L, DW, and EW showed a gradual decrease of the intensity of electric current and power during the application of the different voltages was due to the gradual development of the redox reaction inside the fuel cell.

	mA	**mW**	**mA**	**mW**	**mA**	**mW**	**mA**	**mW**
	HT G		**HT L**		**DW**		**EW**	
0 Volts	63.2±1.8		60.9±2.0		75.9±3.0		68.8±2.1	
0.05 Volts	56.6±1.3	2.8±0.1	54.3±2.3	2.7±0.1	67.7±3.8	3.4±0.2	60.5±4.0	3.0±0.2
0.10 Volts	49.2±0.9	4.9±0.1	48.5±2.7	4.9±0.3	59.2±3.0	5.9±0.3	54.3±2.9	5.4±0.3
0.15 Volts	42.8±1.0	6.4±0.2	41.5±2.2	6.2±0.3	50.6±2.1	7.6±0.3	47.7±2.0	7.1±0.3
0.20 Volts	36.1±0.8	7.2±0.2	35.7±1.6	7.1±0.3	42.2±1.3	8.4±0.3	41.4±1.7	8.3±0.3
0.25 Volts	30.7±0.7	7.7±0.2	30.4±1.4	7.6±0.3	34.1±1.4	8.5±0.3	35.3±1.7	8.8±0.4
0.30 Volts	25.7±0.9	7.7±0.3	25.2±0.9	7.6±0.3	28.0±0.4	8.4±0.1	29.5±1.5	8.9±0.5
0.35 Volts	20.8±0.7	7.3±0.3	20.6±0.9	7.2±0.3	22.2±0.8	7.8±0.3	24.0±1.7	8.4±0.6
0.40 Volts	16.7±0.3	6.7±0.1	16.3±1.0	6.5±0.4	17.2±1.0	6.9±0.4	19.2±1.5	7.7±0.6
0.45 Volts	14.1±0.5	6.4±0.3	12.4±1.0	5.6±0.5	13.3±0.6	6.0±0.3	15.0±1.4	6.7±0.6
0.50 Volts	9.7±1.0	4.8±0.6	9.1±1.1	4.5±0.6	9.8±0.5	4.9±0.2	11.2±1.1	5.6±0.6

0.55 Volts	6.4±0.6	3.5±0.4	6.0±1.0	3.3±0.5	6.6±0.6	3.6±0.3	6.9±0.5	3.8±0.3
0.60 Volts	3.3±0.4	2.0±0.3	2.9±0.5	1.7±0.3	3.2±0.5	1.9±0.3	3.0±0.5	1.8±0.3
0.65 Volts	0.0	0.0	0.0	0.0	0.0	0.0	0.0	0.0

Table 8.4: Electrochemical measurements on the heads and tails from grape pomace. mA: intensity of electric current; mW: apparent power. HT G: grape pomace heads and tails; DW: demethylation waste; EW: epuration waste; HT L: lees head and tails.

The composition of the fuel cell at the end of each experiment was considered (Table 8.5). The results are very difficult to explain and there are many differences among the different experiments, not only passing from one sample to one another, but also using the same sample under different operative conditions. Indeed, samples were treated either for 2 h (2-h experiment) without considering the electric parameters or stopped when half of the initial electric intensity was reached (½-intensity experiment), thus denoting that the time was variable during the various repetitions.

In general, acetaldehyde, 2-butanone, and acetic acid increased, while all the other substances decreased. The increase of acetic acid was particularly strong and not supported by a similar decrease of ethanol, its natural precursor together with acetaldehyde in an oxidation pathway (Fig. 8.7). The hydrolysis of ethyl acetate, probably occurred by considering the decrease of its concentration, it was not sufficient to justify such behaviour. Probably other substances were responsible of acetic acid increase, but their reduction rate was not so obvious due to the dilution of the distillation fraction carried out before feeding the fuel cell. All other substances, indeed, can be considered present only in trace amounts and thus below the limit of detection (< 0.1 mg/L). Even if in a lesser extent, the same considerations can be applied to the pair 2-butanol-2-butanone.

The situation does not substantially change by converting the results into “mmol/L” (table 8.6), a more correct procedure for evaluating the mass balance in the reactions that occur at the electrodes. The overwhelming presence of acetic acid persists, except in the case of waste from Epuration column. In the latter case, adding together the values of variations (A-B) obtained for acetaldehyde, ethanol, and acetic acid, the sum is 0.3 mmol/L. This is an acceptable result compared to the others that were 3 or 4 orders of magnitude higher. Unfortunately, the pair 2-butanol-2-butanone did not show a similar situation. The scarcity of cases and the extremely uniform situation should indicate the 0.3 value registered for acetic acid production as random.

	Heads and tail lees							Heads and tail marcs						
	2-h experiment				½-potential experiment			2-h experiment				½-potential experiment		
	mean	st dev	CV	A/B*	mean	st dev	CV	mean	st dev	CV	A/B*	mean	st dev	CV
Acetaldheyde	11	2	16	18	203	21	10	78	13	17	1	92	0	0
Ethyl acetate	697	32	5	0	337	27	8	984	77	8	0	309	7	2
Methanol	206	9	4	0	82	1	2	3603	335	9	0	705	924	131
2-Butanone	76	4	6	4	282	21	7	43	5	12	6	250	114	46
Ethanol	5728	495	9	1	3589	269	7	5053	90	2	1	3749	1387	37
2-Butanol	1309	52	4	1	683	14	2	562	3	1	2	861	909	106
1-Propanol	517	32	6	0	225	2	1	367	8	2	0	96	53	55
2-Methyl-1-propanol	13	12	88	1	16	1	8	24	0	2	0	11	7	69
2-Methyl-1-butanol	9	9	97	1	7	0	5	7	0	1	1	10	8	84
Acetic acid	15	10	67	874	13280	1881	14	92	17	18	97	8942	6122	68

	Demethylation column waste							Epuration column waste						
	2-h experiment				½-potential experiment			2-h experiment				½-potential experiment		
	mean	st dev	CV	A/B*	mean	st dev	CV	mean	st dev	CV	A/B*	mean	st dev	CV
Acetaldheyde	5	0	10	188	958	230	24	10	5	46	107	1114	953	86
Ethyl acetate	1	2	141	626	865	458	53	320	86	27	6	2001	22333	1116
Methanol	585	34	6	1	651	57	9	137	6	4	1	88	136	154
2-Butanone	9	1	9	1	10	4	36	206	29	14	5	1098	2029	185
Ethanol	7950	1364	17	1	7592	225	3	6446	544	8	1	6230	14444	232
2-Butanol	30	1	3	0	3	2	78	1757	8	0	2	2862	1037	36
1-Propanol	8	7	85	0	0	0		115	10	8	1	136	293	215
2-Methyl-1-propanol	3	4	141	0	0	0		12	4	35	1	14	81	593
2-Methyl-1-butanol	2	3	141	0	0	0		11	1	7	1	15	380	2464
Acetic acid	85	6	8	165	13972	2039	15	18869	7507	40	1	17666	13629	77

Table 8.5: Composition of the samples used in the fuel cell before and after the experiments (mg/L). *A/B: ratio of concentration (After the experiment/Before the experiment); CV: coefficient of variation

	Heads and tail lees			Heads and tail marcs		
	BEFORE	**AFTER**	**A-B***	**BEFORE**	**AFTER**	**A-B***
Acetaldheyde	0.3	4.6	4.4	1.8	2.1	0.3
Ethyl acetate	7.9	3.8	-4.1	11.2	3.5	-7.7
Methanol	6.4	2.6	-3.9	112.6	22.0	-90.6
2-Butanone	1.1	3.9	2.9	0.6	3.5	2.9
Ethanol	124.5	78.0	-46.5	109.8	81.5	-28.3
2-Butanol	17.7	9.2	-8.5	7.6	11.6	4.0
1-Propanol	8.6	3.7	-4.9	6.1	1.6	-4.5
2-Methyl-1-propanol	0.2	0.2	0.0	0.3	0.1	-0.2
2-Methyl-1-butanol	0.1	0.1	-0.0	0.1	0.1	0.0
Acetic acid	0.3	221.3	221.1	1.5	149.0	147.5
	sum		**160.5**			**23.5**

	Demethylation column waste			Epuration column waste		
	BEFORE	**AFTER**	**A-B***	**BEFORE**	**AFTER**	**A-B***
Acetaldheyde	0.1	21.8	21.7	0.2	25.3	25.1
Ethyl acetate	0.0	9.8	9.8	3.6	22.7	19.1
Methanol	18.3	20.3	2.1	4.3	2.7	-1.5
2-Butanone	0.1	0.1	0.0	2.9	15.3	12.4
Ethanol	172.8	165.0	-7.8	140.1	135.4	-4.7
2-Butanol	0.4	0.0	-0.4	23.7	38.7	14.9
1-Propanol	0.1	-	-0.1	1.9	2.3	0.4
2-Methyl-1-propanol	0.0	-	-0.0	0.2	0.2	0.0
2-Methyl-1-butanol	0.0	-	-0.0	0.1	0.2	0.1
Acetic acid	1.4	232.9	231.5	314.5	294.4	-20.0
	sum		**256.6**			**45.7**

Table 8.6: Composition of the sample used in the fuel cell before and after the experiments (mmol/L). In red, negative numbers that show a loss of substance.
***A-B: difference of concentration (concentration after the experiment – concentration before the experiment).**

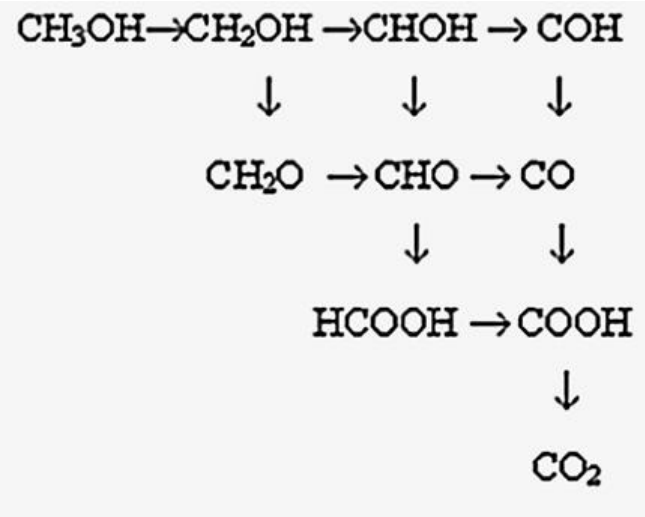

Fig. 8.6: Possible intermediate products of methanol oxidation

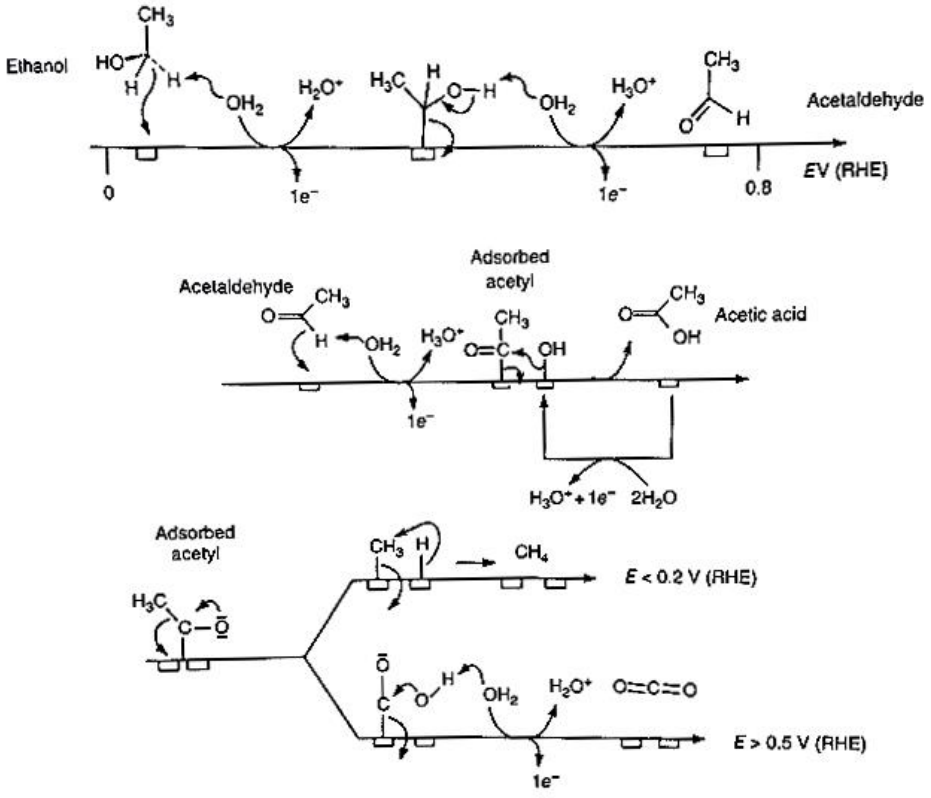

Fig. 8.7: Possible intermediate products of ethanol oxidation

8.2. BIO-COMPOSITES

Biodegradable materials of biological origin and derived from food leftovers are tested as reinforcements and fillers for bio-composite polymers.

The powder subjected to acetylation (Fig. 8.8 B) first gave a yield of 9.83 g (50%) starting from 20.00 g of grape stalks, while the second reaction yielded 31.19 g (62%) starting from 50.00 g of initial material.

The powder subjected to silylation (Fig. 8.8 C) first gave a yield of 24.34 g (97%) starting from 25.00 g of grape stalks.

(A) **(B)** **(C)**

Figure 8.8: Grape stalk powders such as (A), acetylated (B), and silylated (C)

The bulk density of the samples was measured with the 10 mL graduated cylinder. The derivatised samples showed significant lower densities than the untreated powder (Table 8.7), thus confirming the decrease of these as effect of the derivatisation reaction.

	Bulk density (g/cm^3)
ANOVA (F_{values})	87.0**
Grape stalk powder	0.62±0.03 c
Acetylated grape stalk powder	0.36±0.01 a
Silylated grape stalk powder	0.47±0.02 b

Table 8.7: Results of the bulk density measure of the grape stalk powder and derivatised ones. Results of the one-way ANOVA and the Tukey's test applied on values are reported as F_{values} and lowercase letters, respectively. Different letters identify samples significantly different ($P \leq 0.05$): ** $P \leq 0.01$.

8.2.1. STRUCTURAL ANALYSIS OF THE MODIFIED GRAPE STALK POWDER

The structural analysis of the modified grape stalk powder was performed by FT-IR in order to highlight differences in the presence of functional groups between control sample and derivatised ones. Figure 8.9 shows the IR spectra of the control raw material (A) vs. acetylated grape stalk powder (B). In the IR spectrum of the control the stretching band of the hydroxyl group (3300 nm) can be noted, while in the spectrum of acetylated material said band has almost disappeared and, at the same time, the carbonyl-group stretching band was very intense, as a consequence of the acetylation reaction.

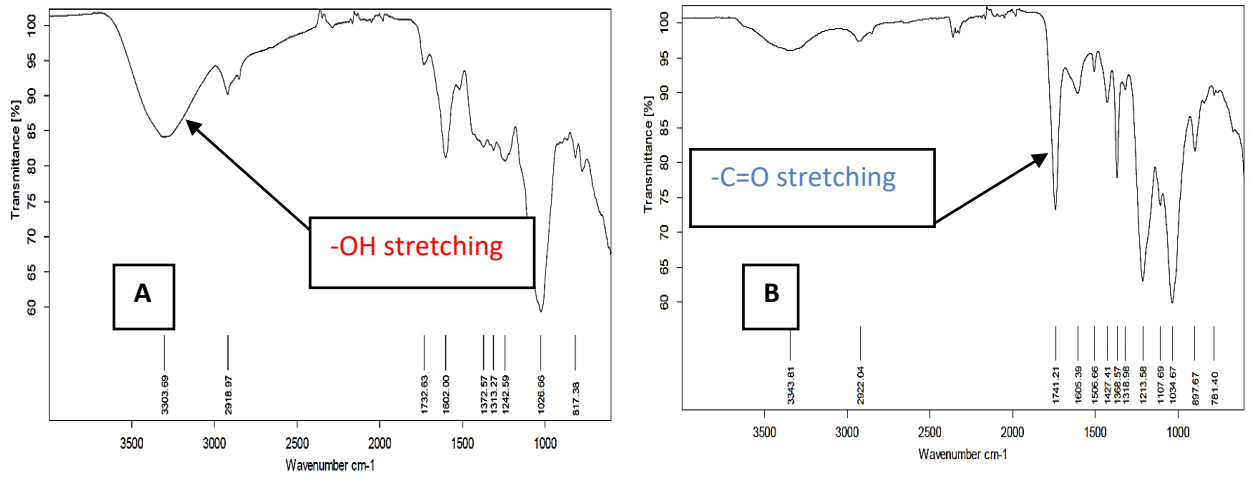

Figure 8.9: Control raw material (A) and acetylated grape stalks powder (B) FT-IR spectra

FT-IR spectra of silylated grape stalk powder were also acquired. Figure 8.10 shows the IR spectra of control raw material (C) vs. silylated grape stalk powder (D). Between these samples there was a high similarity, probably due to the poor reactivity of the silylating reagent to the grape stalk powder.

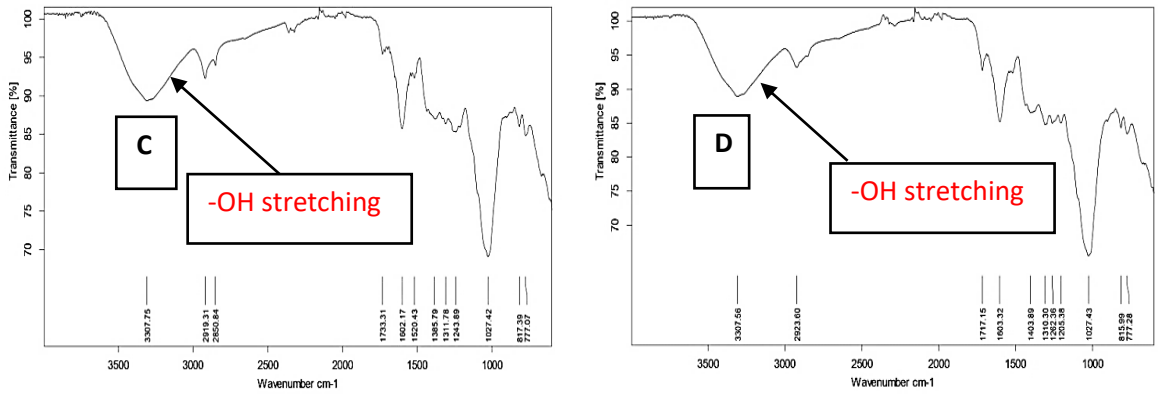

Figure 8.10: Control raw material (C) and silylated grape stalks powder (D) FT-IR spectra

8.2.2. MECHANICAL ANALYSIS OF THE BIO-COMPOSITES OBTAINED FROM THE GRAPE STALK POWDER

The results of the mechanical analysis of the bio-composites are shown in table 8.8. The bio-composite obtained from grape stalks such as, acetylated, and silylated grape stalk powder showed an increase by 14-15% of the stiffness (Young's modulus, E) in comparison with the pure PBS polymer. Such increase in stiffness is due to the hydrophobic interactions and to the hydrogen-bonds electrostatic forces between the modified lignocellulosic material and the co-polymer. The same increase was not shown by the silylated *in situ*, probably as a consequence of the poor derivatization of the substrate as demonstrated by the FTIR spectrum (figure 8.10). Tensile stress and elongation at break showed a inverse trend in grape stalks such as, acetylated, and silylated grape stalk powder showed, with a reduction of values in comparison with the PBS polymer.

	E [MPa]	**σ_M [MPa]**	**ε [%]**
PBS	623 ± 8	31.4 ±2	399 ±93
PBS +10 GS	712 ±6	25.4 ±1	98 ±109
PBS +10 GS acetylated	713 ±15	26.4 ±1	151 ±125
PBS +10 GS silylated	711 ±9	25.5 ±1	89 ±94
PBS + 10 GS silylated *in situ*	635 ±46	28.7 ±2	267 ±123

Table 8.8: Results of the mechanical analysis for the bio-composites. E: Young's modulus; σ_M: tensile stress; ε: elongation at break. PBS: polybutylene succinate; 10 GS: 10% of grape stalk; 10 GS acetylated: 10% of acetylated grape stalk; 10 GS silylated: 10% of silylated grape stalk; 10 GS silylated in situ: 10% of silylated in situ grape stalk.

Furthermore, a colourimetric evaluation using the CIELAB L*, a*, b* color space (McLaren, 1976) and the results are shown in Table 8.9. The most remarkable result is the very high difference between acetylated sample (powder, specimens, and granules) L*, a*, and b* values from those of the control and silylated sample. This is a further confirmation of the strong modification occurred during the acetylation reaction in comparison with the silylated one. The figure 8.11 show a picture of all the specimens.

	L*	a*	b*
ANOVA (F_{values})	4952***	1654***	4984***
GS powder	47.95b ± 0.60	7.95b ± 0.15	20.82b ± 0.26
GS acetylated powder	20.82a ± 0.14	3.38a ± 0.13	6.98a ± 0.25
GS silylated powder	50.34c ± 0.34	9.82c ± 0.14	22.45c ± 0.06
ANOVA (F_{values})	9294***	1152***	388***
PBS (specimens)	76.71d ± 0.61	1.14b ± 0.12	0.84a ± 0.64
PBS 10 GS (specimens)	34.00c ± 0.36	5.09c ± 0.24	7.69b ± 0.42
PBS 10 GS acetylated (specimens)	25.79a ± 0.17	0.48a ± 0.08	0.43a ± 0.10
PBS 10 GS silylated (specimens)	32.49b ± 0.31	7.26e ± 0.12	8.31b ± 0.08
PBS 10 GS silylated *in situ* (specimens)	32.71b ± 0.24	5.66d ± 0.14	8.18b ± 0.20
ANOVA (F_{values})	89.5***	383***	260***
PBS 10 GS (granules)	44.29b ± 1.43	6.72b ± 0.05	14.73b ± 0.37
PBS 10 GS acetylated (granules)	26.96a ± 1.56	2.12a ± 0.28	4.69a ± 0.64
PBS 10 GS silylated (granules)	46.56b ± 1.87	9.05c ± 0.31	17.26c ± 0.75
PBS 10 GS silylated *in situ* (granules)	46.93b ± 0.43	7.54b ± 0.11	17.70c ± 0.17

Table 8.9: Results of the colour analysis of the bio-composites. Results of the one-way ANOVA and the Tukey's test applied on values are reported as F_{values} and lowercase letters, respectively. Different letters identify samples significantly different ($P \leq 0.05$): ***$P \leq 0.001$. PBS: polybutylene succinate; PBS 10 GS: 10% of grape stalk with PBS; PBS 10 GS silylated: 10% of silylated grape stalk with PBS; PBS 10 GS acetylated: 10% of acetylated grape stalk with PBS; PBS 10 GS silylated situ: 10% of silylated in situ grape stalk with PBS.

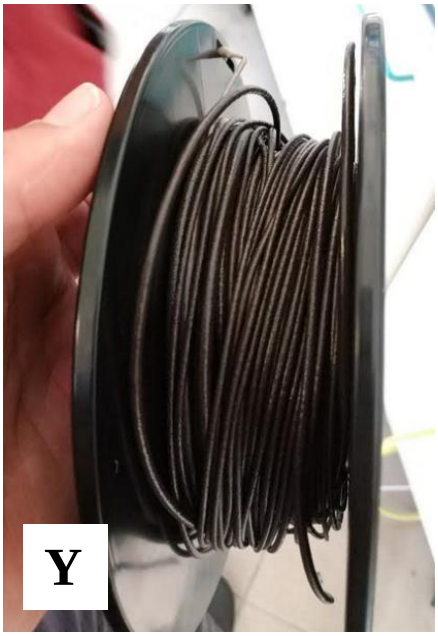

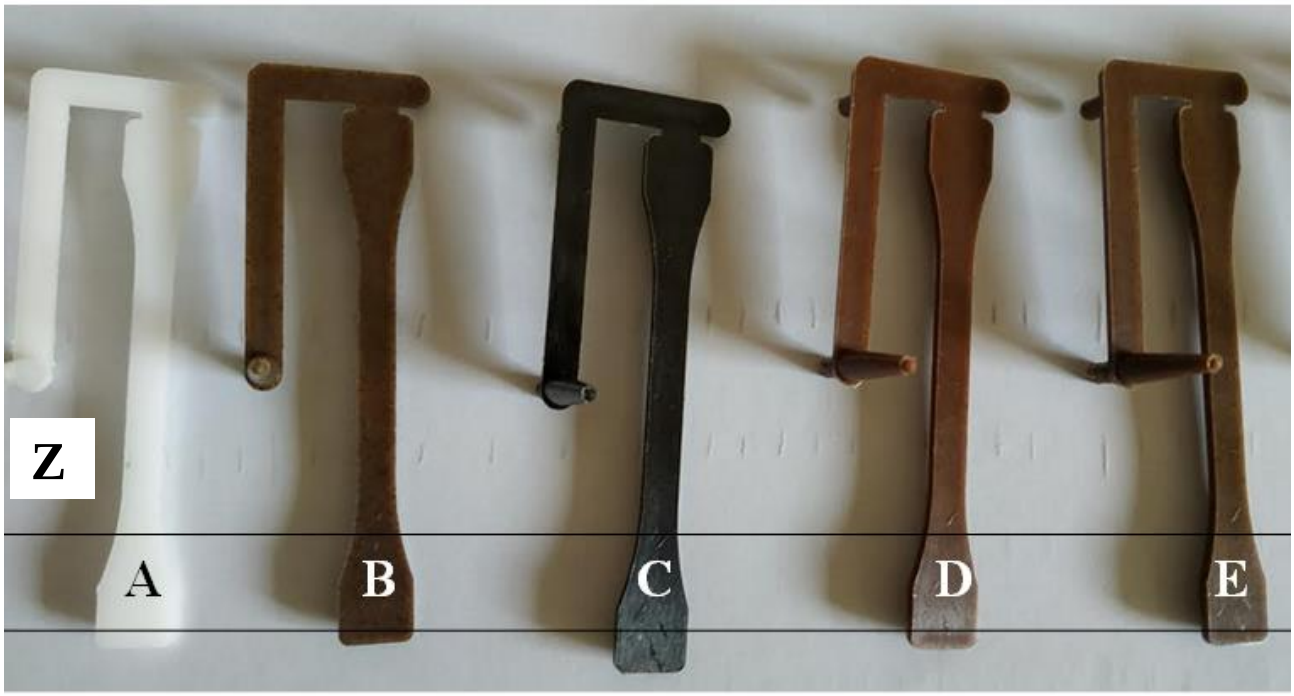

Figure 8.11: (Y) Extruded bio-composite materials wrapped in reels. (Z) Bio-composites obtained from grape stalk powders. From left to right: (A) PBS specimen, (B) PBS 10 GS specimen, (C) PBS 10 GS acetylated specimen, (D) PBS 10 GS specimens, and (E) PBS 10 GS silylated in situ.

8.3. ELECTROSTATIC SEPARATION OF GRAPE STALK POWDER

Electrostatic separation of grape-stalks powder with a particle size less than 63 μm was carried out in two steps. Table 8.10 shows the percentages of recovery in the first separation in correspondence of two electrodes and the jars placed under them.

	Mass of product recovered	Yield
Jar +	94.2 g	38.01%
Jar -	80.6 g	32.53%
Electrode +	22.3 g	9.00%
Electrode -	12.6 g	5.08%
Total mass recovered	209.7 g	84.62%
Total loss	38.1 g	15.38%

Table 8.10: Yields obtained in the first step of electrostatic separation.

Table 8.11 shows the yields in the second electrostatic separation of grape stalk powder when the two fractions. In the second phase of electrostatic separation the percentage of loss is higher by 9%.

	Mass of product recovered	Yield
Jar +	53.5 g	36.77%
Jar -	44.9 g	30.86%
Electrode +	8.7 g	5.98%
Electrode -	4.5 g	3.09%
Total mass recovered	111.6 g	76.70%
Total loss	34.9 g	23.99%

Table 8.11: Yields obtained in the second step of electrostatic separation.

8.3.1. GRANULOMETRIC ANALYSIS OF THE FRACTIONS DERIVING FROM THE ELECTROSTATIC SEPARATION

Table 8.12 shows the results of the granulometric analysis carried out on the nine fractions of the grape stalk powder. The granulometry of the samples collected at all the electrodes showed values of d (0.9) lower than those at all the jars, as well as the control. This is probably due to the weight of the particles with higher size that tended to fall down into the jars.

#	Sample Name	Span	Specific surface area	d (0.1) micron	d (0.5) micron	d (0.9) micron
1	**Control**	2.393	0.539	7.357	30.098	79.393
2	**Electrode-, I step**	2.542	0.736	4.427	19.892	54.990
3	**Jar-, I step**	3.181	0.780	3.526	21.687	72.514
4	**Electrode+, I step**	2.788	0.726	4.363	19.702	59.296
5	**Jar+, I step**	3.061	0.737	3.762	23.785	76.556
6	**Electrode+, I step**	2.784	0.746	4.121	19.409	58.150
7	**Jar-, I step**	3.008	0.760	3.528	23.995	75.711
8	**Electrode-, I step**	2.624	0.728	4.455	20.395	57.981
9	**Jar+, I step**	2.832	0.713	3.820	26.362	78.472

Table 8.12: Particle size analysis of the grape stalk powder fractions; d (0.1), d (0.5), d (0.9): these parameters indicate respectively that 10, 50, and 90% of the analyzed particles are lower the corresponding microns. Span: width of the distribution; index that correlates the d (0.9), d (0.1) and d (0.5), through the following formula: (d 0.9-d 0.1)/d 0.5.

8.3.2. FT-IR SPECTROSCOPY ANALYSIS OF GRAPE STALK POWDER FRACTIONS

Spectroscopic infrared analyses were performed on the nine fractions of grape stalks. There are some differences in the relative intensity of some functional group bands (figure 8.12 A), in particular the sample Electrode- (II step) showed the hydroxyl stretching band of lower intensity than the other samples. Instead, the sample Electrode+ (II step) showed the highest intensity related to the same band. However, this technique was not able to completely discriminate the fractions. Chemometric tools should be applied to deconvolute the spectra and obtain the latent information.

Figure 8.12 B shows the FT-IR spectrum of fraction 2 (Electrode-, I step) as an exemplification of the FT-IR spectra obtained from the stalk powder fractions. The wide absorption band at 3300 cm^{-1} is the hydroxyl-group stretching, while the stretching of carbonyl groups at 1602 cm^{-1} is due to the high abundance of the functional group in the lignin structure.

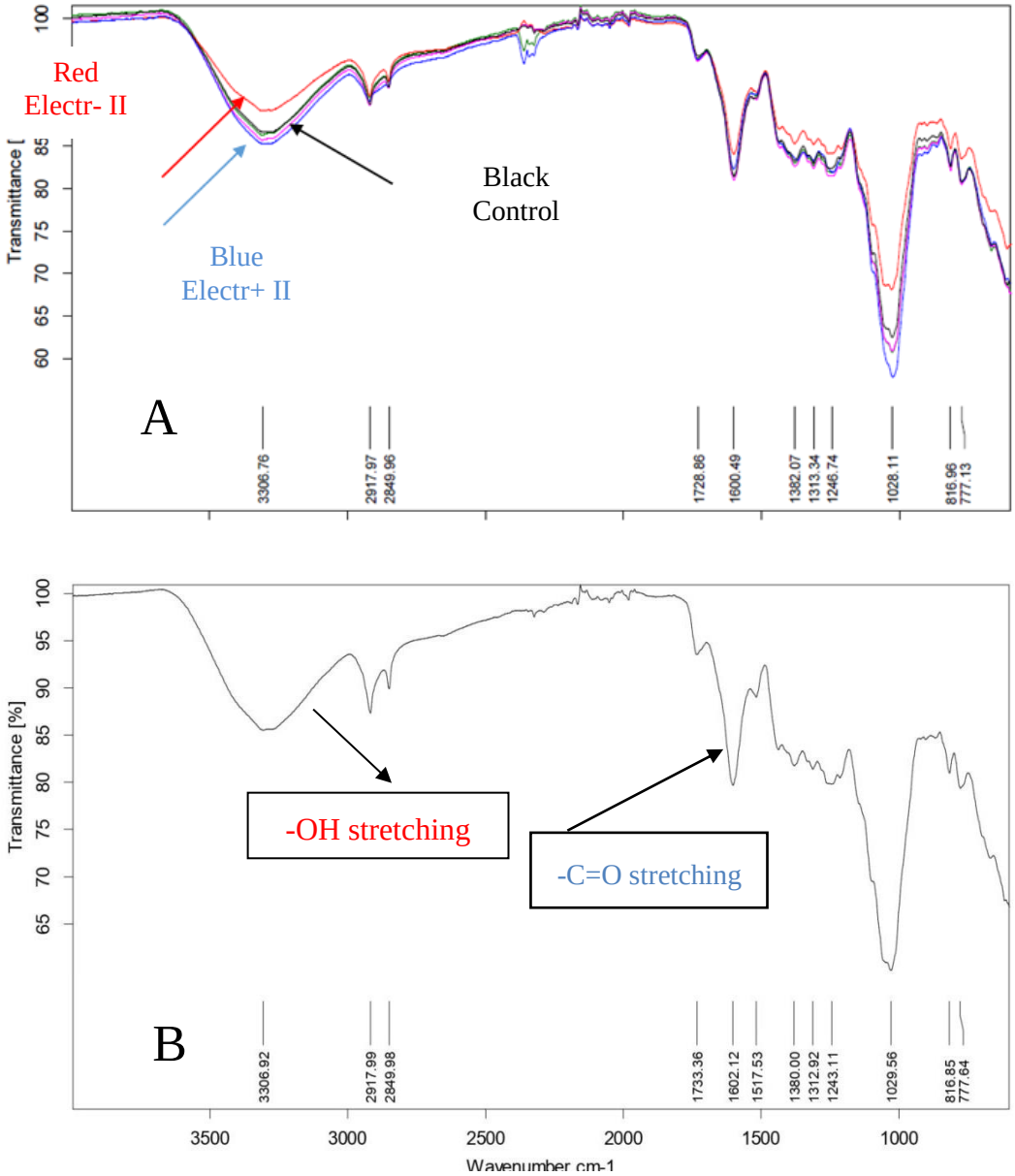

Figure 8.12: FT-IR of the overlaid spectra of all the fractions (A); FT-IR fraction 2 (Electrode-, I step) (B) of the grape stalk powder.

8.3.3. COLOUR ANALYSIS OF THE GRAPE STALK POWDER FRACTIONS

Grape stalks color analyses were performed on the nine powder fractions and the results are shown in the table 8.13. The lightness (L*) values were significantly ($P \leq 0.001$) lower in the samples E- I, E- II, and J- I. These samples are associated by the capacity to selectively migrate towards the positive electrode. E- II showed also the significantly highest values of a* followed by E- I, as well as of b*. These differences in hue were evident even with the naked eye. This represents a first clue of the ability of the electrostatic separation technique to obtain a partial separation of the main components based on their different physico-chemical characteristics.

The browning index measured as the absorbance at 440 nm of both aqueous and acid extracts showed significant differences among the fractions. However, only the high value of acid-extraction control was noteworthy. The absorbance at 440 nm of the aqueous extracts showed a significant positive correlation (r = 0.54, $P \leq 0.05$) with a*, while a* showed a negative positive correlation (r = -0.84, $P \leq 0.001$) with L*. The more a fraction is brown the less is bright and this assumption is particularly relevant to the fractions collected at the negative electrode.

		L*	a*	b*	440 nm aqueous extract	440 nm acid extract
ANOVA (F_{value})		34.68***	623.5***	14.07***	3.54*	14.78***
1	**Control**	53.8 ± 0.95^{b}	11.8 ± 0.10^{c}	23.4 ± 0.22^{a}	0.96 ± 0.07	1.13 ± 0.14^{b}
2	**E- I**	49.7 ± 0.95^{a}	13.7 ± 0.09^{d}	24.5 ± 0.09^{ab}	1.14 ± 0.10	0.57 ± 0.12^{a}
3	**J- I**	49.7 ± 0.50^{a}	11.8 ± 0.11^{c}	23.4 ± 0.07^{a}	1.02 ± 0.09	0.34 ± 0.09^{a}
4	**E+ I**	59.0 ± 0.33^{c}	10.4 ± 0.04^{a}	24.5 ± 0.03^{ab}	1.10 ± 0.16	0.43 ± 0.07^{a}
5	**J+ I**	55.0 ± 0.06^{b}	11.9 ± 0.03^{c}	24.7 ± 0.08^{ab}	0.96 ± 0.01	0.56 ± 0.01^{a}
6	**E+ II**	54.9 ± 1.12^{b}	11.4 ± 0.03^{b}	24.9 ± 1.02^{b}	0.92 ± 0.02	0.36 ± 0.03^{a}
7	**J- II**	53.8 ± 1.28^{b}	11.8 ± 0.01^{c}	24.5 ± 0.13^{ab}	1.06 ± 0.06	0.43 ± 0.05^{a}
8	**E- II**	49.2 ± 0.48^{a}	14.0 ± 0.02^{e}	26.5 ± 0.03^{c}	1.23 ± 0.01	0.46 ± 0.09^{a}
9	**J+ II**	53.3 ± 0.09^{b}	11.8 ± 0.06^{c}	25.4 ± 0.01^{bc}	0.95 ± 0.03	0.63 ± 0.11^{a}

Table 8.13: Colour analysis of the fractions of the grape stalk powder. Results of the one-way ANOVA and the Tukey's test applied on values are reported as F_{values} and lowercase letters, respectively. Different letters identify samples significantly different ($P \leq 0.05$): *$P \leq 0.05$; ***$P \leq 0.001$. E-: Negative electrode; E-: Positive electrode; J-: Negative jar, J+: Positive jar; I: first electrostatic separation; II: second electrostatic separation

8.3.4. DETERMINATION OF THE IMBIBITION RATIO (i.r.) OF THE FRACTIONS OF THE GRAPE STALK POWDER

During the extraction with water, r of the nine powder fractions was calculated and the results are shown in table 8.14. Also in this case, the significantly highest r values ($P \leq 0.001$) were shown by a homogeneous group of samples, notably E+ I, E+ II, and J+ II. These fractions selectively attracted by the negative electrode showed a higher water-absorption capacity in comparison with those driven to positive electrode. The ability of the fiber to hydrate and dissolve in water is usually associated with a low molecular weight. Conversely, high molecular weight polysaccharides, such as cellulose and hemicellulose, as well as lignin, are scarcely soluble in cold water, but they are soluble in a different extent in hot water and under acid and basic conditions.

The correlation evaluation showed a significant positive correlation between i.r. and L* (r = 0.85, $P \leq 0.001$) and negative correlations between i.r. and the absorbance at 440 nm of the aqueous extracts, as well as a* (r = -0.49, $P \leq 0.05$ and r = -0.83, $P \leq 0.001$, respectively).

		i.r. (mL/g d.w.)
ANOVA (F_{value})		32.48***
1	**Control**	2.05 ± 0.04^{cd}
2	**E- I**	1.78 ± 0.06^{b}
3	**J- I**	1.74 ± 0.06^{b}
4	**E+ I**	2.33 ± 0.05^{e}
5	**J+ I**	1.89 ± 0.12^{bc}
6	**E+ II**	2.20 ± 0.08^{de}
7	**J- II**	1.80 ± 0.08^{b}
8	**E- II**	1.43 ± 0.01^{a}
9	**J+ II**	1.94 ± 0.04^{bcd}

Table 8.14: Imbibition ratio of the extracts fractions of the grape stalk powder. Results of the one-way ANOVA and the Tukey's test applied on values are reported as F_{values} and lowercase letters, respectively. Different letters identify samples significantly different ($P \leq 0.05$): ***$P \leq 0.001$. i.r.: imbibition ratio; E-: Negative electrode; E-: Positive electrode; J-: Negative jar, J+: Positive jar; I: first electrostatic separation; II: second electrostatic separation

8.3.5. DETERMINATION OF THE °BX OF THE GRAPE STALK POWDER EXTRACTS

The soluble solids content expressed as °Bx normalised by the specific sample weight was measured after each cycle of aqueous extraction of each sample (table 8.15) to evaluate the progressive exhaustion of the sugars from the residue and the effectiveness of the extraction method. Extraction effectiveness after three cycles of extraction was considered satisfactory. Although this measures were not repeated, and as a consequence the ANOVA was not applied, °Bx showed similar values for all the sample except for E- I and E- II. The soluble solids content represents with a good approximation the concentration of soluble sugars. The sugary liquid that comes out of the berries during the pressing of the grapes impregnates the grape stalks and it is also responsible for the fermentation process that takes place inside the grape stalks heap.

		°Bx I cycle	°Bx II cycle	°Bx III cycle
1	**Control**	8.61	3.00	1.60
2	**E- I**	7.69	2.70	1.25
3	**J- I**	8.72	2.70	1.25
4	**E+ I**	9.20	3.13	1.76
5	**J+ I**	9.09	2.90	1.55
6	**E+ II**	9.21	3.28	1.43
7	**J- II**	8.67	2.89	1.54
8	**E- II**	7.71	2.24	0.99
9	**J+ II**	8.98	2.99	1.40

Table 8.15: °Bx normalised by the specific sample weights of each aqueous extract of the nine fractions of grape stalk powder obtained through electrostatic separation. E-: Negative electrode; E-: Positive electrode; J-: Negative jar, J+: Positive jar; I: first electrostatic separation; II: second electrostatic separation

8.3.6. DETERMINATION OF THE SUGARS IN THE AQUEOUS EXTRACTS OF THE GRAPE STALK POWDER FRACTIONS

The concentrations of glucose and fructose, ranging from 9.46 to 13.50 g/100 g and from 7.39 to 11.61 g/100 g respectively, did not show any significant differences in the nine fractions (table 8.16). However, their sum showed significant differences, although the associated F_{value} was quite low and Tukey's was not able to discriminate the samples. The particles containing the highest concentrations of sugars seemed to fall selectively into the jars placed under the electrodes, perhaps due to a reduction effect in the net charge.

Fructose showed a significant negative correlation ($r = -0.47$, $P \leq 0.05$) with the absorbance at 440 nm of the aqueous extracts.

8.3.7. DETERMINATION OF THE SUGARS AND FURANIC COMPOUNDS IN THE ACID EXTRACTS OF THE GRAPE STALK POWDER FRACTIONS

The concentrations of xylose deriving from the hemicellulose hydrolysis ranged from 8.26 to 17.53 g/100 g and showed significant differences (table 8.17). Unlike the previous case of sugars extracted in aqueous solution, xylose seemed to selectively accumulate on the electrodes rather than in the jars. Nevertheless, the concentration of xylose in the control was significantly higher than in all the other fractions. The higher values of the standard deviations recorded for all analytes compared to those obtained with the aqueous extraction show either that the hydrolysis process

under these conditions has a poor repeatability or the hemicellulose content is not homogeneous within each sample. Indeed, hemicellulose is linked to other cellular structures, such as microfibrils (glycoproteins and cellulose) and lignin. In each single particle, the net charge provided by the triboelectric effect is, in fact, the result of the presence or not of the various components.

		Glucose (g/100 g d.w.)	Fructose (g/100 g d.w.)	Sum (g/100 g d.w.)
	ANOVA (F_{value})	n.s.	n.s.	3.38*
1	**Control**	12.12±1.45	9.09±0.66	21.21
2	**E- I**	9.46±1.08	7.39±0.89	16.84
3	**J- I**	9.46±1.08	9.55±1.50	18.62
4	**E+ I**	9.60±0.90	8.59±0.52	18.20
5	**J+ I**	13.50±1.29	10.75±1.44	24.25
6	**E+ II**	12.03±0.53	11.51±2.00	23.54
7	**J- II**	13.49±0.46	10.78±0.65	24.28
8	**E- II**	13.00±0.08	9.85±0.01	22.86
9	**J+ II**	13.33±2.14	11.61±2.42	24.94

Table 8.16: Concentration of sugars in the aqueous extracts of grape stalk powder fractions. Results of the one-way ANOVA and the Tukey's test applied on values are reported as F_{values} and lowercase letters, respectively. n.s.: not significant. E-: Negative electrode; E-: Positive electrode; J-: Negative jar, J+: Positive jar; I: first electrostatic separation; II: second electrostatic separation

Glucose did not show significant differences due to high standard deviations. Furanic compounds are formed during the acid treatment of the simple sugars. Furfural mainly derived from xylose, while HMF from glucose. The former showed significant differences, as already observed for xylose, while HMF, just like glucose, did not.

Significant positive correlations were highlighted between both the sugars (glucose and xylose) and i.r. ($r = 0.63$, $P \leq 0.01$, respectively and $r = 0.57$, $P \leq 0.05$, respectively). This effect suggests that the more is the absorbed by a fraction the higher is the extent of hydrolysis, and at the same time the material showing higher water affinity is also the one that has the highest concentration of simple sugars. Xylose concentrations also showed a positive correlation ($r = 0.77$, $P \leq 0.001$) with the absorbances at 440 nm of the acid extracts. This relation is easily explainable, indeed the high the concentration of xylose, the high the non-enzymatic browning effect on the sample due to the heating process under acid condition.

		Glucose (g/100 g d.w.)	Xylose (g/100 g d.w.)	HMF (mg/kg d.w.)	Furfural (mg/kg d.w.)
	ANOVA (F_{value})	n.s.	6.8**	n.s.	4.48*
1	**Control**	4.47±1.06	17.53±3.08^{c}	166.72±88.54	2272.36±118.59^{ab}
2	**E- I**	1.67±0.97	11.93±0.66^{ab}	144.41±64.30	2005.16±217.28^{a}
3	**J- I**	2.61±0.59	9.33±0.34^{a}	197.57±189.16	2109.59±49.14^{ab}
4	**E+ I**	3.38±3.79	12.87±2.36^{ab}	290.58±8.68	2035.97±81.09^{a}
5	**J+ I**	3.77±2.31	10.17±1.15^{a}	230.98±182.24	2093.75±218.96^{a}
6	**E+ II**	5.32±0.12	12.14±0.36^{ab}	252.30±61.39	2178.83±50.57^{ab}
7	**J- II**	4.17±0.42	10.15±0.60^{a}	204.24±75.41	1996.19±127.24^{a}
8	**E- II**	0.34±0.60	8.26±1.30^{a}	171.74±19.18	2605.24±25.21^{b}
9	**J+ II**	4.69±0.81	11.07±0.22^{a}	228.79±18.54	2074.49±93.30^{a}

Table 8.17: Concentration of sugars and furanic compounds in the acid extracts of grape stalk powder fractions. Results of the one-way ANOVA and the Tukey's test applied on values are reported as F_{values} and lowercase letters, respectively. Different letters identify samples significantly different ($P \leq 0.05$): *$P \leq 0.05$; **$P \leq 0.01$. E-: Negative electrode; E-: Positive electrode; J-: Negative jar, J+: Positive jar; I: first electrostatic separation; II: second electrostatic separation

8.3.8. YIELDS OF THE SOLID RESIDUES AFTER EACH EXTRACTION

The percentage values of the yields after each cycle of extraction are shown in table 8.18. Significant higher values were found for both the fractions collected at negative electrode, while those one collected at positive electrode showed some of the lowest percentage yields. These data suggest that the fractions that selectively migrate towards to negative electrodes are less susceptible to release substances adhered to them and less prone to hydrolysis of the polymeric components. This is a further confirmation of the difference that was found in the fractions collected on the different electrodes. This is clearly due to a different average composition. The high correlation between the two data sets of yields (r = 0.82, $P \leq 0.001$) also suggests that a acid residue likely still present on the grape stalks surface could trigger the hydrolysis process even in the aqueous extraction, although to a lesser extent.

The two data sets of yields (related to aqueous and acid extractions) also showed negative significant correlations with i.r. (r = -0.52, $P \leq 0.05$ and r = -0.76, $P \leq 0.001$, respectively). This means

that the lower water-absorption capacity already noticed for these fractions brought about higher yields in solid residue, and in turn, lower yields in soluble compounds. In a few words, the negative electrode was able to selectively attract the particles containing the polymeric structures most recalcitrant to hydrolysis. Significant correlations leading to the same conclusions were highlighted between the percentage yields and the concentrations of glucose and fructose.

		Initial weights of the samples (g)	Sample weights after aqueous extraction (g) and % yield	Sample weights after acid extraction (g) and % yield
ANOVA (F_{value})			7.09**	58.39***
1	**Control**	0.500 ± 0.002	0.234 ± 0.006 (46.75% a)	0.152 ± 0.002 (30.33% ab)
2	**E- I**	0.491 ± 0.014	0.266 ± 0.000 (54.09% c)	0.175 ± 0.011 (35.64% c)
3	**J- I**	0.492 ± 0.014	0.241 ± 0.006 (48.99% ab)	0.151 ± 0.006 (30.81% b)
4	**E+ I**	0.507 ± 0.006	0.247 ± 0.011 (48.73% ab)	0.144 ± 0.000 (28.44% a)
5	**J+ I**	0.509 ± 0.011	0.242 ± 0.017 (47.62% a)	0.149 ± 0.005 (29.19% ab)
6	**E+ II**	0.494 ± 0.008	0.237 ± 0.001 (48.02% ab)	0.140 ± 0.002 (28.32% a)
7	**J- II**	0.512 ± 0.010	0.255 ± 0.002 (49.80% abc)	0.156 ± 0.002 (30.54% b)
8	**E- II**	0.402 ± 0.000	0.212 ± 0.004 (52.70% bc)	0.142 ± 0.002 (35.30% c)
9	**J+ II**	0.502 ± 0.001	0.245 ± 0.004 (48.73% ab)	0.146 ± 0.001 (29.07% ab)

Table 8.18: Weights of the samples and yields after each extraction. Results of the one-way ANOVA and the Tukey's test applied on values are reported as F_{values} and lowercase letters, respectively. Different letters identify samples significantly different ($P \leq 0.05$): ** $P \leq 0.01$; *** $P \leq 0.001$. E-: Negative electrode; E-: Positive electrode; J-: Negative jar, J+: Positive jar; I: first electrostatic separation; II: second electrostatic separation

8.3.9. FLUORESCENCE MICROSCOPY

The fluorescence microscope is an instrument used to study organic and inorganic samples by exploiting the phenomena of fluorescence and phosphorescence induced in the sample through the application of an appropriate electromagnetic source of electronic excitation.

The analysis of the samples allowed to highlight the prevalence of trachea and fibers with lignified tissues in the samples selectively isolated to the positive electrode (figure 8.13; E+, I). From these images it emerges that the fragments with higher amounts of lignin selectively moved towards the positive electrode due to the higher presence of phenolic substances, characterized by the presence of the electronic cloud in the aromatic rings. In the control sample, the presence of these elements was fair limited (figure 8.14; Control), while they were not found at all in the samples isolated from the negative electrode. A similar behaviour has been already described in a study on the electrostatic separation of sunflower oil cake (Barakat et al., 2015), in which the authors showed that proteins selectively migrated to the positive electrode, while the lignocellulosic material was massively directed to the negative one.

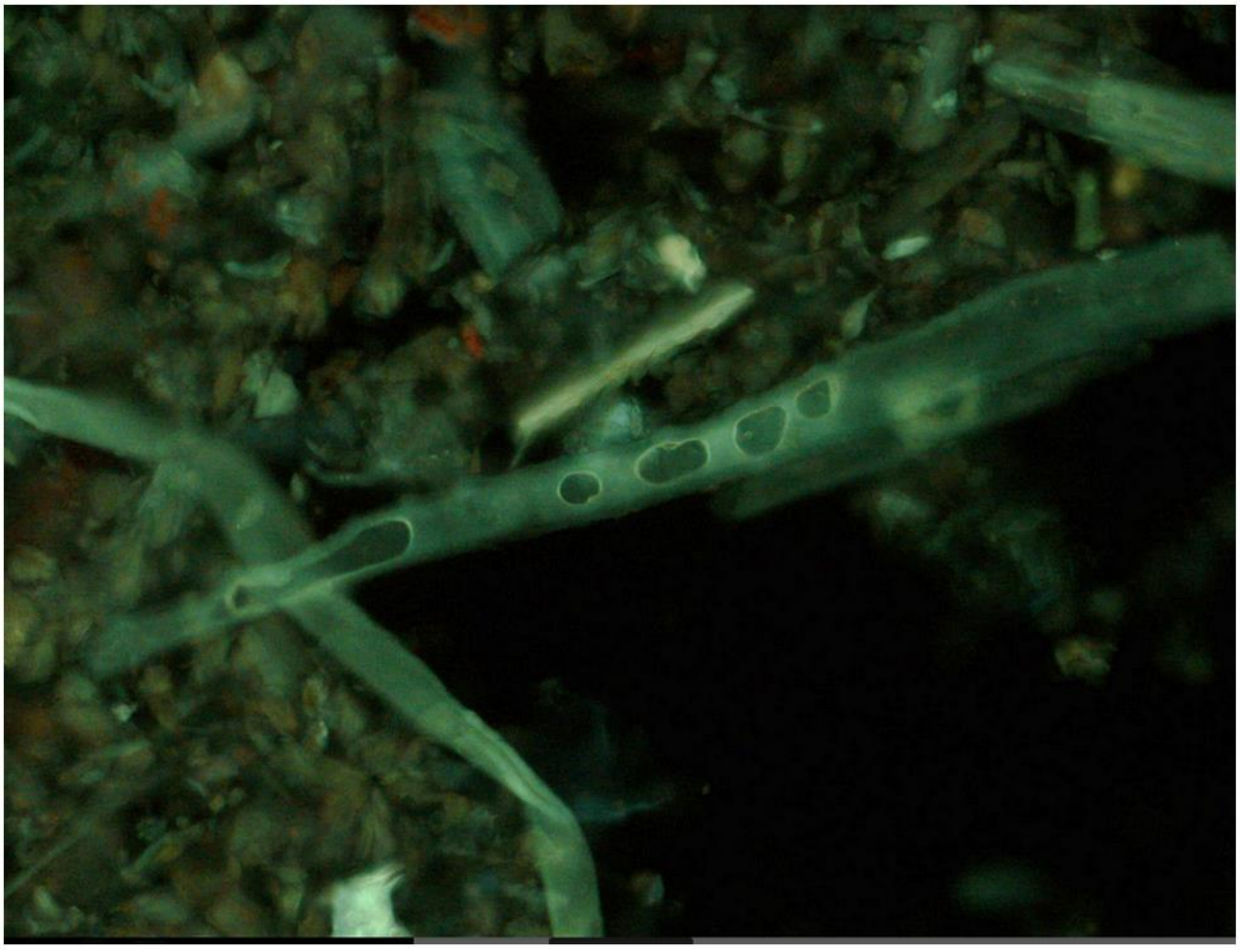

Figure 8.13: Fluorescence microscopy picture of the grape stalk powder sample E+ I

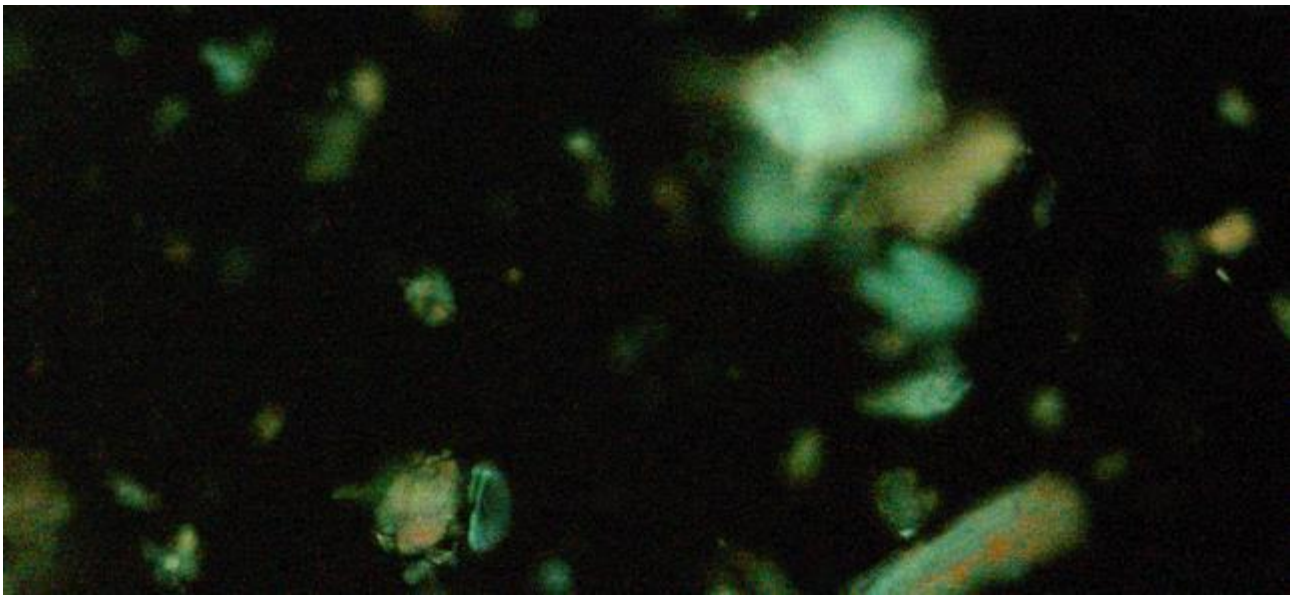

Figure 8.14: Fluorescence microscopy of the control grape stalk powder control

8.4. ENZYMATIC TESTS ON THE GRAPE STALK POWDER

The figures 8.14 and 8.15 show the histograms of absorbance values according to the biocatalytic activity of the enzymatic groups during 24 and 48 h, respectively. The absorbance at 280 nm increase in both 24 and 48 h samples by increasing laccase amount from 25 to 100 U. In the 24 h, the enzymatic mixtures that yielded the highest absorbance values are the combination of 100 U of laccase and 200 U cellulase, and the triple combination of 100 U laccase, 200 U hemicellulase, and 100 U cellulase.

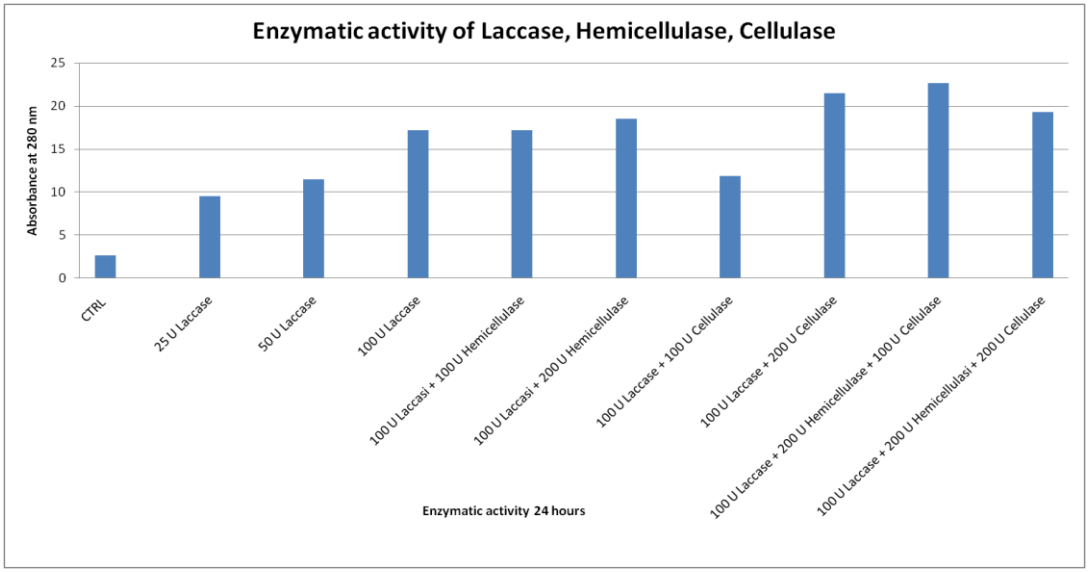

Figure 8.14: Enzymatic activity during 24 h and absorbance at 280 nm. Ctrl: non-treated control sample

By prolonging the experiment up to 48 h, very similar results were obtained (Fig. 8.15). This suggests that 24 h are sufficient to achieve the maximum result from each combination of enzymes.

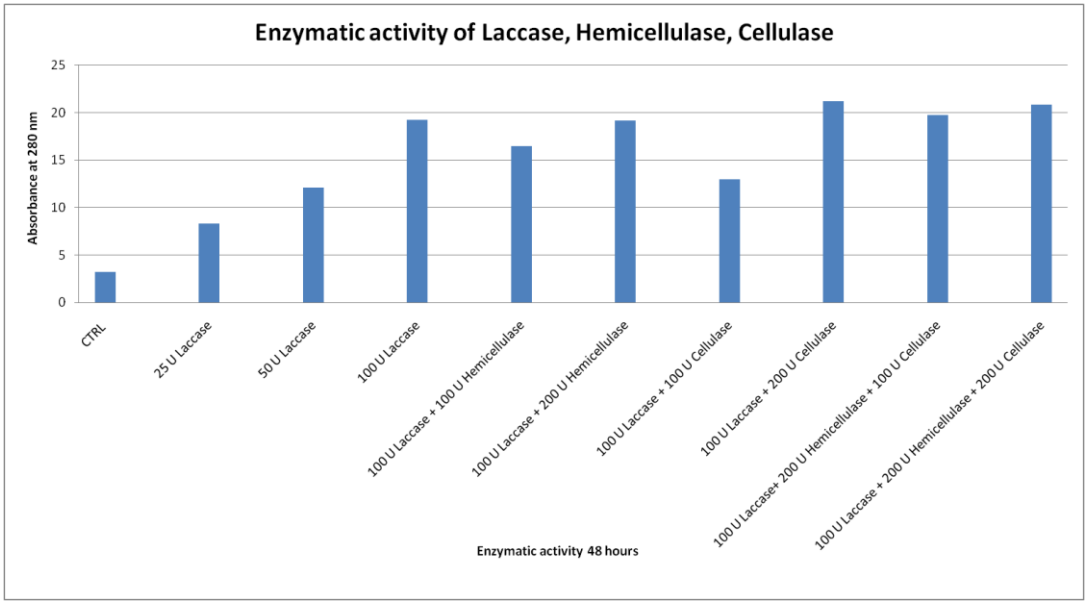

Figure 8.15: Enzymatic activity during 48 hours and absorbance at 280 nm

Keeping the concentration of laccase constant (100 U) and increasing that one of hemicellulase and cellulase (200 U), values of absorbance at 500 nm (Molisch assay) showed a sharp increase comparing samples at 24 h with those one at 48 h (Fig. 8.16 and Fig. 8.17). The enzymatic system that provided the highest absorbance value at 500 nm at 24 and 48 h was that constituted by the laccase 100 U, hemicellulase 200 U, and cellulase 200 U. These results indicated that the release by hydrolysis of simple sugars keeps on increasing during 48 h. A further experiment should consider a higher time of enzymatic reaction.

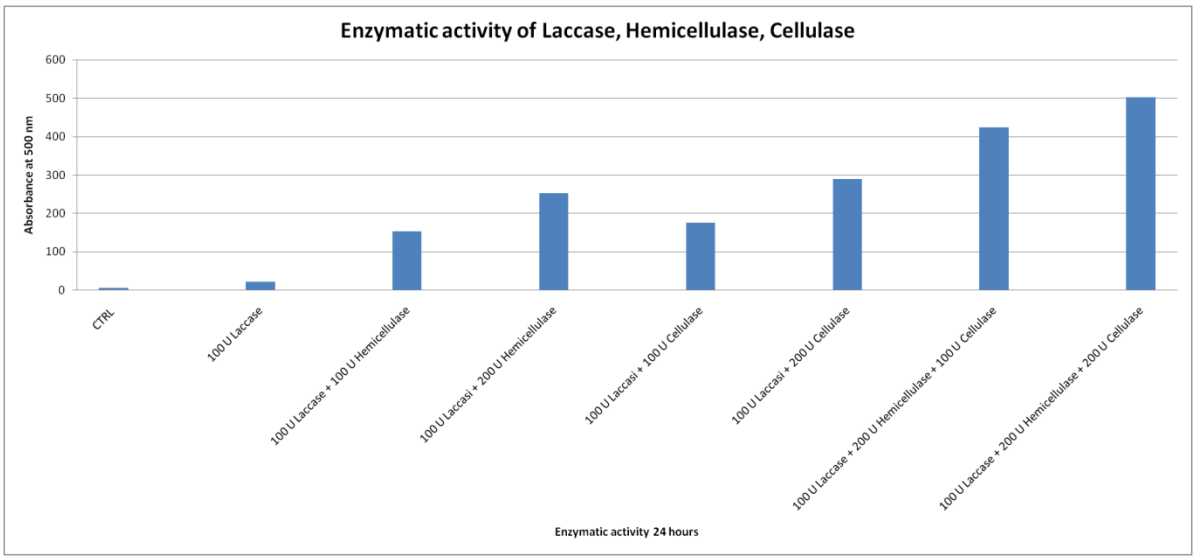

Figure 8.16: Measure of the enzymatic activity at 500 nm (Molisch assay) during 24 h

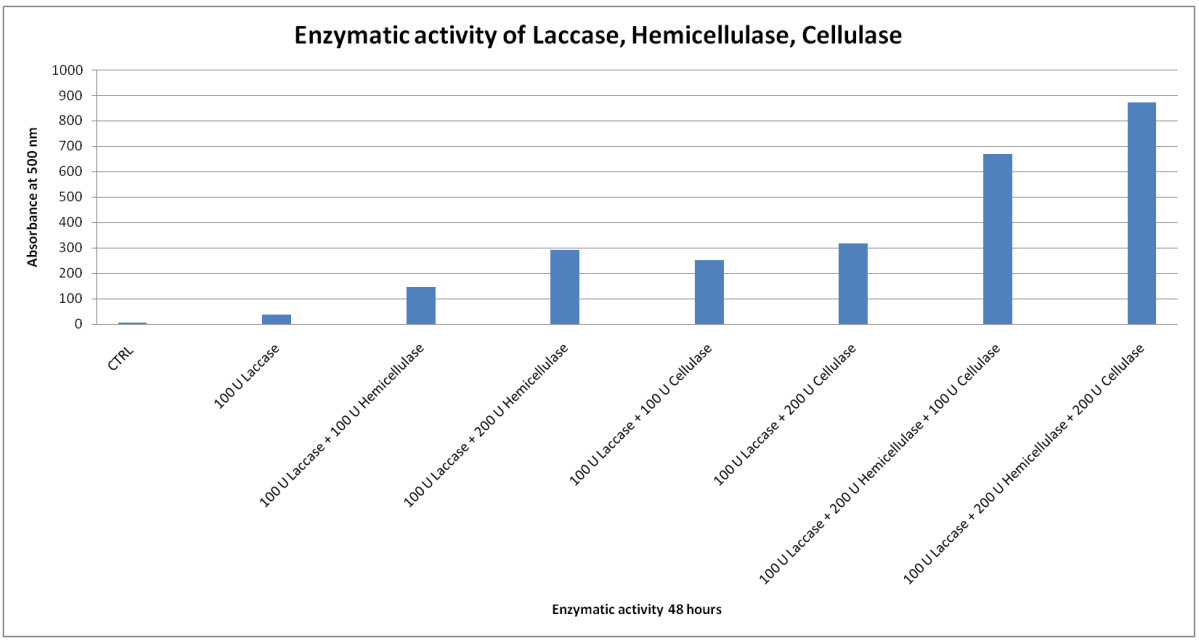

Figure 8.17: Measure of the enzymatic activity at 500 nm (Molisch assay) during 48 h

9. CONCLUSIONS

This Ph.D. project focused on the circular economy strategy applied to the wine industry in order to valorise leftovers with a scarce value and difficult to dispose, such as grape stalks and some distillation fractions.

The results of the experiment on distillation fractions showed an actual possibility of exploiting the still-high grade fraction resulting from ethanol distillation as potential fuel for fuel cells. Undoubtedly, fuel cells work with this fuel even if at a reduced regime. At the moment we are not able to understand the chemistry occurring in the cell by utilising a complex mixture compared to a mere diluted solution of MeOH. On the other hand, better results can be probably achieved using larger fuel cell, and even better results with direct-ethanol fuel cells, specifically studied for EtOH. Another item worth of investigation is the ability of cells in converting volatile congeners in other chemicals. Scaling up the system, thus yielding high amount of energy, fuel cell would produce remarkable quantities of low-concentrated chemicals in its wastewater. Also, it could be interesting to study the economical sustainability of chemical recovery from this waste.

The use of grape stalk powder as filler to improve mechanical properties of bio-composites materials showed satisfactory results, in particular when grape stalk powder was subjected to acetylation. Aside from the improvement of the mechanical properties, the incorporation of grape stalk powder 10% into a biodegradable polymer as polybutylene succinate allows the rate of the polymer to reduce and complessive cost of the material as well, and provides various woody hues.

The electrostatic separation of grape stalks is a cutting-edge technique already successfully applied to sunflower oil cake to separate proteins from polysaccharides, lignin, and polyphenol. Starting from this previous experience, it was applied to grape stalk powder to verify the possibility of their fractionament. The aqueous extraction of the obtained fractions showed appreciable concentration of simple sugars that residuated from the grape pressing. Another quite high rate of simple sugars was obtained through an acid hydrolysis of the residual pellet. This source of sugars can find applications in the microbial fermentations for the production of various metabolites. The acid extraction led to the formation of furanic compounds derived from the sugars. A proper modulation of the acid-extraction condition is needed to drive the reaction towards either the highest yield in simple sugars or in furanic compounds. Indeed the latter, represents useful building blocks that find employment in the fine chemistry. For this reason other strategies, such as pyrolysis and electrochemical could be taken into consideration for an extensive production of these compounds.

The enzymatic treatment on grape stalk powder showed promising results in terms of carbohydrate hydrolysis, while the hydrolysis of lignin to release phenolic compounds did not show evident results. The very complex nature of the starting material still represents a challenge for chemists that aims at disassembling and separating its structure. Nevertheless, further investigation should be carry out using a hybrid chemical and enzymatic approach.

REFERENCES

Abdul Manan, M., & Webb, C. (2017). Modern microbial solid state fermentation technology for future biorefineries for the production of added-value products. *Biofuel Research Journal*, *4*(4), 730-740.

Agbor, G. A., Vinson, J. A., & Donnelly, P. E. (2014). Folin-Ciocalteu reagent for polyphenolic assay. *International Journal of Food Science, Nutrition and Dietetics (IJFS)*, *3*(8), 147-156.

Alañón, M. E., Pérez-Coello, M. S., & Marina, M. L. (2015). Wine science in the metabolomics era. *TrAC Trends in Analytical Chemistry*, *74*, 1-20.

Allison, G. G. (2011). Application of Fourier transform mid-infrared spectroscopy (FTIR) for research into biomass feed-stocks. *Fourier Transforms–New Analytical Approaches and FTIR Strategies*, 71-88.

Alvira, P., Tomás-Pejó, E., Ballesteros, M., & Negro, M. J. (2010). Pretreatment technologies for an efficient bioethanol production process based on enzymatic hydrolysis: a review. *Bioresource technology*, *101*(13), 4851-4861.

Alvira, P., Negro, M. J., Ballesteros, I., González, A., & Ballesteros, M. (2016). Steam explosion for wheat straw pretreatment for sugars production. *Bioethanol*, *2*(1).

Arora, D. S., & Sharma, R. K. (2010). Ligninolytic fungal laccases and their biotechnological applications. *Applied biochemistry and biotechnology*, *160*(6), 1760-1788.

Bahrami, H., & Faghri, A., (2013). Review and advances of direct methanol fuel cells: Part II: Modeling and numerical simulation. *Journal of Power Sources*, *230*, 303-320.

Barakat, A., & Rouau, X., (2014). New dry technology of environmentally friendly biomass refinery: glucose yield and energy efficiency. *Biotechnology for biofuels*, *7*(1), 138.

Barakat, A., Jérôme, F., & Rouau, X. (2015). A dry platform for separation of proteins from biomass-containing polysaccharides, lignin, and polyphenols. *ChemSusChem*, *8*(7), 1161-1166.

Barakat, A., & Mayer-Laigle, C., (2017). Electrostatic separation as an entry into environmentally eco-friendly dry biorefining of plant materials. *Journal of Chemical Engineering & Process Technology*, *8*(354). doi: 10.4172/2157-7048.1000354.

Bechthold, I., Bretz, K., Kabasci, S., Kopitzky, R., & Springer, A. (2008). Succinic acid: a new platform chemical for biobased polymers from renewable resources. *Chemical Engineering &*

Technology: Industrial Chemistry-Plant Equipment-Process Engineering-Biotechnology, *31*(5), 647-654.

Behera, B. C., Sethi, B. K., Mishra, R. R., Dutta, S. K., & Thatoi, H. N. (2017). Microbial cellulases–Diversity & biotechnology with reference to mangrove environment: A review. *Journal of Genetic Engineering and Biotechnology*, *15*(1), 197-210.

Belda, I., Ruiz, J., Esteban-Fernández, A., Navascués, E., Marquina, D., Santos, A., & Moreno-Arribas, M. (2017). Microbial contribution to wine aroma and its intended use for wine quality improvement. *Molecules*, *22*(2), 189.

Bevilacqua, N., Morassut, M., Serra, M. C., & Cecchini, F. (2017). Determinazione dell'impronta carbonica dei sottoprodotti della vinificazione e loro valenza biologica. *Ingegneria dell'Ambiente*, *4*(3).

Bhuiyan, N. H., Selvaraj, G., Wei, Y., & King, J. (2008). Gene expression profiling and silencing reveal that monolignol biosynthesis plays a critical role in penetration defence in wheat against powdery mildew invasion. *Journal of Experimental Botany*, *60*(2), 509-521.

Brandt, A., Gräsvik, J., Hallett, J. P., & Welton, T. (2013). Deconstruction of lignocellulosic biomass with ionic liquids. *Green chemistry*, *15*(3), 550-583.

Brodeur, G., Yau, E., Badal, K., Collier, J., Ramachandran, K. B., & Ramakrishnan, S. (2011). Chemical and physicochemical pretreatment of lignocellulosic biomass: a review. *Enzyme research*, *2011*.

Brostow, W., Datashvili, T., Jiang, P., & Miller, H. (2016). Recycled HDPE reinforced with sol–gel silica modified wood sawdust. *European Polymer Journal*, *76*, 28-39.

Chen, H. Z., & Liu, Z. H. (2015). Steam explosion and its combinatorial pretreatment refining technology of plant biomass to bio-based products. *Biotechnology journal*, *10*(6), 866-885.

Collins, T., Gerday, C., & Feller, G. (2005). Xylanases, xylanase families and extremophilic xylanases. *FEMS microbiology reviews*, *29*(1), 3-23.

Coseri, S. (2017). Cellulose: To depolymerize… or not to? *Biotechnology Advances*, *35*(2), 251-266.

Christopher, L. P., Yao, B., & Ji, Y. (2014). Lignin biodegradation with laccase-mediator systems. *Frontiers in Energy Research*, *2*, 12.

Decloux, M., Coustel, J. (2005). Simulation of a neutral spirit production plant using beer distillation International Sugar Journal 107(1283), 628-643.

De Hoffmann, E., Charette, J., & Stroobant, V. (1997). Mass Spectrometry: Principles and Applications.

Delidovich, I., Hausoul, P. J., Deng, L., Pfützenreuter, R., Rose, M., & Palkovits, R. (2015). Alternative monomers based on lignocellulose and their use for polymer production. *Chemical reviews*, *116*(3), 1540-1599.

de Jong, E., & Jungmeier, G. (2015). Biorefinery concepts in comparison to petrochemical refineries. In *Industrial biorefineries & white biotechnology* (pp. 3-33). Elsevier.

de Jong, E., Higson, A., Walsh, P., & Wellisch, M. (2012). Product developments in the bio-based chemicals arena. *Biofuels, Bioproducts and Biorefining*, *6*(6), 606-624.

de Oliveira Felipe, L., de Oliveira, A. M., & Bicas, J. L. (2017). Bioaromas–Perspectives for sustainable development. *Trends in food science & technology*, *62*, 141-153.

Dettmer, K., Aronov, P. A., & Hammock, B. D. (2007). Mass spectrometry-based metabolomics. *Mass spectrometry reviews*, *26*(1), 51-78.

Diaz, A. B., Blandino, A., & Caro, I. (2018). Value added products from fermentation of sugars derived from agro-food residues. *Trends in Food Science & Technology*, *71*, 52-64.

D'Ischia, M., 2002. *Chimica organica in laboratorio*. Piccin.

Dwivedi, U. N., Singh, P., Pandey, V. P., & Kumar, A. (2011). Structure–function relationship among bacterial, fungal and plant laccases. *Journal of Molecular Catalysis B: Enzymatic*, *68*(2), 117-128.

Ellen MacArthur Foundation. (2015). Towards a circular economy: Business rationale for an accelerated transition.

Elgharbawy, A. A., Alam, M. Z., Moniruzzaman, M., & Goto, M., 2016. Ionic liquid pretreatment as emerging approaches for enhanced enzymatic hydrolysis of lignocellulosic biomass. *Biochemical Engineering Journal*, *109*, 252-267.

Escamilla-Alvarado, C., Pérez-Pimienta, J. A., Ponce-Noyola, T., & Poggi-Varaldo, H. M., 2017. An overview of the enzyme potential in bioenergy-producing biorefineries. *Journal of Chemical Technology & Biotechnology*, *92*(5), 906-924.

Esposito, D., & Antonietti, M. (2015). Redefining biorefinery: the search for unconventional building blocks for materials. *Chemical Society Reviews*, *44*(16), 5821-5835.

Fache, M., Boutevin, B., & Caillol, S. (2015). Vanillin production from lignin and its use as a renewable chemical. *ACS sustainable chemistry & engineering*, *4*(1), 35-46.

Faraji, M., Fonseca, L. L., Escamilla-Treviño, L., Barros-Rios, J., Engle, N., Yang, Z. K., Timothy J. Tschaplinski T. J., Dixon, R. A., & Voit, E. O. (2018). Mathematical models of lignin biosynthesis. *Biotechnology for biofuels*, *11*(1), 34.

Gelosia, M., Ingles, D., Pompili, E., D'Antonio, S., Cavalaglio, G., Petrozzi, A., & Coccia, V. (2017). Fractionation of Lignocellulosic Residues Coupling Steam Explosion and Organosolv Treatments Using Green Solvent γ-Valerolactone. *Energies*, *10*(9), 1264.

Ghisellini, P., Cialani, C., & Ulgiati, S. (2016). A review on circular economy: the expected transition to a balanced interplay of environmental and economic systems. *Journal of Cleaner production*, *114*, 11-32.

Giacobbo, A., Meneguzzi, A., Bernardes, A. M., & de Pinho, M. N. (2017). Pressure-driven membrane processes for the recovery of antioxidant compounds from winery effluents. *Journal of Cleaner Production*, *155*, 172-178.

Giardina, P., Faraco, V., Pezzella, C., Piscitelli, A., Vanhulle, S., & Sannia, G. (2010). Laccases: a never-ending story. *Cellular and Molecular Life Sciences*, *67*(3), 369-385.

Gu, Y., & Jérôme, F. (2013). Bio-based solvents: an emerging generation of fluids for the design of eco-efficient processes in catalysis and organic chemistry. *Chemical Society Reviews*, *42*(24), 9550-9570.

Gupta, C., Prakash, D., & Gupta, S. (2015). A biotechnological approach to microbial based perfumes and flavours. *J. Microbiol. Exp*, *3*(1).

Gustavsson, J., Cederberg, C., Sonesson, U., Van Otterdijk, R., & Meybeck, A. (2011). *Global food losses and food waste* (pp. 1-38). Rome: FAO.

Guzik, U., Hupert-Kocurek, K., & Wojcieszyńska, D. (2014). Immobilisation as a strategy for improving enzyme properties-application to oxidoreductases. *Molecules*, *19*(7), 8995-9018.

Hatfield, R., & Vermerris, W. (2001). Lignin formation in plants. The dilemma of linkage specificity. *Plant physiology*, *126*(4), 1351-1357.

Hendriks, A. T. W. M., & Zeeman, G. (2009). Pretreatments to enhance the digestibility of lignocellulosic biomass. *Bioresource technology*, *100*(1), 10-18.

Holm, J., & Lassi, U. (2011). Ionic liquids in the pretreatment of lignocellulosic biomass. In *Ionic Liquids: Applications and Perspectives*. IntechOpen.

Hussain, M. A. (2004). *Alternative routes of polysaccharide acylation: synthesis, structural analysis, properties* (Doctoral dissertation).

Isikgor, F. H., & Becer, C. R. (2015). Lignocellulosic biomass: a sustainable platform for the production of bio-based chemicals and polymers. *Polymer Chemistry*, *6*(25), 4497-4559.

Jacquet, N., Maniet, G., Vanderghem, C., Delvigne, F., & Richel, A. (2015). Application of steam explosion as pretreatment on lignocellulosic material: a review. *Industrial & Engineering Chemistry Research*, *54*(10), 2593-2598.

Jones, S. M., & Solomon, E. I. (2015). Electron transfer and reaction mechanism of laccases. *Cellular and molecular life sciences*, *72*(5), 869-883.

Jørgensen, H., Kristensen, J. B., & Felby, C. (2007). Enzymatic conversion of lignocellulose into fermentable sugars: challenges and opportunities. *Biofuels, Bioproducts and Biorefining*, *1*(2), 119-134.

Juturu, V., & Wu, J. C. 2012). Microbial xylanases: engineering, production and industrial applications. *Biotechnology advances*, *30*(6), 1219-1227.

Juturu, V., & Wu, J. C. (2014). Microbial cellulases: engineering, production and applications. *Renewable and Sustainable Energy Reviews*, *33*, 188-203.

Kalia, S., Thakur, K., Kumar, A., & Celli, A. (2014). Laccase-assisted surface functionalisation of lignocellulosics. *Journal of Molecular Catalysis B: Enzymatic*, *102*, 48-58.

Kärkäs, M. D., Matsuura, B. S., Monos, T. M., Magallanes, G., & Stephenson, C. R. (2016). Transition-metal catalysed valorization of lignin: the key to a sustainable carbon-neutral future. *Organic & biomolecular chemistry*, *14*(6), 1853-1914.

Kdidi, S., Vaca-Medina, G., Peydecastaing, J., Oukarroum, A., Fayoud, N., & Barakat, A. (2019). Electrostatic separation for sustainable production of rapeseed oil cake protein concentrate: Effect of mechanical disruption on protein and lignocellulosic fiber separation. *Powder Technology*, *344*, 10-16.

Kebarle, P., & Tang, L. (1993). From ions in solution to ions in the gas phase-the mechanism of electrospray mass spectrometry. *Analytical chemistry*, *65*(22), 972A-986A.

Knob, A., Terrasan, C. F., & Carmona, E. C. (2010). β-Xylosidases from filamentous fungi: an overview. *World Journal of Microbiology and Biotechnology*, *26*(3), 389-407.

Kumar, P., Barrett, D. M., Delwiche, M. J., & Stroeve, P. (2009). Methods for pretreatment of lignocellulosic biomass for efficient hydrolysis and biofuel production. *Industrial & engineering chemistry research*, *48*(8), 3713-3729.

Lee, H. V., Hamid, S. B. A., & Zain, S. K. (2014). Conversion of lignocellulosic biomass to nanocellulose: structure and chemical process. *The Scientific World Journal*, *2014*.

Lei, Z., Huhman, D. V., & Sumner, L. W. (2011). Mass spectrometry strategies in metabolomics. *Journal of Biological Chemistry*, *286*(29), 25435-25442.

Leo, T., Raso, M., Navarro, E., & Mora, E. (2013). Long term performance study of a direct methanol fuel cell fed with alcohol blends. *Energies*, *6*(1), 282-293.

Levine, V. E. (1930). A General Test for Carbohydrates. *Proceedings of the Society for Experimental Biology and Medicine*, *27*(8), 830-831.

Li, X., & Zheng, Y. (2017). Lignin-enzyme interaction: mechanism, mitigation approach, modeling, and research prospects. *Biotechnology advances*, *35*(4), 466-489.

Li, M., Pu, Y., & Ragauskas, A. J. (2016). Current understanding of the correlation of lignin structure with biomass recalcitrance. *Frontiers in chemistry*, *4*, 45.

Li, X., & Faghri, A. (2013). Review and advances of direct methanol fuel cells (DMFCs) part I: Design, fabrication, and testing with high concentration methanol solutions. *Journal of Power Sources*, *226*, 223-240.

Lin, C. S. K., Pfaltzgraff, L. A., Herrero-Davila, L., Mubofu, E. B., Abderrahim, S., Clark, J. H., ... & Thankappan, S. (2013). Food waste as a valuable resource for the production of chemicals, materials and fuels. Current situation and global perspective. *Energy & Environmental Science*, *6*(2), 426-464.

Lucarini, M., Durazzo, A., Romani, A., Campo, M., Lombardi-Boccia, G., & Cecchini, F. (2018). Bio-based compounds from grape seeds: A biorefinery approach. *Molecules*, *23*(8), 1888.

Lupoi, J. S., Singh, S., Simmons, B. A., & Henry, R. J. (2014). Assessment of lignocellulosic biomass using analytical spectroscopy: an evolution to high-throughput techniques. *BioEnergy Research*, *7*(1), 1-23.

Lupoi, J. S., Singh, S., Parthasarathi, R., Simmons, B. A., & Henry, R. J. (2015). Recent innovations in analytical methods for the qualitative and quantitative assessment of lignin. *Renewable and Sustainable Energy Reviews*, *49*, 871-906

McLaren, K. (1976). XIII—The development of the CIE 1976 (L* a* b*) uniform colour space and colour-difference formula. *Journal of the Society of Dyers and Colourists*, *92*(9), 338-341.

Madadi, M., Tu, Y., & Abbas, A. (2017). Pretreatment of Lignocelollusic Biomass Based on Improving Enzymatic Hydrolysis. *International Journal of Applied Sciences and Biotechnology*, *5*(1), 1-11.

Madadi, M., Penga, C., & Abbas, A. (2017). Advances in genetic manipulation of lignocellulose to reduce biomass recalcitrance and enhance biofuel production in bioenergy crops. *J Plant Biochem Physiol*, *5*(182), 2.

Maina, S., Kachrimanidou, V., & Koutinas, A. (2017). A roadmap towards a circular and sustainable bioeconomy through waste valorization. *Current Opinion in Green and Sustainable Chemistry*, *8*, 18-23.

Marriott, P. E., Gómez, L. D., & McQueen-Mason, S. J. (2016). Unlocking the potential of lignocellulosic biomass through plant science. *New Phytologist*, *209*(4), 1366-1381.

Martinez, G. A., Rebecchi, S., Decorti, D., Domingos, J. M., Natolino, A., Del Rio, D., ... & Fava, F. (2016). Towards multi-purpose biorefinery platforms for the valorisation of red grape pomace: production of polyphenols, volatile fatty acids, polyhydroxyalkanoates and biogas. *Green Chemistry*, *18*(1), 261-270.

Mayer-Laigle, C., Blanc, N., Rajaonarivony, R., & Rouau, X. (2018). Comminution of dry lignocellulosic biomass, a review: part I. From fundamental mechanisms to milling behaviour. *Bioengineering*, *5*(2), 41.

Mayer-Laigle, C., Barakat, A., Barron, C., Delenne, J. Y., Frank, X., Mabille, F., ... & Lullien-Pellerin, V. (2018). Dry biorefineries: Multiscale modeling studies and innovative processing. *Innovative Food Science & Emerging Technologies*, *46*, 131-139.

Medina, F., Aguila, S., Baratto, M. C., Martorana, A., Basosi, R., Alderete, J. B., & Vazquez-Duhalt, R. (2013). Prediction model based on decision tree analysis for laccase mediators. *Enzyme and microbial technology*, *52*(1), 68-76.

Miao, Y. C., & Liu, C. J. (2010). ATP-binding cassette-like transporters are involved in the transport of lignin precursors across plasma and vacuolar membranes. *Proceedings of the National Academy of Sciences*, *107*(52), 22728-22733.

Mimini, V., Kabrelian, V., Fackler, K., Hettegger, H., Potthast, A., & Rosenau, T. (2018). Lignin-based foams as insulation materials: a review. *Holzforschung*, *73*(1), 117-130.

Mollania, N., Heidari, M., & Khajeh, K. (2018). Catalytic activation of Bacillus laccase after temperature treatment: Structural & biochemical characterization. *International journal of biological macromolecules*, *109*, 49-56.

Monier, V., Mudgal, S., Escalon, V., O'Connor, C., Gibon, T., Anderson, G., ... & Morton, G. (2010). Preparatory study on food waste across EU 27. *Report for the European Commission [DG ENV—Directorate C]*.

Monlau, F., Barakat, A., Trably, E., Dumas, C., Steyer, J. P., & Carrère, H. (2013). Lignocellulosic materials into biohydrogen and biomethane: impact of structural features and pretreatment. *Critical reviews in environmental science and technology*, *43*(3), 260-322.

Obeng, E. M., Adam, S. N. N., Budiman, C., Ongkudon, C. M., Maas, R., & Jose, J. (2017). Lignocellulases: a review of emerging and developing enzymes, systems, and practices. *Bioresources and Bioprocessing*, *4*(1), 16.

Ouyang, X., Chen, L., Zhang, S., Yuan, Q., Wang, W., & Linhardt, L. J. (2018). Effect of simultaneous steam explosion and alkaline depolymerization on corncob lignin and cellulose structure. *Chemical and biochemical engineering quarterly*, *32*(2), 177-189.

Paës, G., Berrin, J. G., & Beaugrand, J. (2012). GH11 xylanases: structure/function/properties relationships and applications. *Biotechnology advances*, *30*(3), 564-592.

Pardo, I., & Camarero, S. (2015). Laccase engineering by rational and evolutionary design. *Cellular and molecular life sciences*, *72*(5), 897-910.

Pastrana-Bonilla, E., Akoh, C. C., Sellappan, S., & Krewer, G. (2003). Phenolic content and antioxidant capacity of muscadine grapes. *Journal of agricultural and food chemistry*, *51*(18), 5497-5503.

Philp, J. (2018). The bioeconomy, the challenge of the century for policy makers. *New biotechnology*, *40*, 11-19.

Pleissner, D., Qi, Q., Gao, C., Rivero, C. P., Webb, C., Lin, C. S. K., & Venus, J. (2016). Valorization of organic residues for the production of added value chemicals: a contribution to the bio-based economy. *Biochemical Engineering Journal*, *116*, 3-16.

Polizeli, M. L. T. M., Rizzatti, A. C. S., Monti, R., Terenzi, H. F., Jorge, J. A., & Amorim, D. S. (2005). Xylanases from fungi: properties and industrial applications. *Applied microbiology and biotechnology*, *67*(5), 577-591.

Prajapati, H. V., & Minocheherhomji, F. P. (2018). Laccase-A Wonder Molecule: A Review of its Properties and Applications. *Int. J. Pure App. Biosci*, *6*(1), 766-773.

Ravindran, R., & Jaiswal, A. K. (2016). Exploitation of food industry waste for high-value products. *Trends in Biotechnology*, *34*(1), 58-69.

Richel, A., Vanderghem, C., Simon, M., Wathelet, B., & Paquot, M. (2012). Evaluation of matrix-assisted laser desorption/ionization mass spectrometry for second-generation lignin analysis. *Analytical chemistry insights*, *7*, ACI-S10799.

Rinaldi, R., Jastrzebski, R., Clough, M. T., Ralph, J., Kennema, M., Bruijnincx, P. C., & Weckhuysen, B. M. (2016). Paving the way for lignin valorisation: recent advances in bioengineering, biorefining and catalysis. *Angewandte Chemie International Edition*, *55*(29), 8164-8215.

Riva, S. (2006). Laccases: blue enzymes for green chemistry. *TRENDS in Biotechnology*, *24*(5), 219-226.

Romaní, A., Garrote, G., Ballesteros, I., & Ballesteros, M. (2013). Second generation bioethanol from steam exploded Eucalyptus globulus wood. *Fuel*, *111*, 66-74.

Rose, M., & Palkovits, R. (2011). Cellulose-Based Sustainable Polymers: State of the Art and Future Trends. *Macromolecular rapid communications*, *32*(17), 1299-1311.

Saffarionpour, S., & Ottens, M. (2018). Recent advances in techniques for flavor recovery in liquid food processing. *Food engineering reviews*, *10*(2), 81-94.

Saranraj, P., Stella, D., & Reetha, D. (2012). Microbial cellulases and its applications. *International Journal of Biochemistry and Biotechnology Science*, *1*, 1-12.

Scheller, H. V., & Ulvskov, P. (2010). Hemicelluloses. *Annual review of plant biology*, *61*.

Schutyser, W., Renders, T., Van den Bosch, S., Koelewijn, S. F., Beckham, G. T., & Sels, B. F. (2018). Chemicals from lignin: an interplay of lignocellulose fractionation, depolymerisation, and upgrading. *Chemical society reviews*, *47*(3), 852-908.

Sciubba, L. (2009). *Sviluppo di processi biotecnologici per la produzione e il recupero di vanillina* (Doctoral dissertation, alma).

Sheldon, R. A., & Woodley, J. M. (2017). Role of biocatalysis in sustainable chemistry. *Chemical reviews*, *118*(2), 801-838.

Sibout, R., & Höfte, H. (2012). Plant cell biology: the ABC of monolignol transport. *Current Biology*, *22*(13), R533-R535.

Silveira, M. H. L., Morais, A. R. C., da Costa Lopes, A. M., Olekszyszen, D. N., Bogel-Łukasik, R., Andreaus, J., & Pereira Ramos, L. (2015). Current pretreatment technologies for the development of cellulosic ethanol and biorefineries. *ChemSusChem*, *8*(20), 3366-3390.

Singleton, V. L., Orthofer, R., & Lamuela-Raventós, R. M. (1999). [14] Analysis of total phenols and other oxidation substrates and antioxidants by means of folin-ciocalteu reagent. In *Methods in enzymology* (Vol. 299, pp. 152-178). Academic press.

Spigno, G., Moncalvo, A., De Faveri, D. M., & Silva, A. (2014). Valorisation of stalks from different grape cultivars for sugars recovery. *Chemical Engineering Transactions*, *37*, 745-750.

Styger, G., Prior, B., & Bauer, F. F. (2011). Wine flavor and aroma. *Journal of industrial microbiology & biotechnology*, *38*(9), 1145.

Sumby, K. M., Grbin, P. R., & Jiranek, V (2010). Microbial modulation of aromatic esters in wine: Current knowledge and future prospects. *Food chemistry*, *121*(1), 1-16.

Sun, Z., Fridrich, B., de Santi, A., Elangovan, S., & Barta, K. (2018). Bright side of lignin depolymerization: toward new platform chemicals. *Chemical reviews*, *118*(2), 614-678.

Tomás-Pejó, E., Alvira, P., Ballesteros, M., & Negro, M. J. (2011). Pretreatment technologies for lignocellulose-to-bioethanol conversion. In *Biofuels* (pp. 149-176). Academic press.

Traoré, M., Kaal, J., & Cortizas, A. M. (2016). Application of FTIR spectroscopy to the characterization of archeological wood. *Spectrochimica Acta Part A: Molecular and Biomolecular Spectroscopy*, *153*, 63-70.

Upton, B. M., & Kasko, A. M. (2015). Strategies for the conversion of lignin to high-value polymeric materials: review and perspective. *Chemical reviews*, *116*(4), 2275-2306.

Vanholme, R., Demedts, B., Morreel, K., Ralph, J., & Boerjan, W. (2010). Lignin biosynthesis and structure. *Plant physiology*, *153*(3), 895-905.

Walia, A., Guleria, S., Mehta, P., Chauhan, A., & Parkash, J. (2017). Microbial xylanases and their industrial application in pulp and paper biobleaching: a review. *3 Biotech*, *7*(1), 11.

Wong, D. W. (2009). Structure and action mechanism of ligninolytic enzymes. *Applied biochemistry and biotechnology*, *157*(2), 174-209.

Xu, F., Yu, J., Tesso, T., Dowell, F., & Wang, D. (2013). Qualitative and quantitative analysis of lignocellulosic biomass using infrared techniques: a mini-review. *Applied Energy*, *104*, 801-809.

Yoo, C. G., Pu, Y., & Ragauskas, A. J. (2017). Ionic liquids: Promising green solvents for lignocellulosic biomass utilization. *Current Opinion in Green and Sustainable Chemistry*, *5*, 5-11.